Factors affecting proteasome dynamics and localization

by

Alicia Burris

B.S., Washburn University, 2012

AN ABSTRACT OF A DISSERTATION

submitted in partial fulfillment of the requirements for the degree

DOCTOR OF PHILOSOPHY

Division of Biology
College of Arts and Sciences

KANSAS STATE UNIVERSITY
Manhattan, Kansas

2020

Abstract

Proteasomes are essential, multisubunit complexes that control cellular processes and proteostasis by selectively degrading proteins. Their function depends on the coordination between two major subcomplexes, the regulatory particle (RP) and the core particle (CP). The CP forms a cylindrical structure that cleaves substrates but has closed gates on either end that limits substrate entry. The regulatory particle opens these gates, recognizes the substrates, and unfolds them into the core particle. Besides RP, other proteasome associated proteins, like Blm10, can open the gates and thereby activate the CP. Blm10 is a large, monomeric protein that binds to the same interface of CP as the regulatory particle; however, it remains poorly understood how the mutually exclusive binding between these activators is regulated. The work in this dissertation addresses this by studying Blm10 and Blm10-CP complexes including how their levels are regulated by various stress conditions, and how that affects the proteasome landscape. Our results show that upon overexpression of Blm10, all RP-CP complexes were replaced by Blm10-CP complexes. This indicates that Blm10, which is normally present at substoichiometric levels relative to CP, can compete with RP and change the proteasome landscape. The emergence of almost exclusively Blm10-CP complexes compromised the proteasome's ability to degrade substrates as indicated by an accumulation of ubiquitinated material. However, under stress conditions, like prolonged cell growth, Blm10 and Blm10-CP complexes were targeted for autophagy and vacuolar degradation, while RP-CP complexes were not. Consistent with this difference in fate between complexes, we saw no colocalization of Blm10 and CP in proteasome storage granules (PSGs) following glucose starvation while RP and CP are found in the same granules.

This was surprising as previous work indicated a role for Blm10 in PSG formation. As PSGs require proteasome export from the nucleus we also focused on other factors involved in this process. Interestingly, proteasomes fail to be exported from the nucleus in cells containing a mutant form of Rpn11, a lid subunit of the regulatory particle. This mutant, *rpn11-m1*, has a frameshift mutation resulting in the loss of its terminal alpha helix. Therefore, we created a new mutant, Rpn11-Δ31, which produced a clean truncation. This mutant prevented the proteasome from localizing to PSGs and showed severe growth defects, indicating we could use this mutant to study proteasome nuclear export. Our results showed that truncating Rpn11 affected

incorporation of late stage lid subunits Rpn7 and Rpn12 which themselves contain putative nuclear export signals for the common export protein Crm1. However, further analysis indicated that Crm1 was not involved in export of the proteasome under glucose starvation. Nevertheless, unincorporated Rpn7 and Rpn12 did accumulate in granule-like structures while the remainder of the proteasome remained nuclear. This suggests that unincorporated lid subunits might be stored in granule-like structures until they can be successfully incorporated into the proteasome. In sum, this thesis provides a better understanding of the dynamics of proteasome complexes and how changing these dynamics affects proteasome localization and function.

Factors affecting proteasome dynamics and localization

by

Alicia Burris

B.S., Washburn University, 2012

A DISSERTATION

submitted in partial fulfillment of the requirements for the degree

DOCTOR OF PHILOSOPHY

Division of Biology
College of Arts and Sciences

KANSAS STATE UNIVERSITY
Manhattan, Kansas

2020

Approved by:

Major Professor
Dr. Jeroen Roelofs

Copyright

Abstract

Proteasomes are essential, multisubunit complexes that control cellular processes and proteostasis by selectively degrading proteins. Their function depends on the coordination between two major subcomplexes, the regulatory particle (RP) and the core particle (CP). The CP forms a cylindrical structure that cleaves substrates but has closed gates on either end that limits substrate entry. The regulatory particle opens these gates, recognizes the substrates, and unfolds them into the core particle. Besides RP, other proteasome associated proteins, like Blm10, can open the gates and thereby activate the CP. Blm10 is a large, monomeric protein that binds to the same interface of CP as the regulatory particle; however, it remains poorly understood how the mutually exclusive binding between these activators is regulated. The work in this dissertation addresses this by studying Blm10 and Blm10-CP complexes including how their levels are regulated by various stress conditions, and how that affects the proteasome landscape. Our results show that upon overexpression of Blm10, all RP-CP complexes were replaced by Blm10-CP complexes. This indicates that Blm10, which is normally present at substoichiometric levels relative to CP, can compete with RP and change the proteasome landscape. The emergence of almost exclusively Blm10-CP complexes compromised the proteasome's ability to degrade substrates as indicated by an accumulation of ubiquitinated material. However, under stress conditions, like prolonged cell growth, Blm10 and Blm10-CP complexes were targeted for autophagy and vacuolar degradation, while RP-CP complexes were not. Consistent with this difference in fate between complexes, we saw no colocalization of Blm10 and CP in proteasome storage granules (PSGs) following glucose starvation while RP and CP are found in the same granules.

This was surprising as previous work indicated a role for Blm10 in PSG formation. As PSGs require proteasome export from the nucleus we also focused on other factors involved in this process. Interestingly, proteasomes fail to be exported from the nucleus in cells containing a mutant form of Rpn11, a lid subunit of the regulatory particle. This mutant, *rpn11-m1*, has a frameshift mutation resulting in the loss of its terminal alpha helix. Therefore, we created a new mutant, Rpn11-Δ31, which produced a clean truncation. This mutant prevented the proteasome from localizing to PSGs and showed severe growth defects, indicating we could use this mutant to study proteasome nuclear export. Our results showed that truncating Rpn11 affected

incorporation of late stage lid subunits Rpn7 and Rpn12 which themselves contain putative nuclear export signals for the common export protein Crm1. However, further analysis indicated that Crm1 was not involved in export of the proteasome under glucose starvation. Nevertheless, unincorporated Rpn7 and Rpn12 did accumulate in granule-like structures while the remainder of the proteasome remained nuclear. This suggests that unincorporated lid subunits might be stored in granule-like structures until they can be successfully incorporated into the proteasome. In sum, this thesis provides a better understanding of the dynamics of proteasome complexes and how changing these dynamics affects proteasome localization and function.

.

Table of Contents

List of Figures

List of Tables

Acknowledgements

First, I would like to acknowledge Dr. Jeroen Roelofs for your ongoing support and advice. I am incredibly fortunate to have had the privilege to work and learn from you. I will forever be grateful that you became my Ph.D. advisor as your encouragement and patience has been a contributing factor to my success. Thank you for being so kind and understanding. You embody what it means to be a wonderful advisor and I'm so glad that you gave me the chance to become a better scientist in your lab.

I would also like to thank all the members of supervisory committee, Dr. Stella Lee, Dr. Jocelyn McDonald, Dr. Alina De La Mota-Peynado and Dr. Richard Todd. All of you have been instrumental to my progress. Your support and advice through the years has been invaluable and I will forever be grateful for your guidance.

To the current and past lab members: Akeem, Anjana, Gabrielle, Alina, and Mandeep. Thank you for your constant discussions and suggestions on projects and ideas. We have been through so much together and I feel incredibly lucky to have had you by my side through this chapter of my life. You will forever be lifelong friends and I can't imagine having a better group of people to work and grow with. I would also like to thank Zach, Sam and Shelby for being the most amazing undergraduates to work with. The effort and dedication you showed to our work allowed me to have the best possible experience as a mentor.

I would also like to thank the Division of Biology including Melissa, Becki, Tari, Sarah, and Bob for always being so incredibly helpful in every situation. We could not succeed without your constant assistance and listening ear.

I also want to acknowledge all of the friends I've made in the last five years. I fully believe that the only way to succeed in graduate school is to have an incredible support group. Specifically, I would like to thank Babita, Seton, Kaitlin, Priscila, Josh, Anil, Elsie, and Nirupama. All of you have been such a big part of my life and you've helped me through so much. I can't express what our time together has meant.

Finally I would like to thank my family: Billy, my grandma, Austin and Misty and my mom. None of this would be possible without your love and support. Mom, words cannot describe what you've done for me. You mean everything to me, and I only hope to be half the person you are. Lastly, I would like to thank my best friend, Dr. Sarah. You have been my rock through all of this, and I couldn't have done it without you.

Dedication

I dedicate this work to my mom. You are the person that keeps me grounded and I absolutely would not have succeeded this far in life without your constant support, advice, and love.

Chapter 1 - Introduction

Protein Homeostasis

Proteins perform many important cellular processes and their activity, as well as levels, need to be regulated in order to maintain cellular protein homeostasis or proteostasis. Proteostasis is a complex, coordinated network that works to ensure proteins are correctly folded and present in the correct amounts when and where they are needed in the cell. Proteostasis is achieved through the coordination of multiple cellular process such as translation, protein folding, post-translational modifications, assembly, localization, and degradation of proteins to ensure protein levels are regulated[1]. Abnormalities in these processes can disrupt the balance and have detrimental consequences such as protein accumulation. Excess proteins can form aggregates that result in certain disease states including Huntington's disease, Alzheimer's, and Parkinson's[2–4].

The function of many proteins relies on their 3-dimensional folded structure; however, some proteins are intrinsically disordered meaning they fail to adopt a 3-diminsional structure. This often allows them more flexibility for binding partner proteins [5]. Unfortunately, proteins with intrinsically disordered regions, as well as misfolded proteins that expose hydrophobic residues, tend to aggregate to reduce their exposure to the aqueous environment. While aggregation allows these proteins to become more thermodynamically stable it can also lead to the above mentioned diseases [6]. Chaperones can mediate proper protein folding but for those that are unsalvageable, degradation by the proteasome can prevent their accumulation and aggregation. Failure to degrade these proteins can result in cell toxicity and disease states[6]. The two major protein degradation pathways in the cell are the lysosome, or vacuole for yeast and plants, and the ubiquitin-proteasome system (UPS). These two degradation systems work complementary to each other in that certain proteins or protein aggregates that cannot be degraded by the proteasome are targeted for degradation in the vacuole which contains multiple proteases that degrade these proteins into individual amino acids that can be reused by the cell. Synthesis of amino acids requires a large input of energy making amino acid recycling more energetically favorable, especially under starvation conditions.

As cells age, reduced activity of proteostasis machinery leads to an increase in misfolded proteins which can aggregate in a concentration dependent manner[7]. While protein aggregation

is the most commonly associated phenotype for defects in protein homeostasis, other defects exist such as high protein turnover rates and abnormal localization of proteins. For example, a mutant form of the fibrosis transmembrane conductance regulator (CFTR) remains in the endoplasmic reticulum due to a folding delay which leads to its rapid turnover by the proteasome[8]. Unhealthy lifestyles can also affect the proteostasis network. Diets high in fat can lead to overproduction of insulin in pancreatic β-cells[1]. These increased levels exceed the ER's capacity for folding and secretion which activates the unfolded protein response (UPR), a signaling network that becomes activated to restore ER function and protein levels [9]. Additionally, insulin overproduction monopolizes proteostasis machinery resulting in delayed degradation of other cellular proteins. Overall, prolonged UPR activation and extended protein half-lives affect cell functioning and survival[1]. In addition to activation of the UPR, macroautophagy is also activated by ER stress. Macroautophagy, also termed autophagy, involves bulk packaging of cytosolic material in a double membrane structure, called a phagophore, that fuses with the lysosome (vacuole in yeast). Once in the lysosome, this material is degraded. Autophagy is, therefore, thought to help eliminate the abnormal aggregation of ER proteins [10].

Vacuolar Degradation Pathways

While macroautophagy can be activated by ER stress, other cellular stress conditions, such as nutrient starvation, can also activate autophagy. The process of autophagy involves the formation of a phagophore. Formation of the phagophore, as well as recruitment and engulfment of material for degradation, requires the assembly of multiple protein complexes. Assembly of these complexes begins with TORC1 (target of rapamycin), which monitors nutrient levels in the cell. When nutrient levels are depleted, TORC1 becomes inactivated. The inactivation of TORC1 prevents it from hyperphosphorylating Atg13[11,12]. Unphosphorylated Atg13 is free to bind to other autophagy proteins leading to the formation of a six-protein complex referred to as the autophagy initiation complex [13,14]. Once formed, this complex recruits other autophagy proteins including transmembrane protein, Atg9, which carries vesicles to where the phagophore, or double membrane structure, will be assembled [15]. The formation of this complex is referred to as the nucleation step which is required for expansion of the phagophore [16].

Two conjugation systems utilizing ubiquitin-like (Ubl) proteins, Atg12 and Atg8, also participate in autophagy (Fig. 1.1). The C-terminus of Atg12 has a glycine residue that is

recognized by Atg7, an E1-like enzyme, that forms a thioester bond between itself and Atg12 which serves to activate Atg12 [17]. Once activated, Atg12 is conjugated to Atg10, an E2 enzyme, that further transfers Atg12 onto Atg5 to form the Atg12-Atg5 dimer that can now form a complex with Atg16[18–20]. The Atg12-Atg5-Atg16 complex was proposed to act as an E3 ligase to aide in the formation of an Atg8 complex; however, it is not essential for this process [21,22]. While its function remains elusive, recent structural work has suggested that this complex acts as a platform to bring the components of the Atg8 into close proximity rather than acting as the conjugating enzyme [23–26].

This second required Ubl protein, Atg8, becomes conjugated to the membrane lipid phosphatidylethanolamine (PE) instead of a protein[27]. The C-terminal amino acid of Atg8 (arginine) is initially removed by Atg4, a cysteine protease, which allows it to be recognized and conjugated to Atg7[28]. From Atg7, Atg8 is transferred to the E2-like enzyme Atg3 which catalyzes the conjugation of Atg8 to phosphatidylethanolamine (PE). This complex is recruited to the growing phagophore where it functions to recruit cargo, or material that will eventually be engulfed by the phagophore and degraded in the lysosome. Specific autophagy proteins act as linkers as they simultaneously bind cargo for degradation and the Atg8 complex. Binding of both the cargo as well as Atg8 recruits the material to the phagophore [29]. Once the cargo has been recruited, the phagophore continues to elongate and the two ends eventually fuse together to form a double membranous, circular structure now termed an autophagosome which houses the cargo inside the lumen (Fig. 1-1). From here, the autophagosome fuses with the lysosomal membrane to release the autophagic body, the single membrane structure housing the cargo, into the lysosomal lumen [30]. Once inside, lysosomal hydrolases degrade the autophagic body and cargo[31,32]. The process of macroautophagy can be energetically favorable under stress conditions as misfolded proteins and aggregates can be degraded without needing to first unfold them.

A secondary nutrient pathway involves the Ras/PKA signaling pathway which activates autophagy in response to cellular glucose levels[33–37]. Two GTPases (Ras1 & Ras2) activate adenylyl cyclase which produces cAMP in the presence of glucose. cAMP binds to the regulatory subunit of PKA (Bcy1). Binding of cAMP leads to the dissociation of the PKA catalytic subunits leading to their activation[38]. Activated PKA phosphorylates Atg13 and Atg1 which inhibits autophagy. The kinase Sch9 acts in parallel to PKA as a secondary glucose sensor as its inactivation induces autophagy [37]. This overall model involves the cooperative

effect of TORC1, PKA, and Sch1 in autophagy induction, nutrient sensing, and the regulation of cell growth[39].

In addition to macroautophagy (autophagy), two other autophagy pathways exist (Fig. 1.1). Chaperone-mediated autophagy involves the identification of misfolded proteins by the chaperone Hsc70. Hsc70 recognizes the specific amino acid motif KFERQ which is normally buried in approximately one-third of folded, cytosolic proteins[40,41]. Misfolding can expose this sequence thus allowing for its recognition by the Hsc70 chaperone. Once bound by Hsc70, the substrate is unfolded and directly translocated into the lysosomal lumen for degradation. Binding of the Hsc70 bound substrate to LAMP-2a, a lysosomal membrane protein, leads to its multimerization which forms a translocation channel for the substrate [42]. The second, microautophagy, involves direct uptake of degradable material by the lysosome typically by direct invagination of the lysosomal membrane. Some evidence suggests microautophagy is involved in maintaining membrane composition as well as the overall size of certain organelles[43].

Figure 1-1 – Types of Autophagy

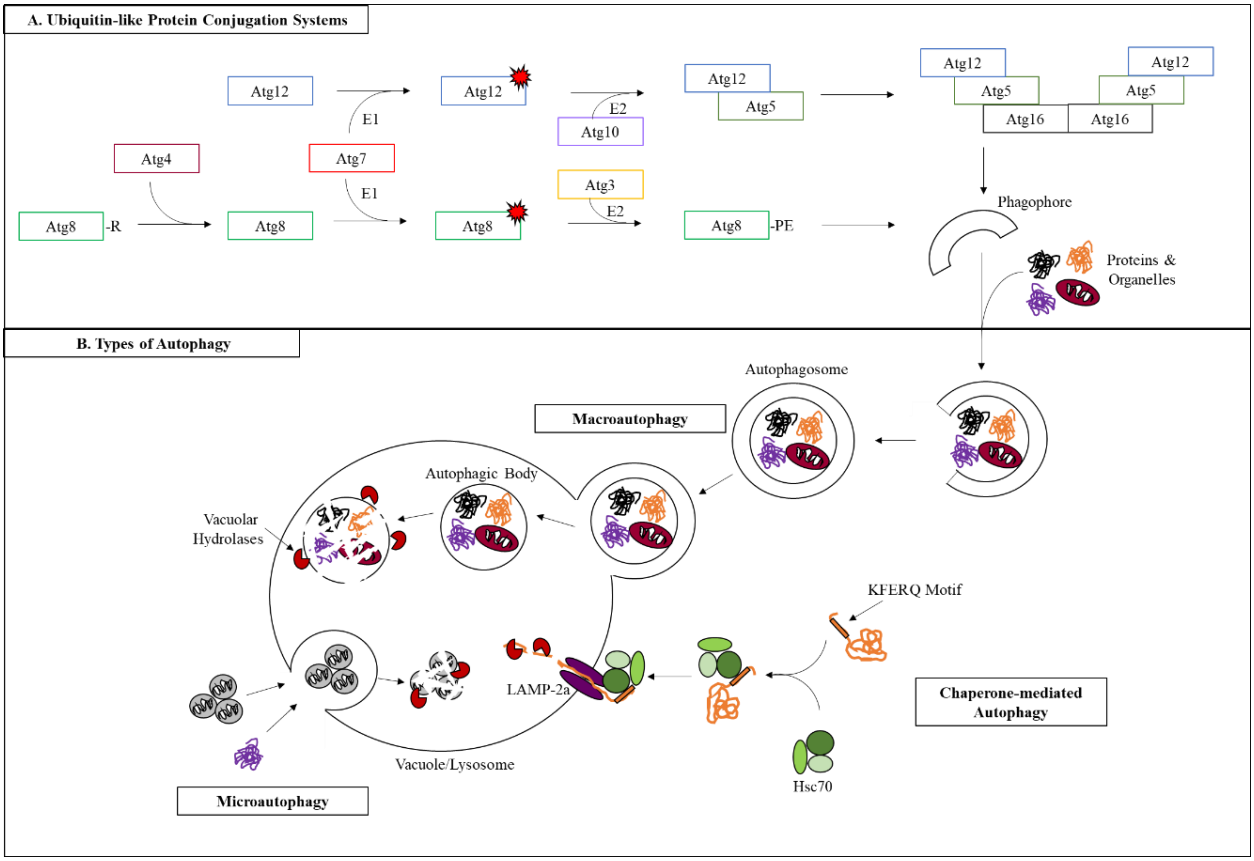

(A) Schematic representation of the two ubiquitin conjugation systems involving Atg8 and Atg12. In the Atg12 conjugation system, Atg12 becomes activated by the E1-like enzyme Atg7. The E2-like enzyme Atg10 conjugates the activated Atg12 to Atg5 creating the Atg12-Atg5 dimer. This conjugate can now bind Atg16 which leads to its dimerization. The resulting complex was proposed to aide in Atg8 conjugation; however, it was not essential to the conjugation process. Recent structural work has suggested that the Atg12-Atg5-Atg16 complex works as a scaffold to bring Atg components in close proximity rather than a conjugating enzyme. The second conjugation system involving Atg8 begins when the C-terminal arginine residue of Atg8 is removed by the cysteine protease, Atg4. Similar to the Atg12 conjugation system, Atg7 also functions to activate Atg8 which then becomes conjugated to phosphatidylethanolamine (PE) by the E2-like enzyme Atg3. Once conjugated to PE, Atg8 is recruited to the growing phagophore where it is responsible for recruiting degradable material to the phagophore. (B) Depictions of the three types of autophagy. (1) Macroautophagy involves the sequestration of bulk material in a structure called a phagophore. As the phagophore grows, it eventually fuses together to form a double membrane structure called an autophagosome which contains the cargo material inside the lumen. Macroautophagy substrates include proteins, cytosolic material and organelles. Once formed, the autophagosome fuses with the lysosomal membrane which expels a single membrane structure called an autophagic body into the lumen of the vacuole. This autophagic body, along with encased cargo, are degraded by the proteolytic enzymes within the vacuole. (2) Microautophagy involves the uptake of cargo into the vacuole through interactions and direct invagination of the vacuolar membrane. This produces a luminal vesicle containing the invaginated material which are both degraded by lysosomal hydrolases. (3) Chaperone-mediated autophagy involves the recognition of proteins, containing the conserved KFERQ motif, by the HSC70 chaperone complex. Once bound by HSC70, the substrate is trafficked to the lysosome membrane. Binding of this complex to LAMP-2a, a lysosomal transmembrane protein, causes its multimerization into a translocation channel. This channel then allows the substrate to be translocated across the lysosomal membrane and into the lumen for degradation. Adapted from (20) & (44).

The process of autophagy is generally considered to be bulk degradation of nonselective material; however, selective types of autophagy do exist. Mitophagy, ribophagy, xenophagy, and proteaphagy are all processes that selectively target and degrade mitochondria, ribosomes, bacteria, and proteasomes respectively. Autophagy is therefore involved in the degradation of organelles, large protein complexes or aggregates, and many long-lived proteins[44]. Conversely, regulated proteins including short-lived, denatured, damaged, or abnormal proteins that make up the bulk of degraded proteins are selectively targeted for degradation by an alternate, conserved mechanism used by all organisms, the ubiquitin-proteasome system (UPS).

Ubiquitin-Proteasome System

An important component of maintaining cellular homeostasis is selectively degrading proteins involved in such processes as cell cycle progression, transcription, apoptosis, DNA repair, and the cell stress response. Covalent attachment of ubiquitin, a small polypeptide of 76 amino acids, targets them to the proteasome for degradation. Ubiquitin serves as a recognition tag for downstream targeting of the substrate which affects both its function and fate. Ubiquitin molecules are attached to either one or multiple lysine residues of substrate proteins and can be bound as single ubiquitin molecules or chains of ubiquitins (Fig. 1-2). Single monoubiquitylation tends to affect protein localization, structure, activity, and interactions with partner proteins[45,46]. For example, monoubiquitylation of cell surface receptors lead to their

subsequent endocytosis and degradation by the lysosome[46]. Other cell processes regulated by single monoubiquitylation include histone function, nuclear export and DNA repair. In addition to single monoubiquitination, there is also multiple monoubiquitination where multiple single ubiquitin molecules can be attached to various lysine residues on the same protein. Furthermore, substrates can also be polyubiquitylated meaning ubiquitin can be attached onto substrates as chains. Ubiquitin itself contains seven lysine residues (Lys63, Lys48, Lys33, Lys29, Lys27, Lys11, and Lys6), as well as the N-terminal methionine, which can all be ubiquitinated ultimately forming a unique chain of ubiquitin molecules.

Addition of multiple ubiquitins in varying linkages provides this system the flexibility needed to regulate various processes. While K48 chains are the most common for targeting proteins to the proteasome for degradation, K11 and K29 chains have also been implicated in this process [47,48]. K63 branched ubiquitin chains are often involved in endocytosis, DNA repair, inflammatory signaling, and selective forms of autophagy [49,50]. Interestingly, while some chains can be homogeneous, meaning they consist of the same linkages, others can be heterogeneous and contain different linkages such as K11/K48 or K29/K48 [47,48,51].

Figure 1-2 – Types of Ubiquitination

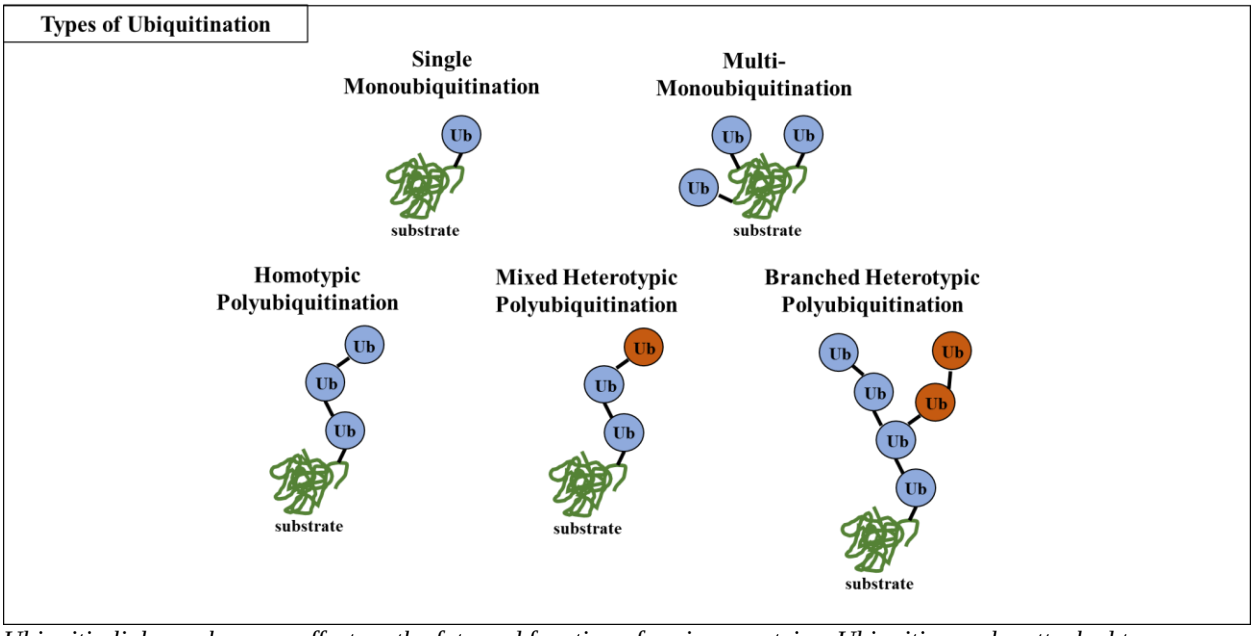

Ubiquitin linkages have an effect on the fate and function of various proteins. Ubiquitin can be attached to one or multiple lysine residues in the target protein allowing for single monoubiquitination or multi-monoubiquitination. Ubiquitin itself contains seven lysine residues that can all be ubiquitinated, in addition to Met1. This provides a wide array of polyubiquitin linkages and chains which all have specific effects on their target proteins. Ubiquitin chains can be homotypic, containing the same linkages, or heterotypic, containing different linkages. Furthermore, ubiquitin can be ubiquitinated at 2 or more positions allowing for the formation of branched chains.

Despite the variations in ubiquitination, the process of attaching the ubiquitin molecules follows a three-step process: activation, conjugation, and ligation (Fig. 1-3). The cascade begins with an E1 enzyme, also referred to as a ubiquitin activating enzyme. Initially, the ubiquitin molecule becomes C-terminally adenylated with AMP which is attacked by the catalytic cysteine of an E1 enzyme[52]. The formation of this bond and subsequent release of AMP allows a secondary active site of the E1 enzyme to noncovalently bind another ubiquitin to ultimately produce an asymmetrical, doubly loaded E1 enzyme. While the purpose of a dual loaded E1 enzyme is not completely understood, it has been shown that its formation accelerates the second step of the ubiquitination cascade, which is the transfer of the thioester bound ubiquitin molecule to the catalytic cysteine of an E2 enzyme [53–55]. Furthermore, interaction of the second ubiquitin molecule causes a conformational change within the E1 structure exposing its E2 binding sites. These sites allow for recruitment of E2 enzymes to the E1 charged ubiquitin conjugate which further allows the E1 enzyme to facilitate the transthiolation reaction to transfer the ubiquitin molecule from the E1 to the active site cysteine of the E2 enzyme[56–58].

Figure 1-3 – Process of Substrate Ubiquitination

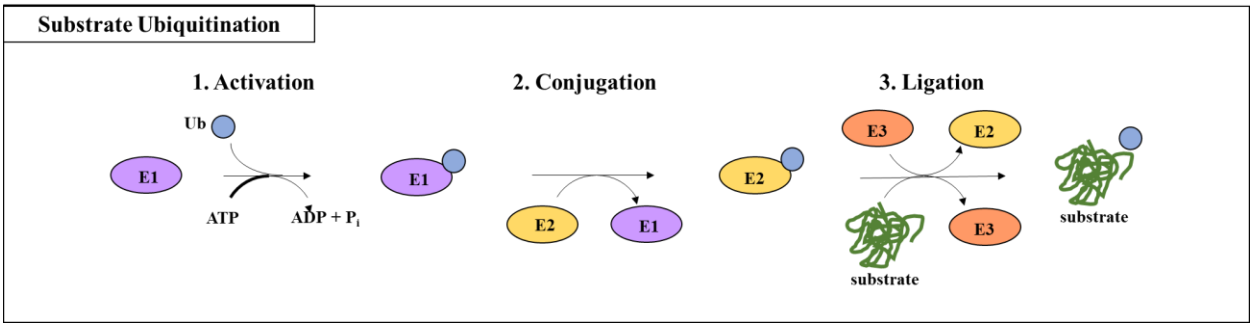

The process of ubiquitination involves three steps: activation, conjugation, and ligation. (1) Ubiquitin activation requires ATP and occurs through the formation of a thioester bond between itself and an E1 enzyme. (2) Once activated, ubiquitin is transferred from the E1 enzyme to an E2 enzyme. (3) Once bound to ubiquitin, the E2 enzyme can interact with an E3 enzyme which facilitates ubiquitin conjugation to the substrate. Adapted from (48).

Once charged with ubiquitin, E2 enzymes can bind to E3 enzymes from one of two classes, either the HECT or RING domain family ligases. The HECT domain of HECT E3 ligases are bilobed with the N-lobe interacting with the E2 enzyme and the C-lobe containing an active site cysteine that allows for the transfer of the ubiquitin from the E2 enzyme to itself [59]. Alternatively, RING finger E3 ligases do not bind to ubiquitin but instead coordinate Zn^{2+} ions that facilitate the transfer of ubiquitin directly from the E2 enzyme to the target substrate[60]. The lysine amino on the substrate ultimately attacks the thioester bond between the ubiquitin and E2 or E3 enzyme to facilitate the formation of a covalent bond between the substrate protein and

ubiquitin. For polyubiquitination to occur, this cycle continues where a lysine on the most recently added ubiquitin attacks the incoming ubiquitin conjugate. An interesting aspect of this system is understanding how E3 ligases can recognize which substrates need to be degraded. E3 ligases typically recognize a short degradation signal, called a degron, which is present on the substrate and leads to its ubiquitination. Various types of degrons exist and below are some examples discussed in detail.

N-degron: Short-lived proteins can be recognized and ubiquitinated upon exposure of an N-degron which is a destabilizing N-terminal amino acid. Destabilizing residues include positively charged residues, such as arginine, or bulky, hydrophobic amino acids [61]. Often, the substrate protein develops an N-degron whenever its N-terminus becomes modified . For example, proteolytic cleavage of the substrate can expose either an asparagine or glutamine residue which can be deamidated to produce an aspartate or glutamate. These two resides can further be arginylated by arginine transferases to create an N-terminal arginine residue which is recognized as a degron by specific E3 ligases [62,63,64,65]. N-degrons can also be generated upon acetylation of the N-terminal amino acid [66]. Three major NAT complexes found in *Saccharomyces cerevisiae* are responsible for N-terminal acetylation. Following methionine removal, the resulting N-terminal amino acid can be acetylated by NatA. In comparison, NatB and NatC can directly acetylate the N-terminal methionine residue if the following amino acid is hydrophobic or acidic[67,68]. These N-terminal degrons or modifications lead to substrate recognition by N-recognins, or E3 ligases, that target substrates to the proteasome for degradation [69,70].

Phosphodegron: Phosphorylation can also affect degron recognition as in the case of phosphodegrons. Certain motifs found on substrate proteins are only recognized for degradation following their phosphorylation. Conversely, constitutively active degradation motifs can be phosphorylated to cover the degradative signal thus allowing the protein to be maintained in the cell until the motif has been dephosphorylated[71]. A well-studied phosphodegron involves the substrate Sic1 in yeast. Upon phosphorylation, Sic1 becomes recognized by SCF, a multisubunit ubiquitin-ligase complex that binds and further ubiquitinates Sic1 for degradation by the proteasome [72,73]. As Sic1 is degraded, the cell can progress into S phase of the cell cycle [74].

Recognition of degrons within substrate proteins leads to their delivery to E2/E3 enzyme complexes. Here, they are ubiquitinated. The ubiquitinated proteins are recognized and

degraded by the 26S proteasome. The proteasome is a large protein complex found in the cytosol and nucleus of eukaryotic cell. It consists of two subcomplexes, the 19S regulatory particle (RP) and the 20S core particle (CP). The core particle is composed of 28 subunits that form four heteroheptameric rings axially stacked to form a barrel shaped complex with pores at either end of the cylinder. The regulatory particle is composed of 19 subunits that can bind to one or both ends of the core particle. The regulatory particle is involved in the recognition, deubiquitylation, and unfolding of substrate proteins. The RP is situated directly above the core particle pore which allows the unfolded substrates to be threaded into the core particle. Once inside, three proteolytic active sites cleave the substrates into short peptides that are released.

Core Particle Assembly and Function

As mentioned, the core particle is composed of four heteroheptameric rings that form a cylindrical structure with a hollow inner chamber. The two inner rings are composed of beta subunits (β1-β7) while the two outer rings consist of alpha subunits (α1-α7). β1-, β2-, and β5- are the subunits of the core particle that are responsible for proteolytically cleaving substrate proteins once they enter the inner chamber. Each of these subunits cleave after specific substrate residues to maximize the ability of the proteasome to degrade a wide variety of substrates. β2 has trypsin-like activity and cleaves after basic amino acids while β1 has peptidylglutamyl peptide hydrolyzing activity to cleave after acidic residues. Lastly, β5 has chymotrypsin-like activity for cleaving substrates after hydrophobic residues[75–77]. Amino acid specificity results from the specific residues that fit within each subunit's active site. The active site catalytic triad for the proteasome beta subunits consists of Thr1, Lys33, and Asp/Glu17. This triad is conserved amongst all archaeal, bacterial, and eukaryotic proteasome subunits. For peptidase activity, the threonine hydroxyl group nucleophilically attacks the target while the lysine amino group acts as the proton acceptor [78]. Aspartic acid helps this transfer by positioning lysine in a suitable conformation for protonation to occur. For peptide cleavage, the mature, positively charged α-amino group of threonine forms a bond with the amide nitrogen of the substrate protein. This interaction then allows for proteolytic cleavage of the substrate's peptide bond by the active gamma oxygen of the same threonine residue[79,80].

For the core particle to become active, multiple steps in assembly must occur successfully. Assembly of the core particle requires both intrinsic and extrinsic factors. Each of the three proteolytically active subunits β-subunits, as well as two inactive ones, are translated

containing N-terminal propeptides that are removed after proper assembly[75,78,81]. Propeptides often function to either inhibit protease activity until maturation or help in the assembly of multisubunit complexes[82]. For the proteasome, the β-subunit propeptides prevent premature acetylation and inactivation until the subunit has successfully been incorporated into the mature core particle. Without the propeptide, the N-terminal residue of these subunits would be a threonine which is susceptible to acetylation by the Nat1-Ard1 acetyltransferase[80,83,84]. Once the core particle has assembled, the propeptide can be removed allowing the threonine to become active while being protected inside the inner chamber of the core particle[80]. Furthermore, recent work in bacteria has suggested an additional role where the beta propeptides help regulate CP assembly and activation[85]. The same catalytic triad responsible for substrate cleavage is also involved in maturation. For autocatalysis, the lysine amino group accepts a proton from threonine which can then nucleophilically attack the preceding peptide bond with glycine to release the propeptide[86,87].

In addition to intrinsic assembly factors, there are five extrinsic factors that play a role in CP assembly. Assembly requires the formation of two immature (half) core particles which dimerize to form a fully assembled core particle (Fig. 1-4). The first step in immature CP assembly is the formation of the alpha ring which involves two sets of heterodimeric chaperones, Pba3-Pba4 and Pba1-Pba2 in yeast (mammalian orthologs are PAC3-PAC4 and PAC1-PAC2 respectively). In the early stages of assembly, Pba3-Pba4 enhances the interaction between α5 and its neighboring subunits, α4 and α6[88,89]. Pba3-Pba4 interacts with multiple alpha subunits and its deletion can lead to incorporation of two α4 subunits; therefore, it is thought to act as a scaffold to ensure proper incorporation of all subunits into the ring[89–91]. The fully formed alpha ring can then act as a scaffold for the incorporation of beta subunits in the following order: β2, β3, β4, β5, β6, β1, β7[92]. Pba3-4 sterically clashes with the incoming β4 subunit resulting in its displacement premature of immature core particle assembly[90]. One of the earliest core particle intermediates formed is the 15S complex that contains a full alpha ring, β1-6, Pba1-2 and Ump1, a core particle chaperone that associates either concurrently or prior to β2 incorporation. A proposed function of Ump1 is to structurally position the β5 propeptide in a conformation that facilitates its autocatalysis and activation upon half CP dimerization[93]. A secondary function for Ump1 is to prevent premature dimerization of two half core particles before the incorporation of β7, the rate limiting step of core particle assembly[92].

The last extrinsic core particle chaperone is the Pba1-Pba2 dimer. Both components contain an HbYX motif which allows them to bind to the pockets formed between alpha 5/6 and alpha6/7[94,95]. The positioning of Pba1-2 on the outer surface of the alpha ring aides in the incorporation of α5 and α6. This allows the beta subunits to incorporate onto the alpha ring scaffold[96]. A second function of Pba1-2 is to prevent premature docking of proteasome activators until the core particle is fully assembled. Pba1-2 has a high affinity for immature core particles but a low affinity for fully assembled, active core particles. Its high affinity for immature CP allows it to bind tightly and prevent RP from binding prematurely. Once the core particle has matured, the affinity of Pba1-2 decreases leading to its dissociation and allowing RP to bind. This affinity switch is likely due to conformational changes within the core particle resulting from propeptide cleavage of beta subunits that impact the structure of the alpha ring[97,98].

Figure 1-4 – Assembly process of the core particle

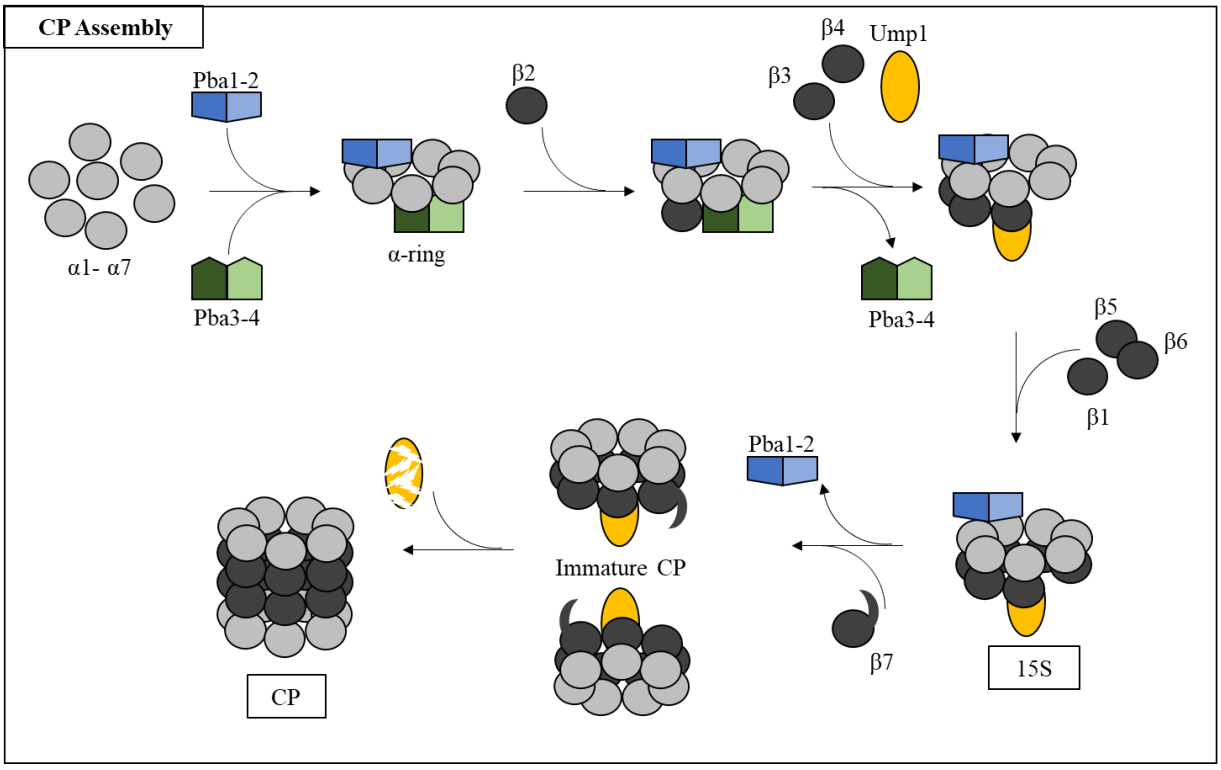

The core particle is composed of four heteroheptameric rings that stack to form a cylinder with an internal chamber. The two inner rings are composed of β-subunits while the two outer rings are composed of α-subunits. Assembly of the core particle begins with the formation of an α ring which involves two pairs of extrinsic heterodimeric chaperones, Pba3-4 and Pba1-2. Once the α ring has formed, it acts as a scaffold to aid in the incorporation of the β-subunits, which assemble in the following order β2, β3, β4, β5, β6, β1, β7. Pba3-4 sterically clashes with β4 and

is released upon its incorporation. At this point, the fifth extrinsic chaperone, Ump1 incorporates which prevents premature dimerization of two immature core particles as well as positions the β5 subunit in the correct conformation for activation. Incorporation of β5, β6, and β1produces the 15S assembly complex which retains Pba1-2 and Ump1. Incorporation of β7 completes the formation of an immature CP. Dimerization of two immature CPs results in completion of the core particle and subsequent degradation of Ump1. Adapted from (139).

Over the course of assembly, some beta subunit C-terminal extensions are required at various steps of the maturation process. β2 possesses a long C-terminal tail that helps incorporate its neighboring subunit (β3) and allows it to interact with β4 of the adjacent beta ring [99,100]. The long C-terminal extension of β7 forms interactions with β1 *in trans* to promote dimerization of two half CPs[100,101]. This dimerization process also requires the β5 propeptide which is thought to function as an intramolecular chaperone that aides to align the two half CPs[102]. Additionally, the β5 propeptide is involved in β6 incorporation which itself possesses an N-terminal extension thought to aide in the incorporation of β7. This, in turn, helps overcome the assembly checkpoint put in place by Ump1[102]. Upon dimerization, Ump1 becomes trapped inside the inner chamber of the core particle. The association of two half core particles leads to autocatalysis of the beta propeptides resulting in an active core particle that ultimately degrades the encased Ump1[93].

Fully assembled core particles are still considered inactive as substrates cannot gain access into the inner chamber until it associates with an activator complex[103]. The N-termini of specific alpha subunits extend across the substrate entry pore to block entrance into the catalytic chamber[104,105]. Activators of the core particle often contain the conserved HbYX motif which binds to one or more alpha ring pockets[106,107]. Once bound, a salt bridge between the lysine amine group in the alpha pocket and the C-terminal carboxyl group of the HbYX motif is formed. This bond causes conformational changes within the alpha ring that displaces the N-terminal alpha tails to produce an open gate conformation[108–110].

While interactions between the core and regulatory particles constitute an active proteasome, substrates still cannot be degraded until they are unfolded. This is due to the narrowness of the translocation channel[104]. As such, the regulatory particle consists of an ATPase ring specifically designed to unfold these substrates.

Regulatory Particle

The 19 subunits that make up the regulatory particle are divided into two subcomplexes, the lid and base. The base consists of Rpn1, Rpn2, Rpn13 and six Rpt subunits (Rpt1-6). The Rpts are AAA-ATPases that form a heterohexameric ring which binds directly to the alpha

ring(s) of the core particle[111]. This ring functions as a motor to unfold and translocate substrates into the core particle using energy from ATP hydrolysis[112].

Each Rpt contains 4 domains: an N-terminal coiled-coil domain (CC), an OB or oligonucleotide/oligosaccharide-binding domain, AAA+ ATPase domain, and a C-terminal domain. The coiled coil domains of Rpt subunits allow for the formation of heterodimers Rpt4-Rpt5, Rpt1-Rpt2, and Rpt3-Rpt6. Rpt5, Rpt3, and Rpt2 contain a proline residue in between the CC and OB domains which is absent in their dimerization partners. Subunits containing this proline adopt a *cis* configuration while their partner forms the *trans*. This slight alteration between subunits encourages interactions between their CC domains, which results in three sets of dimers or three *cis-trans* pairs. This pairing results in alternating *cis* subunits within the Rpt ring (Rpt1-Rpt2-Rpt6-Rpt3-Rpt4-Rpt5)[111,113,114]. The coiled coil is positioned above the OB domain in subunits with the *cis* confirmation and can range in motion from being parallel to the N-ring (closed confirmation) to being at a 45° angle to the N-ring (open confirmation)[114]. The main function of these coiled coils is in the proper assembly of the Rpt ring while secondary functions in lid/base assembly and recognition of substrates have been proposed[115].

Destabilizing mutations in the coiled coil region between each Rpt dimer, excluding Rpt4 and Rpt5, affect assembly of the Rpt ring. This dimer, along with Rpt1-Rpt2, is proposed to assist in substrate recognition as they are both positioned toward the outside of the structure and contain multiple charged residues that may interact with substrates through electrostatic interactions. Comparatively, the Rpt3-Rpt6 coiled coil is located within the lid-base interface and contains hydrophobic residues to strengthen interactions between these two subcomplexes [116]. The N-ring, composed of the six OB domains, lies up to 40 Å away from the ATPase pore loops and it has been suggested that the ATPase motor pulls against the N-ring to induce substrate unfolding. Substrates must be able to span a distance of 35 Å from the N-ring to the pore loops before they can engage the ATPase ring and be translocated into the core particle[117,118].

Each Rpt subunit contains a large and small AAA subdomain. The Walker A and Walker B motifs within the large subdomain are key to ATP binding and hydrolysis. The Walker A motif uses a conserved lysine which is required for ATP binding[119] . Additionally, a conserved glutamate, or sometimes aspartate, within the Walker B motif hydrogen bonds with a water molecule as well as the serine within the Walker A motif to facilitate ATP hydrolysis[120,121].

Folding of the ATP module produces a pocket between the large and small subdomains for nucleotide binding. In addition to the Walker motifs, the large domain also contains an arginine finger composed of two arginine residues that help in nucleotide binding and are thought to act as a sensor between Rpt subunits as the arginine finger interacts with the nucleotide bound by its neighboring Rpt[122,123]. A critical component of the Rpt subunits is the conserved, hydrophobic pore loop which extends into the central channel and engages with substrates[124]. The small subdomain of one Rpt interacts with the large subdomain of its neighboring Rpt to form a rigid body which allows the ring of six rigid bodies to cycle through conformational changes linked to ATP hydrolysis. This allows the pore loops to move in unison to unfold the substrate and pull it through the translocation channel[125,126].

As the ATPase subunits transition through these conformational changes, the RP as a whole also undergoes changes to facilitate substrate processing. These conformations begin with the s1 state (substrate free) and move to the s2 (commitment step), s3 (substrate-processing step), and s4 (gate opening) states[127,128]. Transition from s1 to s2 primarily involves movement of the lid subcomplex while s3 involves multiple changes within the Rpt ring[127,128]. The ATPase domains of Rpt subunits adopt a spiral staircase arrangement in the substrate free (s1) state where the large subdomains (along with pore loops) tilt progressively more downward with Rpt2 being at the bottom and Rpt3 being at the top[129–132]. In the s3 state, the N-ring moves toward Rpn1 while the tilted staircase of the large ATPase domain becomes progressively more linear to resemble the active state of other ATPase motors[127,128,133,134]. Altogether, this creates a larger central pore that now aligns with the translocation channel of the core particle[127,128,133,135]. In the substrate free state, Rpn11, the deubiquitinase subunit, is offset from the Rpt channel. Transition to the s2 state rotates the lid in order to align Rpn11 directly above the Rpt pore. This positions it for removal of the ubiquitin chain which is required for translocation into the core particle. For substrates to pass the translocation channel and enter the core particle, the regulatory particle must transition in to the s4 state. As mentioned previously, Rpt5, Rpt3 and Rpt2 have C-terminal tails that bind to the corresponding alpha ring pockets of the core particle[106]. It has been suggested that the C-terminal tail of Rpt6 forms interactions with the ring to induce this transition to the s4 state and induce gate opening and substrate translocation into the core particle[128,135].

Base Assembly

The base itself requires five external assembly chaperones: Hsm3 (S5b in mammalian cells), Nas2 (p27 in mammalian cells), Nas6 (gankyrin/p28 in mammalian cells), Rpn14 (PAAF1 in mammalian cells), and Adc17[136–141] (Table 1-1).

Table 1-1 Chaperones

	Saccharomyces cerevisiae	*Homo sapiens*
Core Particle Chaperones	Pba1/Pba2 dimer Pba3/Pba4 dimer Ump1	PAC1/PAC2 dimer PAC3/PAC4 dimer UMP1
Regulatory Particle Chaperones	Hsm3 Nas2 Nas6 Rpn14 Adc17	S5b p27 Gankyrin PAAF1

As mentioned previously, base assembly begins with the formation of three *cis-trans* dimers. Adc17 interacts at the N-terminus of Rpt6 to aid in its dimerization with Rpt3[141]. The other four chaperones bind to Rpt dimers, specifically at their C-domains, to form the following assembly intermediates: Nas2-Rpt5-Rpt4, Rpn14-Rpt6-Rpt3-Nas6, and Hsm3-Rpt1-Rpt2-Rpn1 (BP1) (Fig. 1-5)[137,140,142]. Interestingly, these chaperones are structurally quite different yet are capable of binding to the Rpt C-domain similarly[143]. The Nas2 and Nas6 subcomplexes first associate followed by addition of the Hsm3 subcomplex, Rpn13, and Rpn2[111]. The final addition involves association of Rpn10 which allows the fully assembled base and lid to bind one another. For RP and CP to interact, these assembly chaperones must be expelled in order to free the C-terminal HbYX motifs for binding to the alpha ring. Data suggests that binding of ATP leads to conformational changes within the Rpt ring which weakens their interaction with the assembly chaperones leading to their release[144]. Moreover, association of the lid (specifically Rpn5) and the base induce additional conformational changes to Rpt3 that induces release of Nas6[145].

Figure 1-5 – Assembly of the regulatory particle base subcomplex

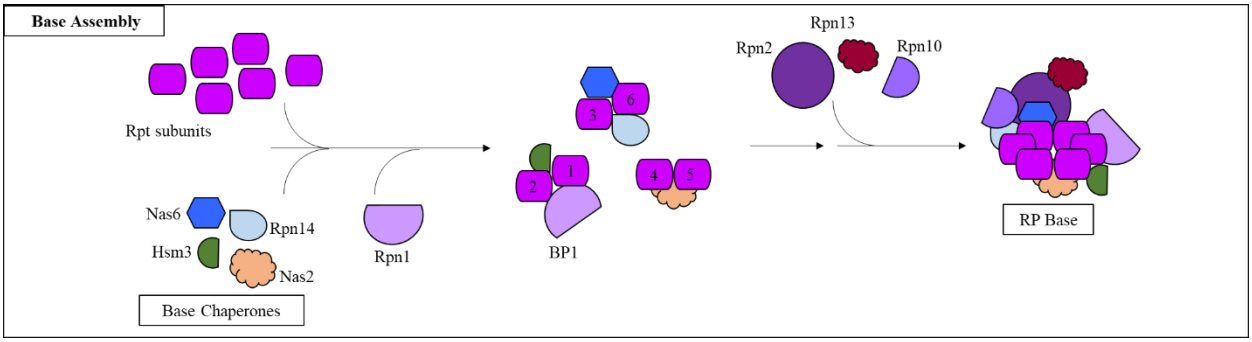

The regulatory particle is assembled first as two subcomplexes, the lid and the base. Base assembly involves the formation of three Rpt dimers using four external chaperones: Hsm3, Nas2, Nas6, and Rpn14. Rpt:chaperone complexes that form include Nas2-Rpt5-Rpt4, Rpn14-Rpt6-Rpt3-Nas6, and Hsm3-Rpt1-Rpt2-Rpn1 (BP1). The Nas2 and Nas6 subcomplexes form first followed by the Hsm3 subcomplex to form a six membered ring with bound chaperones. Ring formation is followed by the addition of Rpn13, Rpn2 and finally Rpn10 which aides in lid-base interactions and RP completion. Binding of ATP is thought to induce conformational changes that allow for chaperone release and binding to the core particle. Adapted from (159).

Proteasome Intrinsic Ubiquitin Receptors

The proteasome is able to degrade substrates with the help of both intrinsic and extrinsic ubiquitin receptors that recognize and bind polyubiquitinated substrates. Intrinsic ubiquitin receptors include proteasome subunits Rpn1, Rpn10, and Rpn13. Rpn1 contains a T1 site responsible for binding ubiquitin and ubiquitin-like (UBL) domains. Its T2 site is a UBL binding site that binds the UBL domain of extrinsic receptors and Ubp6, a deubiquitinating enzyme that aides in disassembling substrate ubiquitin chains[146]. Rpn13 contains a pleckstrin-homology domain-like fold allowing Rpn13 to bind Rpn2 and ubiquitin chains with high affinity[147,148]. While not part of the lid or base, Rpn10 is the third intrinsic ubiquitin receptor of the proteasome and can contain one or more highly flexible ubiquitin-interacting motifs [149]. Loss of Rpn10 destabilizes the regulatory particle indicating its importance in lid-base interactions[150]. Each of these intrinsic receptors can bind the ubiquitin-like domain of extrinsic ubiquitin receptor such as Dsk2, Ddi1 and Rad23. These extrinsic receptors also contain a ubiquitin-associated domain to bind ubiquitinated substrates and shuttle them to the intrinsic ubiquitin receptors[151,152].

Deubiquitinase Activity of the RP

The lid consists of nine subunits, Rpn5, Rpn6, Rpn7, Rpn8, Rpn9, Rpn11, Rpn12, Rpn3, and Rpn15 (Sem1)[150]. Six of these subunits contain PCI domains (Rpn3, Rpn5-7, Rpn9, and Rpn12) while two, Rpn11 and Rpn8, contain MPN domains. The proteasome ubiquitin receptors bind ubiquitinated substrates which can then be translocated through the narrow translocation

channel of the Rpt base and into the core particle for degradation. Due to the narrowness of the channel the attached ubiquitin tag interferes with translocation and must be removed by the only essential deubiquitinating subunit of the proteasome, Rpn11[153,154]. Rpn11 is a Zn^{2+} metalloprotease part of the MPN- and JAMM family of proteins. The aspartate and histidine residues of the JAMM motif (EX_nHS/THX_7SXXD) within the JAMM domain of these proteases (along with a water molecule) coordinates the Zn^{2+} ion[153]. A glutamate residue within the active site hydrogen bonds with the water molecule whose purpose is to initiate the catalytic mechanism to break the isopeptide bond between the ubiquitin chain and the translocating substrate[153–155]. Extending from the MPN of Rpn11 are two loops, Ins-1 and Ins-2[156]. The Ins-1 loop changes conformation upon interaction with ubiquitin which switches Rpn11 into an active state[157]. This regulates Rpn11 activity and prevents deubiquitination of substrates prior to translocation initiation[157]. Ins-1 forms a β-hairpin in the active state and forms part of the active site groove that helps position the ubiquitin C-terminus in the active site of Rpn11 for cleavage[157].

As mentioned above, translocation between s1 and s4 requires multiple conformational rearrangements, of which, Rpn11 repositioning is vital. Rpn11 is positioned directly above the translocation channel following the commitment step of translocation. This repositioning shifts Rpn11 closer to the site of substrate entry so as substrates are translocated through the channel, Rpn11 is positioned to remove the ubiquitin chain. The mechanical force exerted on the substrate by the ATPase ring is hypothesized to increase the rate of deubiquitination by forcing the Ins-1 loop of Rpn11 into the active state[158]. As the N-ring pulls the substrate through the translocation channel, the isopeptide bond between substrates and ubiquitin is forced into the Rpn11 active site where the Ins-1 loop folds over the active site to help stabilize the ubiquitin moiety for cleavage[159].

Lid Assembly

In vitro studies indicate the lid self assembles through the formation of a helical bundle between the PCI and MPN containing subunits of the lid (Fig. 1.6)[160]. Each of these subunits have one or more C-terminal helices that interact to form a helical bundle[160,161]. Dimerization of the MPN domains of Rpn11 and Rpn8 begin assembly followed by incorporation of Rpn9 and Rpn5 through interactions of their C-terminal helices with the Rpn8 helix. Rpn9 forms interactions with Rpn8 to help maintain the inactive state of the Rpn11/Rpn8 dimer. Rpn5

binding is more central in maintaining the inactive conformation as it binds directly to the Ins-1 loop and aids in blocking the active site of Rpn11. In addition, asparagine 275 of Rpn5 coordinates the Zn^{2+} ion of Rpn11 to inhibit its catalytic activity[158]. Next, Rpn6 assembles into the nascent lid complex and its binding is stabilized through interactions of its PCI domain with that of Rpn5. While the PCI domains form interactions between subunits, it seems that assembly is driven by interactions of the C-terminal helices. Addition of Rpn6 is followed by incorporation of the Rpn7/Rpn3/Sem1 complex which forms independently of the rest of the lid. The final subunit to bind is Rpn12 which acts like assembly switch that allows for incorporation of the lid into the proteasome.

Figure 1-6 – Assembly of the regulatory particle lid subcomplex

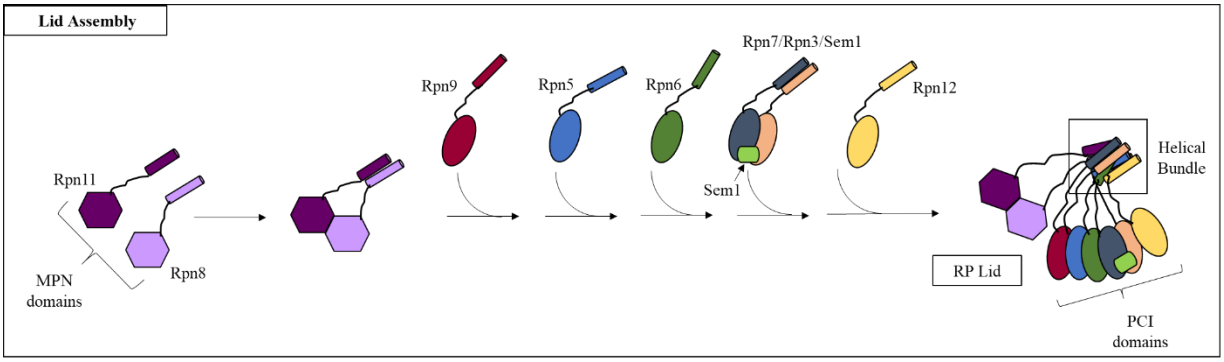

The lid subcomplex of the regulatory particle is composed of nine subunits which include Rpn5, Rpn6, Rpn7, Rpn8, Rpn9, Rpn11, Rpn12, Rpn3, and Rpn15 (Sem1). Rpn11 and Rpn8 contain N-terminal MPN domains while the other subunits, apart from Sem1, contain N-terminal PCI domains all of which aid in lid assembly. Secondly, these subunits contain C-terminal alpha helices which interact to form a helical bundle that is required for lid-base interactions. Lid assembly begins with dimerization of the MPN domains of Rpn11 and Rpn8. This follows incorporation of Rpn9 and Rpn5 through interactions between their C-terminal α helices and the helix of Rpn8. Next, Rpn6 incorporates into the nascent lid complex and is stabilized through interactions between its PCI domain and that of Rpn5. This is followed by incorporation of the Rpn7/Rpn3/Sem1 complex which assembles independently of the rest of the lid. Finally, incorporation of Rpn12 completes lid assembly. Binding of Rpn12, and its C-terminal helix, assesses lid assembly to ensure that all other lid subunit helices have been incorporated. Failure to incorporate all subunits prevents Rpn12 binding which further prevents lid-base interactions. Adapted from (159).

Deletion of any C-terminal helix becomes sensitive to the incorporation of Rpn12. While the Rpn12 alpha helix interacts directly with the helix of Rpn9, it's possible that it can sense a lack of other bundle subunits through conformational changes[160]. Binding of Rpn12 is essential for incorporation of the fully assembled lid[162]. Once the lid incorporates into the proteasome, the Rpn11/Rpn8 dimer rotates relieving its inhibitory interactions with Rpn5 and Rpn9. The incorporation into the proteasome leads to interactions between the Rpn11 Ins-2 loop and Rpn2 which can help stabilize the open state of the Rpn11 active site[158,163].

Proteasome Associated Proteins

Blm10/PA200

In addition to the regulatory and core particle subunits, other proteasome activators exist that bind to the same interface as RP. Interestingly, as binding between these activators is similar, hybrid proteasomes can form where two different activators can be bound to the same core particle. One of these activators is a 200 kDa protein known as Blm10 (PA200 in mammalian cells) which consists of three structural elements. First, there are multiple heat repeats that create an overall curved structure of the protein. Second, Blm10 contains a bromodomain-like region that was suggested to play a role in the degradation of histones[164]. Lastly, Blm10 contains a YYX motif at its C-terminus that allows it to bind to the α5-α6 pocket similarly to the CP chaperone dimer Pba1/2[107,164,165].

Unlike the regulatory particle, Blm10 cannot recognize ubiquitin; therefore, it is unlikely to be directly involved in the degradation of the proteins that are marked for degradation by a ubiquitin chain. It also cannot hydrolyze ATP and utilize that energy to unfold and translocate proteins into the core particle and thus is unlikely to degrade proteins with stable tertiary structures. Due to this inability, one proposed function for Blm10 is in the degradation of small peptides or unstructured proteins like tau[165–167]. In addition, multiple other functions for Blm10 have been proposed including chromatin remodeling, DNA repair, spermatogenesis, histone degradation, nuclear import, proteasome maturation and mitochondrial maintenance[164,166,168–173]. While multiple functions have been proposed, below are some examples discussed in more detail.

Blm10 was shown to associate with mature CP as well as immature CP, which gave rise to its role in core particle maturation as loss of Blm10 was shown to accelerate core particle maturation. While this suggested a role in preventing premature maturation of the core particle, no other assembly defects were identified[168]. Moreover, as an RP mutant that could not bind CP produced the same outcome, it was later suggested that presence of an activator could accelerate maturation.

Another proposed function of Blm10 involves its bromo-like domain which was thought to be involved in histone degradation. While this domain was suggested to bind acetylated histones in a hydrophobic pocket requiring Phe1676, Phe1717, and Asn1716, recent cryo-EM work did not identify this domain and showed Phe1676 was buried in the structure and was not

available for binding[164,174]. However, the structure did reveal non-protein densities mapped to inositol phosphates that are known to be involved in binding and regulating class I histone deacetylase activity[174]. While this link between inositol phosphate and histones could support a role for Blm10 being involved in histone degradation, more work is needed to confirm a role in this process.

Lastly, Blm10 was suspected to play a role in nucleocytoplasmic trafficking of the core particle following nutrient depletion. Under these particular stress conditions, like stationary phase or glucose starvation, the proteasome is exported from the nucleus and forms granules in the cytoplasm called proteasome storage granules (PSGs)[175]. Blm10 was suggested to play a role in targeting CP to these granules as well as importing the core particle back into the nucleus following the addition of nutrients[173].

Most of these papers involving Blm10 attempt to elucidate a mechanism of action; however, we wondered how Blm10 levels affect the proteasome landscape and subsequent cell viability in response to stress conditions. Blm10 and the regulatory particle both bind to the alpha ring of the core particle indicating a potential competition for binding. Normal levels of Blm10 are quite low compared to RP thus resulting in large numbers of 26S proteasomes and low numbers of Blm10 associated CPs. Chapter 2 looks at how changing the levels of Blm10 affect the proteasome under stress conditions and whether proteasome localization and fate are affected if RP and CP are dissociated. In addition, this question led to an interest in understanding if Blm10 is affected similarly to the core particle under stress conditions like nitrogen and carbon starvation.

We, and others, have shown that the 26S proteasome is selectively targeted for degradation through autophagy, but it remains unclear how Blm10 is affected by these same conditions[176,177]. Moreover, while Blm10 was shown by one group to be involved in CP sequestration in proteasome storage granules and nuclear reentry following quiescence, our lab shows contradictory data including Blm10 in its own granules, independent of the core particle.

Ecm29/KIAA0368

While most proteasome associated proteins are found to bind either the core particle or the regulatory particle, Ecm29 (KIAA0368 in mammalian cells) has been shown to bind both Rpt5 of the regulatory particle and α7 of the core particle[178,179]. Its ability to bind both subcomplexes was initially thought to stabilize the 26S proteasome[180]. Ecm29 is 210 kDa with

29 predicted HEAT repeats[181], and like Blm10, its binding to the proteasome has been reported to result in proteasome remodeling, inhibition, and localization to membranes[178,182–186]. For example, Ecm29 is proposed to be a quality control factor due to its ability to recognize, bind, and inhibit the activity of mutant proteasomes [178,187,188]. Ecm29 can inhibit aberrant proteasomes by inducing closure of the translocation channel and inhibiting the ATPase activity of the Rpt ring[186,187]. Furthermore, it has been shown to disrupt the interaction between RP and CP under oxidative stress further suggesting a role in quality control[183].

Nuclear Import/Export

While the majority of proteasomes are found in the nucleus of yeast and mammalian cells, a subset can also be found in the cytoplasm as well as attached to organelles like the ER[189,190]. Fully assembled proteasomes have a width 15-20 nm and are thus expected to be able to pass through the nuclear pore complex (39 nm diameter), at least longitudinally[191–193]. However, multiple studies indicate assembly intermediates and subcomplexes are imported which suggests assembly also occurs inside the nucleus. For nuclear import, immature core particles as well as the base subcomplex are bound by Importin αβ (Srp1/Kap95) through nuclear localization signals (NLSs) on various subunits including α1, α4, α5, Rpt2 and Rpn2[194,195]. None of the lid subunits encode a recognizable NLS so import is dependent on the importin Sts1/Cut8. Sts1 contains an NLS and upon binding to the lid subunit Rpn11 induces import of the whole complex into the nucleus[195,196].

In logarithmically growing cells, nuclear proteasomes can be exported from the nucleus under certain stress conditions such as nitrogen starvation, carbon starvation, and quiescence. Upon nitrogen starvation, proteasomes are exported from the nucleus and are selectively targeted for degradation through autophagy[176,177]. In comparison, carbon starvation induces nuclear export of proteasomes and subsequent delivery to proteasome storage granules (PSGs) in the cytoplasm[175,197]. While the function of these granules is unknown, the name suggests a role in housing proteasomes during nutrient depletion when cell survival relies on conserving vital nutrients rather than wasting them on protein degradation. Nutrient addition results in rapid dissolving of these granules and reentry of proteasomes into the nucleus[173]. The proteasome associated factor Blm10 was shown to be involved in core particle sequestration into granules as well as reentry into the nucleus following nutrient enrichment[173]. Moreover, as Blm10 binds directly to the core particle at the same interface as RP, an alternate import mechanism must

exist for the regulatory particle. A quiescence specific proteasome regulator, Spg5, is involved in proteasome assembly during nutrient deprivation. Loss of Spg5 showed defects in RP sequestration into PSGs which could indicate it has a role in reentry of the RP as well[198,199].

With the multitude of knowledge about nuclear import of proteasomes following synthesis a lack of understanding in how proteasomes are exported from the nucleus under stress conditions exists. Chapter 3 focuses on determining a mechanism for how proteasomes are exported from the nucleus. Our work attempts at identifying potential nuclear export sites on proteasome subunits as well as export factors that recognize, bind, and facilitate exit of the proteasome. Overall, this work provides additional knowledge about proteasome dynamics upon stress conditions as well as a basic understanding of how large complexes move between various intracellular compartments.

References

1. Powers, E. T., Morimoto, R. I., Dillin, A., Kelly, J. W. & Balch, W. E. Biological and Chemical Approaches to Diseases of Proteostasis Deficiency. *Annu. Rev. Biochem.* 78, 959–991 (2009).

2. Krstic, D. & Knuesel, I. Deciphering the mechanism underlying late-onset Alzheimer disease. *Nat. Rev. Neurol.* 9, 25–34 (2013).

3. Labbadia, J. & Morimoto, R. I. Huntington's disease: underlying molecular mechanisms and emerging concepts. *Trends Biochem. Sci.* 38, 378–85 (2013).

4. Trinh, J. & Farrer, M. Advances in the genetics of Parkinson disease. *Nat. Rev. Neurol.* 9, 445–454 (2013).

5. Uversky, V. N., Oldfield, C. J. & Dunker, A. K. Intrinsically Disordered Proteins in Human Diseases: Introducing the D 2 Concept . *Annu. Rev. Biophys.* 37, 215–246 (2008).

6. Gregersen, N., Bross, P., Vang, S. & Christensen, J. H. Protein Misfolding and Human Disease. *Annu. Rev. Genomics Hum. Genet.* 7, 103–124 (2006).

7. Finley, D. Recognition and processing of ubiquitin-protein conjugates by the proteasome. *Annu. Rev. Biochem.* 78, 477–513 (2009).

8. Skach, W. R. CFTR: new members join the fold. *Cell* 127, 673–5 (2006).

9. Hetz, C. The unfolded protein response: Controlling cell fate decisions under ER stress and beyond. *Nature Reviews Molecular Cell Biology* 13, 89–102 (2012).

10. Kroemer, G., Mariño, G. & Levine, B. Autophagy and the Integrated Stress Response. *Molecular Cell* 40, 280–293 (2010).

11. Kamada, Y. *et al.* Tor-mediated induction of autophagy via an Apg1 protein kinase complex. *J. Cell Biol.* 150, 1507–13 (2000).

12. Kamada, Y. *et al.* Tor directly controls the Atg1 kinase complex to regulate autophagy. *Mol. Cell. Biol.* 30, 1049–58 (2010).

13. Kabeya, Y. *et al.* Atg17 functions in cooperation with Atg1 and Atg13 in yeast autophagy. *Mol. Biol. Cell* 16, 2544–53 (2005).

14. Kabeya, Y. *et al.* Characterization of the Atg17–Atg29–Atg31 complex specifically required for starvation-induced autophagy in *Saccharomyces cerevisiae*. *Biochem. Biophys. Res. Commun.* 389, 612–615 (2009).

15. Thomas, L. L., Joiner, A. M. N. & Fromme, J. C. The TRAPPIII complex activates the GTPase Ypt1 (Rab1) in the secretory pathway. *J. Cell Biol.* 217, 283–298 (2018).

16. Kihara, A., Noda, T., Ishihara, N. & Ohsumi, Y. Two distinct Vps34 phosphatidylinositol 3-kinase complexes function in autophagy and carboxypeptidase Y sorting in *Saccharomyces cerevisiae*. *J. Cell Biol.* 152, 519–30 (2001).

17. Tanida, I. *et al.* Apg7p/Cvt2p: A novel protein-activating enzyme essential for autophagy. *Mol. Biol. Cell* 10, 1367–79 (1999).

18. Shintani, T. *et al.* Apg10p, a novel protein-conjugating enzyme essential for autophagy in yeast. *EMBO J.* 18, 5234–41 (1999).

19. Mizushima, N. *et al.* A protein conjugation system essential for autophagy. *Nature* 395, 395–398 (1998).

20. McEwan, D. G. & Dikic, I. The Three Musketeers of Autophagy: Phosphorylation, ubiquitylation and acetylation. *Trends in Cell Biology* 21, 195–201 (2011).

21. Hanada, T. *et al.* The Atg12-Atg5 conjugate has a novel E3-like activity for protein lipidation in autophagy. *J. Biol. Chem.* 282, 37298–37302 (2007).

22. Cao, Y., Cheong, H., Song, H. & Klionsky, D. J. In vivo reconstitution of autophagy in *Saccharomyces cerevisiae*. *J. Cell Biol.* 182, 703–713 (2008).

23. Kaiser, S. E. *et al.* Noncanonical E2 recruitment by the autophagy E1 revealed by Atg7-Atg3 and Atg7-Atg10 structures. *Nat. Struct. Mol. Biol.* 19, 1242–1249 (2012).

24. Noda, N. N., Fujioka, Y., Hanada, T., Ohsumi, Y. & Inagaki, F. Structure of the Atg12-Atg5 conjugate reveals a platform for stimulating Atg8-PE conjugation. *EMBO Rep.* 14, 206–211 (2013).

25. Otomo, C., Metlagel, Z., Takaesu, G. & Otomo, T. Structure of the human ATG12~ATG5 conjugate required for LC3 lipidation in autophagy. *Nat. Struct. Mol. Biol.* 20, 59–66 (2013).

26. Romanov, J. *et al.* Mechanism and functions of membrane binding by the Atg5-Atg12/Atg16 complex during autophagosome formation. *EMBO J.* 31, 4304–4317 (2012).

27. Ichimura, Y. *et al.* A ubiquitin-like system mediates protein lipidation. *Nature* 408, 488–492 (2000).

28. Kirisako, T. *et al.* The reversible modification regulates the membrane-binding state of Apg8/Aut7 essential for autophagy and the cytoplasm to vacuole targeting pathway. *J. Cell Biol.* 151, 263–76 (2000).

29. Noda, N. N., Ohsumi, Y. & Inagaki, F. Atg8-family interacting motif crucial for selective autophagy. *FEBS Lett.* 584, 1379–1385 (2010).

30. Klionsky, D. J. & Eskelinen, E.-L. The vacuole vs. the lysosome. *Autophagy* 10, 185–187 (2014).

31. Baba, M., Takeshige, K., Baba, N. & Ohsumi, Y. Ultrastructural analysis of the autophagic process in yeast: Detection of autophagosomes and their characterization. *J. Cell Biol.* 124, 903–913 (1994).

32. Delorme-Axford, E., Guimaraes, R. S., Reggiori, F. & Klionsky, D. J. The yeast *Saccharomyces cerevisiae*: An overview of methods to study autophagy progression. *Methods* 75, 3–12 (2015).

33. Budovskaya, Y. V, Stephan, J. S., Reggiori, F., Klionsky, D. J. & Herman, P. K. The Ras/cAMP-dependent protein kinase signaling pathway regulates an early step of the autophagy process in *Saccharomyces cerevisiae*. *J. Biol. Chem.* 279, 20663–71 (2004).

34. Furuta, S., Hidaka, E., Ogata, A., Yokota, S. & Kamata, T. Ras is involved in the negative control of autophagy through the class I PI3-kinase. *Oncogene* 23, 3898–3904 (2004).

35. Mavrakis, M., Lippincott-Schwartz, J., Stratakis, C. A. & Bossis, I. Depletion of type IA regulatory subunit (RIα) of protein kinase A (PKA) in mammalian cells and tissues activates mTOR and causes autophagic deficiency. *Hum. Mol. Genet.* 15, 2962–2971 (2006).

36. Schmelzle, T., Beck, T., Martin, D. E. & Hall, M. N. Activation of the RAS/cyclic AMP pathway suppresses a TOR deficiency in yeast. *Mol. Cell. Biol.* 24, 338–51 (2004).

37. Yorimitsu, T., Zaman, S., Broach, J. R. & Klionsky, D. J. Protein kinase A and Sch9 cooperatively regulate induction of autophagy in *Saccharomyces cerevisiae*. *Mol. Biol. Cell* 18, 4180–9 (2007).

38. Thevelein, J. M. & de Winde, J. H. Novel sensing mechanisms and targets for the cAMP-protein kinase A pathway in the yeast *Saccharomyces cerevisiae*. *Mol. Microbiol.* 33, 904–918 (1999).

39. Zurita-Martinez, S. A. & Cardenas, M. E. Tor and Cyclic AMP-Protein Kinase A: Two Parallel Pathways Regulating Expression of Genes Required for Cell Growth. *Eukaryot. Cell* 4, 63 (2005).

40. Massey, A. C., Zhang, C. & Cuervo, A. M. Chaperone-Mediated Autophagy in Aging and Disease. *Curr. Top. Dev. Biol.* 73, 205–235 (2006).

41. Jackson, M. P. & Hewitt, E. W. Cellular proteostasis: degradation of misfolded proteins by lysosomes. *Essays Biochem.* 60, 173–180 (2016).

42. Cuervo, A. M. Chaperone-mediated autophagy: Selectivity pays off. *Trends in Endocrinology and Metabolism* 21, 142–150 (2010).

43. Li, W., Li, J. & Bao, J. Microautophagy: lesser-known self-eating. *Cell. Mol. Life Sci.* 69, 1125–1136 (2012).

44. Parzych, K. R. & Klionsky, D. J. An overview of autophagy: Morphology, mechanism, and regulation. *Antioxidants and Redox Signaling* 20, 460–473 (2014).

45. Haglund, K., Di Fiore, P. P. & Dikic, I. Distinct monoubiquitin signals in receptor endocytosis. *Trends Biochem. Sci.* 28, 598–604 (2003).

46. Hicke, L. & Dunn, R. Regulation of Membrane Protein Transport by Ubiquitin and Ubiquitin-Binding Proteins. *Annu. Rev. Cell Dev. Biol.* 19, 141–172 (2003).

47. Swatek, K. N. & Komander, D. Ubiquitin modifications. *Cell Research* 26, 399–422 (2016).

48. Yau, R. & Rape, M. The increasing complexity of the ubiquitin code. *Nature Cell Biology* 18, 579–586 (2016).

49. Husnjak, K. & Dikic, I. Ubiquitin-Binding Proteins: Decoders of Ubiquitin-Mediated Cellular Functions. *Annu. Rev. Biochem.* 81, 291–322 (2012).

50. Komander, D. & Rape, M. The Ubiquitin Code. *Annu. Rev. Biochem.* 81, 203–229 (2012).

51. Kwon, Y. T. & Ciechanover, A. The Ubiquitin Code in the Ubiquitin-Proteasome System and Autophagy. *Trends in Biochemical Sciences* 42, 873–886 (2017).

52. Haas, A. L., Warms, J. V. B. & Rose, I. A. Ubiquitin adenylate: structure and role in ubiquitin activation. *Biochemistry* 22, 4388–4394 (1983).

53. Hershko, A., Heller, H., Elias, S. & Ciechanover, A. Components of Ubiquitin-Protein Ligase System: Resolution, Affinity Purification, and Role in Protein Breakdown. *J. Biol. Chem.* 258, 8206–8214 (1983).

54. Haas, A. L., Bright, P. M. & Jackson, V. E. Functional Diversity among Putative E2 Isozymes in the Mechanism of Ubiquitin-Histone Ligation. *J. Biol. Chem.* 263, 13268–13275 (1988).

55. Pickart, C. M., Kasperek, E. M., Beal, R. & Kim, A. Substrate properties of site-specific mutant ubiquitin protein (G76A) reveal unexpected mechanistic features of ubiquitin-activating enzyme (E1). *J. Biol. Chem.* 269, 7115–23 (1994).

56. Lois, L. M. & Lima, C. D. Structures of the SUMO E1 provide mechanistic insights into SUMO activation and E2 recruitment to E1. *EMBO J.* 24, 439–451 (2005).

57. Huang, D. T. *et al.* Basis for a ubiquitin-like protein thioester switch toggling E1-E2 affinity. *Nature* 445, 394–398 (2007).

58. Lee, I. & Schindelin, H. Structural Insights into E1-Catalyzed Ubiquitin Activation and Transfer to Conjugating Enzymes. *Cell* 134, 268–278 (2008).

59. Huang, L. *et al.* Structure of an E6AP-UbcH7 complex: insights into ubiquitination by the E2-E3 enzyme cascade. *Science* 286, 1321–6 (1999).

60. Metzger, M. B., Hristova, V. A. & Weissman, A. M. HECT and RING finger families of E3 ubiquitin ligases at a glance. *J. Cell Sci.* 125, 531–7 (2012).

61. Tasaki, T., Sriram, S. M., Park, K. S. & Kwon, Y. T. The N-End Rule Pathway. *Annu. Rev. Biochem.* 81, 261–289 (2012).

62. Balzi, E., Choder, M., Chen, W., Varshavsky, A. & Goffeau, A. Cloning and Functional Analysis of the Arginyl-tRNA-protein Transferase Gene ATE1 of *Saccharomyces cerevisiae*. *J. Biol. Chem.* 265, 7464–7471 (1990).

63. Kwon, Y. T., Kashina, A. S. & Varshavsky, A. Alternative splicing results in differential expression, activity, and localization of the two forms of arginyl-tRNA-protein transferase, a component of the N-end rule pathway. *Mol. Cell. Biol.* 19, 182–93 (1999).

64. Baker, R. T. & Varshavsky, A. Yeast N-terminal amidase. A new enzyme and component of the N-end rule pathway. *J. Biol. Chem.* 270, 12065–74 (1995).

65. Grigoryev, S. *et al.* A mouse amidase specific for N-terminal asparagine. The gene, the enzyme, and their function in the N-end rule pathway. *J. Biol. Chem.* 271, 28521–32 (1996).

66. Hwang, C.-S., Shemorry, A. & Varshavsky, A. N-Terminal Acetylation of Cellular Proteins Creates Specific Degradation Signals. *Science* 327, 973 (2010).

67. Polevoda, B. & Sherman, F. N-terminal Acetyltransferases and Sequence Requirements for N-terminal Acetylation of Eukaryotic Proteins. *J. Mol. Biol.* 325, 595–622 (2003).

68. Frottin, F. *et al.* The proteomics of N-terminal methionine cleavage. *Mol. Cell. Proteomics* 5, 2336–2349 (2006).

69. Tasaki, T. *et al.* A family of mammalian E3 ubiquitin ligases that contain the UBR box motif and recognize N-degrons. *Mol. Cell. Biol.* 25, 7120–36 (2005).

70. Tasaki, T. *et al.* The substrate recognition domains of the N-end rule pathway. *J. Biol. Chem.* 284, 1884–95 (2009).

71. Holt, L. J. Regulatory modules: Coupling protein stability to phopshoregulation during cell division. *FEBS Lett.* 586, 2773–2777 (2012).

72. Skowyra, D., Craig, K. L., Tyers, M., Elledge, S. J. & Harper, J. W. F-box proteins are receptors that recruit phosphorylated substrates to the SCF ubiquitin-ligase complex. *Cell* 91, 209–219 (1997).

73. Feldman, R. M. R., Correll, C. C., Kaplan, K. B. & Deshaies, R. J. A complex of Cdc4p, Skp1p, and Cdc53p/cullin catalyzes ubiquitination of the phosphorylated CDK inhibitor Sic1p. *Cell* 91, 221–230 (1997).

74. Schwob, E., Böhm, T., Mendenhall, M. D. & Nasmyth, K. The B-type cyclin kinase inhibitor p40SIC1 controls the G1 to S transition in *S. cerevisiae. Cell* 79, 233–244 (1994).

75. Chen, P. & Hochstrasser, M. Autocatalytic Subunit Processing Couples Active Site Formation in the 20S Proteasome to Completion of Assembly. *Cell* 86, 961–972 (1996).

76. Arendt, C. S. & Hochstrasser, M. Identification of the yeast 20S proteasome catalytic centers and subunit interactions required for active-site formation. *Proc. Natl. Acad. Sci.* 94, 7156–7161 (1997).

77. Heinemeyer, W., Fischer, M., Krimmer, T., Stachon, U. & Wolf, D. H. The Active Sites of the Eukaryotic 20 S Proteasome and Their Involvement in Subunit Precursor Processing. *J. Biol. Chem.* 272, 25200–25209 (1997).

78. Schmidtke, G. *et al.* Analysis of mammalian 20S proteasome biogenesis: the maturation of 1-subunits is an ordered two-step mechanism involving autocatalysis. *EMBO J.* 15, 6887–6898 (1996).

79. Huber, E. M. *et al.* A unified mechanism for proteolysis and autocatalytic activation in the 20S proteasome. *Nat. Commun.* 7, (2016).

80. Arendt, C. S. & Hochstrasser, M. Eukaryotic 20S proteasome catalytic subunit propeptides prevent active site inactivation by N-terminal acetylation and promote particle assembly. *EMBO J.* 18, 3575–3585 (1999).

81. Seemüller, E., Lupas, A. & Baumeister, W. Autocatalytic processing of the 20S proteasome. *Nature* 382, 468–470 (1996).

82. Khan, A. & James, M. Molecular mechanisms for the conversion of zymogens to active proteolytic enzymes. *Protein Sci.* 7, 815–836 (1998).

83. Huang, S. *et al.* Specificity of cotranslational amino-terminal processing of proteins in yeast. *Biochemistry* 26, 8242–8246 (1987).

84. Lee, F. J., Lin, L. W. & Smith, J. A. Model peptides reveal specificity of N alpha-acetyltransferase from *Saccharomyces cerevisiae*. *J. Biol. Chem.* 265, 11576–80 (1990).

85. Suppahia, A. *et al.* Cooperativity in Proteasome Core Particle Maturation. *iScience* 23, 101090 (2020).

86. Groll, M. *et al.* The catalytic sites of 20S proteasomes and their role in subunit maturation: a mutational and crystallographic study. *Proc. Natl. Acad. Sci. U. S. A.* 96, 10976–83 (1999).

87. Ditzel, L. *et al.* Conformational constraints for protein self-cleavage in the proteasome. *J. Mol. Biol.* 279, 1187–1191 (1998).

88. Takagi, K. *et al.* Pba3–Pba4 heterodimer acts as a molecular matchmaker in proteasome α-ring formation. *Biochem. Biophys. Res. Commun.* 450, 1110–1114 (2014).

89. Kusmierczyk, A. R., Kunjappu, M. J., Funakoshi, M. & Hochstrasser, M. A multimeric assembly factor controls the formation of alternative 20S proteasomes. *Nat. Struct. Mol. Biol.* 15, 237–244 (2008).

90. Yashiroda, H. *et al.* Crystal structure of a chaperone complex that contributes to the assembly of yeast 20S proteasomes. *Nat. Struct. Mol. Biol.* 15, (2008).

91. Velichutina, I., Connerly, P. L., Arendt, C. S., Li, X. & Hochstrasser, M. Plasticity in eucaryotic 20S proteasome ring assembly revealed by a subunit deletion in yeast. *EMBO Joumal* 23, 500–510 (2004).

92. Hirano, Y. *et al.* Dissecting β-ring assembly pathway of the mammalian 20S proteasome. *EMBO J.* 27, 2204–2213 (2008).

93. Ramos, P. C., Höckendorff, J., Johnson, E. S., Varshavsky, A. & Dohmen, R. J. Ump1p is required for proper maturation of the 20S proteasome and becomes its substrate upon completion of the assembly. *Cell* 92, 489–99 (1998).

94. Kusmierczyk, A. R., Kunjappu, M. J., Kim, R. Y. & Hochstrasser, M. A conserved 20S proteasome assembly factor requires a C-terminal HbYX motif for proteasomal precursor binding. *Nat. Struct. Mol. Biol.* 18, 622–629 (2011).

95. Stadtmueller, B. M. *et al.* Structure of a proteasome Pba1-Pba2 complex: implications for proteasome assembly, activation, and biological function. *J. Biol. Chem.* 287, 37371–82 (2012).

96. Hirano, Y. *et al.* A heterodimeric complex that promotes the assembly of mammalian 20S proteasomes. *Nature* 437, 1381–1385 (2005).

97. Wani, P. S., Rowland, M. A., Ondracek, A., Deeds, E. J. & Roelofs, J. Maturation of the proteasome core particle induces an affinity switch that controls regulatory particle association. *Nat. Commun.* 6, 6384 (2015).

98. Kock, M. *et al.* Proteasome assembly from 15S precursors involves major conformational changes and recycling of the Pba1-Pba2 chaperone. *Nat. Commun.* 6, 6123 (2015).

99. De, M. *et al.* Beta 2 subunit propeptides influence cooperative proteasome assembly. *J. Biol. Chem.* 278, 6153–9 (2003).

100. Ramos, P. C., Marques, A. J., London, M. K. & Dohmen, R. J. Role of C-terminal Extensions of Subunits β2 and β7 in Assembly and Activity of Eukaryotic Proteasomes. *J. Biol. Chem.* 279, 14323–14330 (2004).

101. Marques, A. J., Glanemann, C., Ramos, P. C. & Dohmen, R. J. The C-terminal extension of the beta7 subunit and activator complexes stabilize nascent 20 S proteasomes and promote their maturation. *J. Biol. Chem.* 282, 34869–76 (2007).

102. Li, X., Kusmierczyk, A. R., Wong, P., Emili, A. & Hochstrasser, M. b-Subunit appendages promote 20S proteasome assembly by overcoming an Ump1-dependent checkpoint. *EMBO J.* 26, 2339–2349 (2007).

103. Groll, M. *et al.* Structure of 0 205 proteasome from yeast at 2.4A resolution. *Nature* 386, 463–471 (1997).

104. Groll, M. *et al.* A gated channel into the proteasome core particle. *Nat. Struct. Biol.* 7, 1062–1067 (2000).

105. Groll, M. & Huber, R. Substrate access and processing by the 20S proteasome core particle. *Int. J. Biochem. Cell Biol.* 35, 606–616 (2003).

106. Smith, D. M. *et al.* Docking of the Proteasomal ATPases' Carboxyl Termini in the 20S Proteasome's α Ring Opens the Gate for Substrate Entry. *Mol. Cell* 27, 731–744 (2007).

107. Sadre-Bazzaz, K., Whitby, F. G., Robinson, H., Formosa, T. & Hill, C. P. Structure of a Blm10 Complex Reveals Common Mechanisms for Proteasome Binding and Gate Opening. *Mol. Cell* 37, 728–735 (2010).

108. Yu, Y. *et al.* Interactions of PAN's C-termini with archaeal 20S proteasome and implications for the eukaryotic proteasome-ATPase interactions. *EMBO J.* 29, 692–702 (2010).

109. Förster, A., Masters, E. I., Whitby, F. G. & Robinson, H. The 1.9 Å Structure of a Proteasome-11S Activator Complex and Implications for Proteasome-PAN/PA700 Interactions. *Mol. Cell* 18, 589–599 (2005).

110. Rabl, J. *et al.* Mechanism of gate opening in the 20S proteasome by the proteasomal ATPases. *Mol Cell* 30, 360–368 (2008).

111. Tomko, R. J., Funakoshi, M., Schneider, K., Wang, J. & Hochstrasser, M. Heterohexameric Ring Arrangement of the Eukaryotic Proteasomal ATPases: Implications for Proteasome Structure and Assembly. *Mol. Cell* 38, 393–403 (2010).

112. Nyquist, K. & Martin, A. Marching to the beat of the ring: polypeptide translocation by AAA+ proteases. *Trends Biochem. Sci.* 39, 53–60 (2014).

113. Zhang, F. *et al.* Mechanism of substrate unfolding and translocation by the regulatory particle of the proteasome from *Methanocaldococcus jannaschii*. *Mol Cell* 34, 485–496 (2009).

114. Djuranovic, S. *et al.* Structure and Activity of the N-Terminal Substrate Recognition Domains in Proteasomal ATPases. *Mol. Cell* 34, 580–590 (2009).

115. Beck, F. *et al.* Near-atomic resolution structural model of the yeast 26S proteasome. *Proc. Natl. Acad. Sci. U. S. A.* 109, 14870–14875 (2012).

116. Inobe, T. & Genmei, R. N-terminal coiled-coil structure of ATPase subunits of 26S proteasome is crucial for proteasome function. *PLoS One* 10, (2015).

117. Finley, D., Chen, X. & Walters, K. J. Gates, Channels, and Switches: Elements of the Proteasome Machine. *Trends Biochem. Sci.* 41, 77–93 (2016).

118. Bard, J. A. M. *et al.* Structure and Function of the 26S Proteasome. *Annu. Rev. Biochem.* 87, 697–724 (2018).

119. Walker, J. E., Saraste, M., Runswick, M. J. & Gay, N. J. Distantly related sequences in the α-and β-subunits of ATP synthase, myosin, kinases and other ATP-requiring enzymes and a common nucleotide binding fold. *EMBO Joumal* 945–951 (1982).

120. Story, R. The structure of the *E. coli* RecA protein monomer and polymer. *Nature* 355, 318–325 (1992).

121. Bell, C. E. Structure and mechanism of *Escherichia coli* RecA ATPase. *Mol. Microbiol.* 58, 358–366 (2005).

122. Ogura, T., Whiteheart, S. W. & Wilkinson, A. J. Conserved arginine residues implicated in ATP hydrolysis, nucleotide-sensing, and inter-subunit interactions in AAA and AAA+ ATPases. *Journal of Structural Biology* 146, 106–112 (2004).

123. Karata, K., Inagawa, T., Wilkinson, A. J., Tatsuta, T. & Ogura, T. Dissecting the Role of a Conserved Motif (the Second Region of Homology) in the AAA Family of ATPases. *J. Biol. Chem.* 274, 26225–26232 (1999).

124. Martin, A., Baker, T. A. & Sauer, R. T. Pore loops of the AAA+ ClpX machine grip substrates to drive translocation and unfolding. *Nat. Struct. Mol. Biol.* 15, 1147–51 (2008).

125. Maillard, R. A. *et al.* ClpX(P) generates mechanical force to unfold and translocate its protein substrates. *Cell* 145, 459–469 (2011).

126. Aubin-Tam, M. E., Olivares, A. O., Sauer, R. T., Baker, T. A. & Lang, M. J. Single-molecule protein unfolding and translocation by an ATP-fueled proteolytic machine. *Cell* 145, 257–267 (2011).

127. Unverdorben, P. *et al.* Deep classification of a large cryo-EM dataset defines the conformational landscape of the 26S proteasome. *Proc. Natl. Acad. Sci. U. S. A.* 111, 5544–9 (2014).

128. Wehmer, M. *et al.* Structural insights into the functional cycle of the ATPase module of the 26S proteasome. *Proc. Natl. Acad. Sci. U. S. A.* 114, 1305–1310 (2017).

129. Gates, S. N. *et al.* Ratchet-like polypeptide translocation mechanism of the AAA+ disaggregase Hsp104. *Science (80).* 357, 273–279 (2017).

130. Glynn, S. E., Martin, A., Nager, A. R., Baker, T. A. & Sauer, R. T. Structures of Asymmetric ClpX Hexamers Reveal Nucleotide-Dependent Motions in a AAA+ Protein-Unfolding Machine. *Cell* 139, 744–756 (2009).

131. Thomsen, N. D. & Berger, J. M. Running in Reverse: The Structural Basis for Translocation Polarity in Hexameric Helicases. *Cell* 139, 523–534 (2009).

132. Lander, G. C. *et al.* Complete subunit architecture of the proteasome regulatory particle. *Nature* 482, 186–191 (2012).

133. Matyskiela, M. E., Lander, G. C. & Martin, A. Conformational switching of the 26S proteasome enables substrate degradation. *Nat. Publ. Gr.* 20, 781–788 (2013).

134. Förster, F., Unverdorben, P., Śledź, P. & Baumeister, W. Unveiling the Long-Held Secrets of the 26S Proteasome. *Structure* 21, 1551–1562 (2013).

135. Chen, S. *et al.* Structural basis for dynamic regulation of the human 26S proteasome. *Proc. Natl. Acad. Sci. U. S. A.* 113, 12991–12996 (2016).

136. Kaneko, T. *et al.* Assembly Pathway of the Mammalian Proteasome Base Subcomplex Is Mediated by Multiple Specific Chaperones. *Cell* 137, 914–925 (2009).

137. Funakoshi, M., Tomko, R. J., Kobayashi, H. & Hochstrasser, M. Multiple Assembly Chaperones Govern Biogenesis of the Proteasome Regulatory Particle Base. *Cell* 137, 887–899 (2009).

138. Le Tallec, B., Barrault, M.-B., Guérois, R., Carré, T. & Peyroche, A. Hsm3/S5b Participates in the Assembly Pathway of the 19S Regulatory Particle of the Proteasome. *Mol. Cell* 33, 389–399 (2009).

139. Roelofs, J. *et al.* Chaperone-mediated pathway of proteasome regulatory particle assembly. *Nature* 459, 861–865 (2009).

140. Saeki, Y., Toh-e, A., Kudo, T., Kawamura, H. & Tanaka, K. Multiple Proteasome-Interacting Proteins Assist the Assembly of the Yeast 19S Regulatory Particle. *Cell* 137, 900–913 (2009).

141. Hanssum, A. *et al.* An Inducible Chaperone Adapts Proteasome Assembly to Stress. *Mol. Cell* 55, 566–577 (2014).

142. Marshall, R. S. & Vierstra, R. D. Dynamic regulation of the 26S proteasome: From synthesis to degradation. *Frontiers in Molecular Biosciences* 6, (2019).

143. Bedford, L., Paine, S., Sheppard, P. W., Mayer, R. J. & Roelofs, J. Assembly, structure, and function of the 26S proteasome. *Trends Cell Biol.* 20, 391–401 (2010).

144. Park, S. *et al.* Reconfiguration of the proteasome during chaperone-mediated assembly. *Nature* 497, 512–516 (2013).

145. Nemec, A. A., Peterson, A. K., Warnock, J. L., Reed, R. G. & Tomko, R. J. An Allosteric Interaction Network Promotes Conformation State-Dependent Eviction of the Nas6 Assembly Chaperone from Nascent 26S Proteasomes. *Cell Rep.* 26, 483–495 (2019).

146. Shi, Y. *et al.* Rpn1 provides adjacent receptor sites for substrate binding and deubiquitination by the proteasome. *Science (80-.).* 351, 9421-1-9421–10 (2016).

147. Schreiner, P. *et al.* Ubiquitin docking at the proteasome via a novel PH domain interaction. *Nature* 453, 548–552 (2008).

148. Husnjak, K. *et al.* Proteasome subunit Rpn13 is a novel ubiquitin receptor. *Nature* 453, 481–488 (2008).

149. Zhang, D. *et al.* Together, Rpn10 and Dsk2 Can Serve as a Polyubiquitin Chain-Length Sensor. *Mol. Cell* 36, 1018–1033 (2009).

150. Glickman, M. H. *et al.* A subcomplex of the proteasome regulatory particle required for ubiquitin-conjugate degradation and related to the COP9-signalosome and eIF3. *Cell* 94, 615–23 (1998).

151. Raasi, S., Varadan, R., Fushman, D. & Pickart, C. M. Diverse polyubiquitin interaction properties of ubiquitin-associated domains. *Nat. Struct. Mol. Biol.* 12, 708–714 (2005).

152. Spyracopoulos, L. The Proteasome: More Than a Means to an End. *Structure* 24, 1221–1223 (2016).

153. Verma, R. Role of Rpn11 metalloprotease in deubiquitination and degradation by the 26S proteasome. *Science (80-.).* 298, 611–615 (2002).

154. Yao, T. & Cohen, R. A cryptic protease couples deubiquitination and degradation by the proteasome. *Nature* 419, 403–407 (2002).

155. Maytal-Kivity, V., Reis, N., Hofmann, K. & Glickman, M. H. MPN+, a putative catalytic motif found in a subset of MPN domain proteins from eukaryotes and prokaryotes, is critical for Rpn11 function. *BMC Biochem.* 3, 1–12 (2002).

156. Sato, Y. *et al.* Structural basis for specific cleavage of Lys 63-linked polyubiquitin chains. *Nature* 455, 358–362 (2008).

157. Worden, E. J., Dong, K. C. & Martin, A. An AAA Motor-Driven Mechanical Switch in Rpn11 Controls Deubiquitination at the 26S Proteasome. *Mol. Cell* 67, 799–811 (2017).

158. Dambacher, C. M., Worden, E. J., Herzik, M. A., Martin, A. & Lander, G. C. Atomic structure of the 26S proteasome lid reveals the mechanism of deubiquitinase inhibition. *Elife* 5, e13027 (2016).

159. Worden, E. J., Padovani, C. & Martin, A. Structure of the Rpn11-Rpn8 dimer reveals mechanisms of substrate deubiquitination during proteasomal degradation. *Nat. Struct. Mol. Biol.* 21, 220–227 (2014).

160. Estrin, E., Lopez-Blanco, J. R., Chacón, P. & Martin, A. Formation of an Intricate Helical Bundle Dictates the Assembly of the 26S Proteasome Lid. *Structure* 21, 1624–1635 (2013).

161. Beck, F. *et al.* Near-atomic resolution structural model of the yeast 26S proteasome. *Proc. Natl. Acad. Sci.* 109, 14870–14875 (2012).

162. Tomko, R. J. & Hochstrasser, M. Incorporation of the Rpn12 Subunit Couples Completion of Proteasome Regulatory Particle Lid Assembly to Lid-Base Joining. *Mol. Cell* 44, 907–917 (2011).

163. Pathare, G. R. *et al.* Crystal structure of the proteasomal deubiquitylation module Rpn8-Rpn11. *Proc. Natl. Acad. Sci. U. S. A.* 111, 2984–9 (2014).

164. Qian, M. X. *et al.* Acetylation-mediated proteasomal degradation of core histones during DNA repair and spermatogenesis. *Cell* 153, 1012–1024 (2013).

165. Dange, T. *et al.* Blm10 Protein Promotes Proteasomal Substrate Turnover by an Active Gating Mechanism. *J. Biol. Chem.* 286, 42830–42839 (2011).

166. Ustrell, V., Hoffman, L., Pratt, G. & Rechsteiner, M. PA200, a nuclear proteasome activator involved in DNA repair. *EMBO J.* 21, 3516–25 (2002).

167. Ustrell, V., Pratt, G., Gorbea, C. & Rechsteiner, M. Purification and Assay of Proteasome Activator PA200. in *Methods in enzymology* 398, 321–329 (2005).

168. Fehlker, M., Wendler, P., Lehmann, A. & Enenkel, C. Blm3 is part of nascent proteasomes and is involved in a late stage of nuclear proteasome assembly. *EMBO Rep.* 4, 959–963 (2003).

169. Khor, B. *et al.* Proteasome Activator PA200 Is Required for Normal Spermatogenesis. *Mol. Cell. Biol.* 26, 2999–3007 (2006).

170. Blickwedehl, J. *et al.* Role for proteasome activator PA200 and postglutamyl proteasome activity in genomic stability. *Proc. Natl. Acad. Sci. U. S. A.* 105, 16165–70 (2008).

171. Mandemaker, I. K. *et al.* DNA damage-induced replication stress results in PA 200-proteasome-mediated degradation of acetylated histones. *EMBO Rep.* 19, (2018).

172. Tar, K. *et al.* Proteasomes associated with the blm10 activator protein antagonize mitochondrial fission through degradation of the fission protein dnm1. *J. Biol. Chem.* 289, 12145–12156 (2014).

173. Weberruss, M. H. *et al.* Blm10 facilitates nuclear import of proteasome core particles. *EMBO J.* 32, 2697–2707 (2013).

174. Toste Rêgo, A. & da Fonseca, P. C. A. Characterization of Fully Recombinant Human 20S and 20S-PA200 Proteasome Complexes. *Mol. Cell* 76, 138-147.e5 (2019).

175. Laporte, D., Salin, B., Daignan-Fornier, B. & Sagot, I. Reversible cytoplasmic localization of the proteasome in quiescent yeast cells. *J. Cell Biol.* 181, 737–745 (2008).

176. Marshall, R. S., Li, F., Gemperline, D. C., Book, A. J. & Vierstra, R. D. Autophagic Degradation of the 26S Proteasome Is Mediated by the Dual ATG8/Ubiquitin Receptor RPN10 in Arabidopsis. *Mol. Cell* 58, 1053–66 (2015).

177. Waite, K. A., De-La Mota-Peynado, A., Vontz, G. & Roelofs, J. Starvation Induces Proteasome Autophagy with Different Pathways for Core and Regulatory Particles. *J. Biol. Chem.* 291, 3239–53 (2016).

178. De La Mota-Peynado, A. *et al.* The proteasome-associated protein Ecm29 inhibits proteasomal ATPase activity and in vivo protein degradation by the proteasome. *J. Biol. Chem.* 288, 29467–29481 (2013).

179. Wani, P. S., Suppahia, A., Capalla, X., Ondracek, A. & Roelofs, J. Phosphorylation of the C-terminal tail of proteasome subunit α7 is required for binding of the proteasome quality control factor Ecm29 OPEN. *Nat. Publ. Gr.* (2016). doi:10.1038/srep27873

180. Leggett, D. S. *et al.* Multiple associated proteins regulate proteasome structure and function. *Mol. Cell* 10, 495–507 (2002).

181. Kajava, A. V., Gorbea, C., Ortega, J., Rechsteiner, M. & Steven, A. C. New HEAT-like repeat motifs in proteins regulating proteasome structure and function. *J. Struct. Biol.* 146, 425–430 (2004).

182. Wang, X., Yen, J., Kaiser, P. & Huang, L. Regulation of the 26S proteasome complex during oxidative stress. *Sci. Signal.* 3, ra88 (2010).

183. Wang, X. *et al.* The proteasome-interacting Ecm29 protein disassembles the 26S proteasome in response to oxidative stress. *J. Biol. Chem.* 292, 16310–16320 (2017).

184. Gorbea, C., Goellner, G. M., Teter, K., Holmes, R. K. & Rechsteiner, M. Characterization of mammalian Ecm29, a 26 S proteasome-associated protein that localizes to the nucleus and membrane vesicles. *J. Biol. Chem.* 279, 54849–61 (2004).

185. Gorbea, C. *et al.* A protein interaction network for Ecm29 links the 26 S proteasome to molecular motors and endosomal components. *J. Biol. Chem.* 285, 31616–33 (2010).

186. Lee, S. Y.-C., De la Mota-Peynado, A. & Roelofs, J. Loss of Rpt5 protein interactions with the core particle and Nas2 protein causes the formation of faulty proteasomes that are inhibited by Ecm29 protein. *J. Biol. Chem.* 286, 36641–51 (2011).

187. Park, S., Kim, W., Tian, G., Gygi, S. P. & Finley, D. Structural defects in the regulatory particle-core particle interface of the proteasome induce a novel proteasome stress response. *J. Biol. Chem.* 286, 36652–66 (2011).

188. Lehmann, A., Niewienda, A., Jechow, K., Janek, K. & Enenkel, C. Ecm29 Fulfils Quality Control Functions in Proteasome Assembly. *Mol. Cell* 38, 879–888 (2010).

189. Enenkel, C., Lehmann, A. & Kloetzel, P. M. Subcellular distribution of proteasomes implicates a major location of protein degradation in the nuclear envelope-ER network in yeast. *EMBO J.* 17, 6144–54 (1998).

190. Russell, S. J., Steger, K. A. & Johnston, S. A. Subcellular localization, stoichiometry, and protein levels of 26 S proteasome subunits in yeast. *J. Biol. Chem.* 274, 21943–52 (1999).

191. Panté, N. & Kann, M. Nuclear pore complex is able to transport macromolecules with diameters of ~39 nm. *Mol. Biol. Cell* 13, 425–434 (2002).

192. Savulescu, A. F. *et al.* Nuclear import of an intact preassembled proteasome particle. *Mol. Biol. Cell* 22, 880–891 (2011).

193. Burcoglu, J., Zhao, L. & Enenkel, C. Nuclear Import of Yeast Proteasomes. *Cells* 4, 387–405 (2015).

194. Andrea Lehmann, Katharina Janek, B. B. & Peter-Michael Kloetzel and Cordula Enenkel. 20 S proteasomes are imported as precursor complexes into the nucleus of yeast. *J. Mol. Biol. (* 317, 401–413 (2002).

195. Wendler, P., Lehmann, A., Janek, K., Baumgart, S. & Enenkel, C. The Bipartite Nuclear Localization Sequence of Rpn2 Is Required for Nuclear Import of Proteasomal Base Complexes via Karyopherin αβ and Proteasome Functions. *J. Biol. Chem.* 279, 37751–37762 (2004).

196. Chen, L. *et al.* Sts1 plays a key role in targeting proteasomes to the nucleus. *J. Biol. Chem.* 286, 3104–18 (2011).

197. Enenkel, C. *et al.* Ubiquitin orchestrates proteasome dynamics between proliferation and quiescence in yeast. *Mol. Biol. Cell* 28, 2479–2491 (2017).

198. Hanna, J., Waterman, D., Boselli, M. & Finley, D. Spg5 protein regulates the proteasome in quiescence. *J. Biol. Chem.* 287, 34400–9 (2012).

199. Marshall, R. S. & Vierstra, R. D. Proteasome storage granules protect proteasomes from autophagic degradation upon carbon starvation. *Elife* 7, e34532 (2018).

Chapter 2 - Overexpression of Proteasome Activator, Blm10, Affects the Proteasome Landscape

Alicia Burris[1,2], Kenrick A. Waite[1], Zach Reuter[2], Sam Ockerhausen[2], and Jeroen Roelofs[1,2#]

[1] Department of Biochemistry and Molecular Biology, University of Kansas Medical Center, Kansas City, 3901 Rainbow Blvd, HLSIC 1077,Kansas, USA

[2] Molecular, Cellular, and Developmental Biology Program, Division of Biology, Kansas State University, 338 Ackert Hall, Manhattan, Kansas 66506 USA

Abstract

The proteasome selectively degrades proteins. It consists of a core particle (CP) which contains proteolytic active sites that can associate with different regulators to form various complexes. How these different complexes are regulated and affected by changing physiological conditions, however, remains poorly understood. In this study, we focused on the activator Blm10 and the regulatory particle (RP). In yeast, increased expression of Blm10 outcompeted RP for CP binding, which suggests that controlling the cellular levels of Blm10 can affect the relative amounts of RP bound CP. By fluorescently tagging Blm10, we observed that strong overexpression of Blm10 did not cause the phenotypes one would expect to observe in cells lacking 26S proteasomes. This was due to the induction of Blm10-CP autophagy under prolonged growth in YPD which led to the reformation of RP-CP complexes. Similarly, under conditions of endogenous Blm10 expression, Blm10 was degraded through autophagy as well. This suggests that reducing the levels of Blm10 allows for more CP binding surfaces and the formation of RP-CP complexes under nutrient stress. This work provides important insights into maintaining the proteasome landscape and how protein expression levels affect proteasome function.

Introduction

Most protein degradation in eukaryotic cells is performed by a large complex known as the proteasome. Unlike lysosomal or secreted proteases, proteasomes sequester proteolytic active sites away from potential substrates as they are located within a barrel shaped structure known as the core particle (also known as CP or 20S). CP is composed of two sets of 14 unique subunits. These subunits are arranged in four stacked heptameric rings. α subunits 1 to 7 form the outer rings while the two inner rings are composed of β subunits 1 to 7. Three pairs of proteolytic β subunits, each with distinct specificity, are responsible for cleaving substrates into short polypeptides [200,201]. Peptides released by the proteasome are further processed by cytosolic peptidases to produce intermediates for various metabolic processes [202,203].

While the CP alone appears to be able to degrade certain classes of substrates, e.g. under oxidative stress, it is well established that the majority of substrates cannot be degraded by CP alone [104]. The reason for this is threefold; first, most substrates are labelled for degradation with a post-translational modification on lysine residues known as ubiquitination. The receptors that recognize this modification are not part of the CP. Second, most substrates contain stable tertiary and quaternary structures, which require unfolding before they can enter the CP. Third, even when substrates are unfolded or disordered, entry into the catalytic chamber is restricted by a gate composed of the N-termini of α subunits [104,105].

The association of CP with the regulatory particle (RP or 19S) eliminates all of these limitations and results in the formation of the 26S proteasome (here used to refer to CP complexes with one or two RPs). The RP is composed of 19 polypeptides. Three of these function as intrinsic ubiquitin receptors, Rpn1, Rpn10, and Rpn13, and thus are able to bind substrates [147,148,204,205]. These substrates are deubiquitinated by various deubiquitinating enzymes including the intrinsic RP subunit Rpn11. A hexameric ring of six AAA-ATPases (Rpt1-6) utilizes ATP to unfold substrates and translocate them into the CP for degradation. Several of the ATPase subunits have C-terminal tails with a conserved Hb-Y-X motif (Hb refers to a hydrophobic amino acid, Y is tyrosine, and X can be any amino acid). Docking of these tails into pockets on the surface of the CP α-ring contribute to the affinity between RP and CP as well as induce conformational changes that open the gate and allow for substrate entry into the core particle [107,110,206]. Thus, 26S proteasomes bind, unfold and subsequently degrade the majority of physiologically important substrates.

Besides RP, several other complexes can associate with the same surface of CP that is occupied by RP, namely the 11S activator (REGα-β and REGγ, a.k.a. as PA28αβ and PA28γ; not found in yeast), Pba1-Pba2/PAC1-PAC2, Blm10/PA200, and Fub1/PI31 [107,207–209]. However, none of these can hydrolyze ATP or are able to recognize ubiquitinated substrates suggesting their function is either different or more specialized. In general terms, they could function as a competitor to prevent RP binding. Competitive binding has the potential to negatively regulate proteasome activity, as has been initially proposed and found for PI31 [209,210]. A second possible function involves a role during CP assembly or maturation. Pba1-2 was shown to stimulate α-ring assembly and binding to the ring prevented RP from associating with immature CP [97,211]. Another possible function is in regulating the localization or transport of CP, e.g. into or out of the nucleus. Such a role has been proposed for Blm10 in yeast [173]. Finally, these CP associated proteins may function as distinct, specialized degradation complexes. Here, the degradation would not depend on ubiquitination-based substrate targeting (considering the lack of ubiquitin receptors) or protein unfolding (considering the lack of ATPase activity in these regulators). This role is consistent with the proposed function for REGγ in degrading intrinsically disordered proteins in the nucleus [212–216].

The above models act under the assumption that CP forms homogeneous complexes where one type of activator binds both ends of the core particle; however, CP can actually form hybrid complexes where RP binds to one end, while the other end is occupied by one of these alternative regulators. Such complexes have been purified from cells and detected in cell lysates [217–219]. The formation of hybrid complexes could cause a change in cellular localization of RP-CP complexes. Binding of other activators may also induce allosteric changes inside the CP that affect the specificity of proteolytic cleavage or change cleavage dynamics and peptide retention in the catalytic chamber. As such, hybrid complexes could degrade ubiquitinated proteins, but produce peptides of different composition and length as final products that are released by the proteasome. For mammals, this might be beneficial as proteasome-generated peptides are crucial for MHC class I antigen presentation. Here, IFN-γ induces expression of alternate core particle subunits that form immunoproteasomes used to generate unique peptides due to the exchange of proteolytic active sites. Like these immunoproteasome subunits, REGα-β (a.k.a. PA28αβ) is also induced by IFN-γ suggesting it might contribute to this process [220]. Consistent with the co-evolution and shared functional importance, the loss of immunoCP subunits in birds is

accompanied by the loss of REGα-β [221]. REGα-β forms heptameric rings that stimulate gate opening through a mechanism different from RP. The C-terminal Hb-Y-X motifs of REGα-β contribute to CP binding but are not involved in gate opening. Instead, gate opening occurs through an activation loop within REGα-β that induces conformational changes required for access [222]. Binding of the 19S RP is similar to that of REGα-β (PA28), but the RP lacks this activation loop as interactions of the Rpt C-termini with the core particle allow for both binding and gate opening [223].

Blm10 is a unique regulator as it has been observed bound to both mature and immature CP. Blm10 can be bound to CP alone or in hybrid complexes with RP. Blm10 in *Saccharomyces cerevisiae* (PA200 in humans) is a single ~ 240 kDa polypeptide that contains multiple heat repeats, a bromodomain-like region and a Hb-Y-X motif at its C-terminus. Similar to other activators, this motif allows Blm10 to bind to a pocket on the surface of the α ring, specifically the α5-α6 pocket [107]. However, unlike other regulators, Blm10 binds proteasomes as a monomeric protein. Binding of Blm10 to the core particle induces partial gate opening and increases peptidase activity; therefore, Blm10 has been described as an activator [165]. Indeed, Blm10-CP complexes have been reported to be involved in degradation of short peptides and unstructured proteins like tau, which is reasonable considering those do not require ubiquitination or ATPase-dependent unfolding [165]. In addition, Blm10 appears to be required for the degradation of Sfp1 and histones, further supporting a role for Blm10 in protein degradation [164,171,224]. The presumably folded nature of these substrates might indicate a role for hybrid RP-CP-Blm10 complexes. However, a clear mechanism of action for these hybrid complexes is unknown and other factors might assist in the degradation.

Considering that Blm10 is also found on an immature form of CP, a role in CP maturation has also been proposed. However, its function here seems very different from the assembly chaperones Pba1-2, which seems to exclusively bind to immature CP. Pba1-2 has a very low affinity for mature CP and a high affinity for the immature form [97,208]. Consistent with this, Pba1-2 is more embedded in the α ring of immature CP compared to mature CP, thus restricting RP-CP interactions [98]. While Blm10 could potentially perform a similar role for immature CP, there is no apparent difference in Blm10 affinity for mature versus immature CP that would allow for an exchange of regulators in maturation. Consistent with this, deletion of Blm10 showed no obvious defect in core particle maturation [101,168].

Over the years, many other roles for Blm10 have been suggested, including involvement in processes such as spermatogenesis, DNA repair, histone degradation, CP sequestration into proteasome storage granules (PSGs), and degradation of mitochondrial proteins [101,164,166,168–173,225]. The predicted bromodomain-like region of Blm10/PA200 was shown to specifically bind acetylated histones which led to their subsequent degradation by PA200-CP complexes [164,171]. While recent structural work on the PA200-CP complex fails to establish this bromo-domain-like region, they do assign non-protein densities on the surface of PA200 to inositol phosphates which have been shown to bind and regulate histone deacetylases [174]. Furthermore, binding of PA200 results in an unusually wide α ring. These conformational changes are propagated to the active site β subunits thus changing the structure of the active sites and affecting proteasome activity. Specifically, activation of β2 trypsin-like activity was observed along with a slight inhibition of β5 and β1 activity [174].

In order to gain insight into the physiological role of Blm10 containing complexes, we altered the abundance of this protein in yeast and monitored the effects of its overexpression on the proteasome landscape. Further, we sought to determine how Blm10 bound complexes were affected by various starvation conditions compared to RP-CP complexes.

Materials and Methods

Strains – Strain information is listed in Table 2-1. All strains except sJR1486 (YMW3) and sJR1487 (YMW1) come from a DF5 background with genotype (*lys2-801 leu2-3, 2-112 ura3-52 his3Δ200 trp1-1*). sJR1486 and sJR1487 were provided by C. Enenkel with a WCGa background and genotype *MATa his3-11,15 leu2-3,112 ura3-52 can GAL*. Gene disruptions or the introduction of tags at the endogenous locus were achieved using standard PCR-based approaches [226,227]. To keep the Blm10 endogenous promoter, we utilized a Cre-Lox-based approach to tag endogenous Blm10 [228]. For replacing the endogenous promoter and concomitantly tagging Blm10 with eGFP, we used a PCR based approach to insert the promoters from the *CYC1*, *ADH*, or *GPD* genes. The primers and plasmids used for each of these manipulations are listed in Table 2-2.

Table 2-1 - Strains

Strain	Genotype	Figure
sUB61	*MATα lys2-801 leu2-3, 2-112 ura3-52 his3Δ200 trp1-1*	2A-C, 3B-E,S2A,S3B
Ump1Tap	*MATA ump1::UMP1-CBP-TEV-ZZ-(His3MX6)*	S1A-B
sDL135	*MATα pre1::PRE1-TevProA (HIS3)*	S1A
sJR287	*MATα rpn4::KAN*	3D
sJR395	*MATα blm10::CloNAT*	2C,3C-D
sJR858	*MATα pre2::PRE2-GFP (HIS)*	6C
sJR917	*MATα pre2::PRE2-GFP (HIS) blm10::CloNAT*	2B,S2A,6C
sJR966	*MATα blm10::VENUS-BLM10*	2A,2B,5A-C,S3A
sJR989	*MATα blm10::CYC1pGFP-BLM10 (CloNAT)*	2A-2C,3C,S2A
sJR990	*MATα blm10::GPDpGFP-BLM10 (CloNAT)*	2A-2C,3B-E,S2A,4A-C,S3B
sJR991	*MATα blm10::ADHpGFP-BLM10 (CloNAT)*	2A,2B,S2A
sJR1001	*MATα blm10::VENUS-BLM10 blm10Y2141-A2143Δ (KanMX)*	5A-C,S3A
sJR1004	*MATα blm10::GPDpGFPBLM10 (CloNAT) atg7::URA*	4A-C
sJR1006	*MATα blm10::VENUS-BLM10 atg7::URA*	5B-C
sJR1007	*MATα blm10::VENUS-BLM10 blm10Y2141-A2143Δ (KanMX) atg7::URA*	5B-C
sJR1012	*MATA ump1::UMP1-CBP-TEV-ZZ-(His3MX6) blm10::GPDpGFPBLM10 (CloNAT)*	S1A
sJR1013	*MATA ump1::UMP1-CBP-TEV-ZZ-(His3MX6) blm10::VENUS-BLM10 blm10Y2141-A2143Δ (KanMX)*	S1B
sJR1014	*MATα blm10::GPDpGFPBLM10 (CloNAT) blm10Y2141-A2143Δ (KanMX)*	2C,3B-D
sJR1016	*MATα blm10::CYC1pGFPBLM10 (CloNAT) blm10Y2141-A2143Δ (KanMX)*	2C,3C
sJR1034	*MATα ura3-1::pGPD-Ubi-Y-eGFP unstable (HIS)*	3G
sJR1035	*MATα ura3-1::pGPD-Ubi-M-eGFP stable (HIS)*	3G
sJR1047	*MATα ura3-1::pBLM10-Ubi-Y-eGFP unstable (HIS)*	3A
sJR1062	*MATα pre1::PRE1-TevProA (HIS3) blm10::GPDpGFPBLM10 (CloNAT)*	S1A
sJR1084	*MATα scl1::SCL1-GFP (HIS)*	1A-1C,6D
sJR1199	*MATα scl1::SCL1-GFP (HIS) blm10::CloNAT*	1B-1C,6D
sJR1202	*MATα blm10::GFP-BLM10 scl1::SCL1-mCherry (KanMX)*	6B,6E
sJR1337	*MATA scl1::SCL1-mCherry (KanMX) blm10::GPDpGFPBLM10 (CloNAT)*	3F,6A
sJR1486 (YMW3)	*MATA his3-11,15 leu2-3,112 ura3-52 can GAL pre2::PRE2-GFPS (HIS3-URA3) HTA2-RFP (natMX) blm10::HIS3*	6C
sJR1487 (YMW1)	*MATA his3-11,15 leu2-3,112 ura3-52 can GAL pre2::PRE2-GFPS (HIS3-URA3) HTA2-RFP (natMX)*	6C
sJR1503	*MATα blm10::GPDpBLM10 (CloNAT) ura3-1::pBLM10-Ubi-Y-eGFP unstable (HIS)*	3A
sJR1569	*MATA ump1::UMP1-CBP-TEV-ZZ-(His3MX6) blm10::GPDpGFPBLM10 (CloNAT) blm10Y2141-A2143Δ (KanMX)*	S1C

Table 2-2 - Primers

Manipulation	Frwd 5' – 3'	Rvrs 5' – 3'	Template
Venus-Blm10	pRL375 GTTAGCTAGCTTTGCACATTAATTTTTCGAT TTGTTACCGcggccgccagggg	pRL376GAATGGGTGATTTGATATCATCGTC ATTGTTAGCGGTCATtttgtacaattcatccataccatggg	pJR 543 (pSH47)
blm10Δ	pf2Blm10 CTGTCATCAGGGCTTG	pr2Blm10 GTTGATCATTCTCAGTGG	sJR395 gDNA
pre3-GFP	Frwd/Beta5 TAT TTT GGA AGG TCA AGG AAG AGG AAG GAT CTT TCA ACA ACG TTA TTG GCC GTA CGC TGC AGG TCG AC	S2- Beta5 TAA TGT ATC ATT AAT ATA GAT GTG CAT ATA CAT ATG TTT GAT GCT TCT ATA TCG ATG AAT TCG AGC TCG	pNU293 (pYM28)
P_{CYC1}*GFP-Blm10*	pRL426 GTTAGCTAGCTTTGCACATTAATTTTTCGAT TTGTTACCGCGTACGCTGCAGGTCGAC	pRL427 GAATGGGTGATTTGATATCATCGTCATTGT TAGCGGTCATCATCGATGAATTCTCTGTCG	pNU325 (pYM-N13)
P_{ADH}*GFP-Blm10*	pRL426	pRL427	pNU321 (pYM-N9)
P_{GPD}*GFP-Blm10*	pRL426	pRL427	pNU329 (pYM-N17)
blm10Δ3	pRL408 AGG AAC TGG AAG ACC TGG AGG GTG TCC TAT GGA GAA GTG CCG CCG CCT GAG CGA ATT TCT TAT GA	pRL409 GAT GTA CAT ATA TGT CTA GAT ATG TGC TTA ATA TCC TAT ACT AAT ATG AAA TCG ATG AAT TCG AGC TCG	pNU170 pFA6a-GFP (S65T)-kanMX6
atg7Δ	pRL236 - TTC ATT ATA TTT CAA CAA ATA TAA GAT AAT CAA GAA TAA ACG TAC GCT GCA GGT CGA CG	pRL237 CGG AAA GTG GCA CCA CAA TAT GTA CCA ATG CTA TTA TAT GCA TCG ATG AAT TCG AGC TCG	pNU166 (pAG60)
P_{GPD}*unstable-GFP*	pRL495 ATGCAGATTTTCGTCAAGACTTTGACCGG	pRL496 GGGTACCGGGTAATAACTG	pJR740 (pNC1124)
P_{GPD}*stable-GFP*	pRL495 ATGCAGATTTTCGTCAAGACTTTGACCGG	pRL496 GGGTACCGGGTAATAACTG	pJR741 (pNC1125)
scl1-GFP	pRL589 TGC TGA GAA CAT CGA AGA AAG GCT AGT AGC AAT TGC TGA ACA AGA TCG TAC GCT GCA GGT CGA C	pRL36 GTG TTG ACG CGT GTG ATT TCA CAT TAT GTT GTG GCA GGA AGA TCG ATG AAT TCG AGC TCG	pNU293 (pYM28)
scl1-mCherry	pRL600 TGCTGAGAACATCGAAGAAAGGCTAGTAGC AATTGCTGAACAAGATggtcgacggatccccggg	pRL36 GTG TTG ACG CGT GTG ATT TCA CAT TAT GTT GTG GCA GGA AGA TCG ATG AAT TCG AGC TCG	pJR655-(pBS34)

Yeast Growth Conditions – Yeast strains were grown in yeast peptone dextrose (YPD) media at 30 ºC unless stated otherwise. To induce starvation, overnight cultures were inoculated in fresh YPD at an OD_{600} of 0.5. Cells were grown to an OD_{600} between 1 and 1.5 (~ 4 hours). Cells were collected by centrifugation, washed with sterile water, and resuspended in SD complete media lacking indicated nutrients (starvation media) to a final OD_{600} of 1.5. Media used for glucose starvation contained 0.17 % yeast nitrogen base with 0.5 % $(NH_4)_2SO_4$ supplemented

with 1X amino acid mix, 1X uracil, and 1X adenine. Nitrogen starvation media contained 0.17 % yeast nitrogen base (without $(NH_4)_2SO_4$ and amino acids) and 2 % dextrose. Log phase and starvation induced cells were grown either at 30 ºC or 37 ºC with constant shaking. Samples for specific timepoints were harvested by centrifugation, frozen dropwise in liquid nitrogen, and stored at – 80 ºC for further processing [229].

Phenotype Screen – Yeast cells were grown in YPD to an OD_{600} of 1. Cells from 1 ml of culture were collected by centrifugation (17,000 x g for 1 minute) and washed using sterile water. Cell pellets were resuspended in sterile water and 4-fold serial dilutions were performed for each sample using a 96 well plate. Using a pin array, a droplet of each dilution of cells was spotted onto YPD plates. Plates were incubated at either 30 ºC or 37 ºC for 1-3 days.

Western Blot Analysis – Depending on the purpose of the assay, cell lysates were made using different methods as indicated in figure legends. Cell lysis by grinding in N_2 (l) was achieved as described in Roelofs et al. (2018). In short, cell pellets from – 80º C were transferred to pre-chilled mortars and ground with a pestle to powder in the presence of liquid nitrogen. The powder was transferred to an Eppendorf tube, resuspended in lysis buffer (50 mM Tris-HCl [pH 7.5], 5 mM $MgCl_2$, 1 mM ATP, 1 mM EDTA) and incubated on ice for 10 minutes. Next, lysates were cleared by centrifugation in a microfuge at 17,000 x g for 2 minutes at 4 ºC. Supernatants were collected, and protein concentrations were measured using the NanoDrop. Equal amounts of protein for each sample was loaded for both SDS-PAGE as well as native gel electrophoresis. For alkaline cell lysis, 2 ODs of cells were frozen and then resuspended in 100 µL water followed by the addition of 100 µL 200 mM NaOH. Samples were incubated at room temperature for 5 minutes and collected by centrifugation in a microcentrifuge for 2 minutes at 17,000 x g. Following aspiration, pellets were resuspended in 50 µL alkaline lysis buffer (60 mM Tris-HCl [pH 6.8], 5 % glycerol, 2 % SDS, 4 % β-mercaptoethanol, 0.0025 % bromophenol blue). Samples were boiled at 96 ºC for 3 minutes and cleared by centrifugation at 17,000 x g. 6 µL of supernatant was loaded for SDS-PAGE. After separation of the lysate, gels were transferred to PVDF membranes and immunoblotted for proteins of interest. Primary antibodies used for immunoblotting were against GFP (1:500; Roche, #11814460001), Blm10 (1:1000; Enzo Life Sciences #XO8100), Rpn8 (1:10,000; #4797, generous gift from Dan Finley, Harvard Medical School, Boston, MA), Pba1 and Pba2 (1:500; [97]), α7 (1:1000; Enzo Life Sciences, #02081203), and Pgk1 (1:4000; Invitrogen, #459250). Secondary antibodies conjugated to

horseradish-peroxidase were purchased from Rockland Immunochemicals. Peroxidase activity was visualized using the Immobilon Forte Western HRP substrate from Millipore. Immunoblot images of luminescence were captured using a Syngene G-box imager from Syngene with GeneSnap software. Pgk1 was utilized for a loading control.

Fluorescence Microscopy – For imaging live yeast cells expressing GFP, Venus, or mCherry fusion proteins, was conducted as described previously [230]. In brief, the equivalent of 2 ODs of cells were spun down and resuspended in 20 µL of the culture media. 3 µL of this cell suspension was sandwiched between an agarose padded slide and coverslip. The agarose padded slides were prepared by resuspending agarose to a 1% final concentration in SD complete media (0.17 % yeast nitrogen base containing 0.5 % $(NH_4)_2SO_4$, amino acids, uracil, adenine, and 2 % dextrose) by heating the solution to 96 ºC. Next, 30 µL of the agarose solution was spread out onto the slide by placing a second slide on top of the droplet. Once solidified, the top slide was removed leaving the agar pad upon the original slide. Images were acquired using fluorescence microscopy on a Nikon Eclipse TE2000-S microscope at room temperature using a 600X magnification (Plan Apo 60x/1.40 objective) and a Retiga R3^{tm} camera from QImaging. Images were collected using the Metamorph software (Molecular Devices) and analyzed with ImageJ.

Native Gel Electrophoresis and Activity Assay– Native gel analyses optimized for proteasome complexes were used to determine the composition/distribution of proteasome complexes in the cell. For each sample, 300 µg of cell lysate prepared by cryogrinding was loaded on native gel. Electrophoresis was performed at 96 V for 2.5 hours at 4 ºC to separate the protein complexes. Gels were imaged to visualize fluorescently tagged proteins using a Typhoon 9410 imager. Fluorescent tags were visualized using the following excitations and filters: GFP (488 nm and 526SP) and Venus (532 nm and 526SP). Next, to visualize bands with proteasome activity, an in gel LLVY-AMC hydrolysis (activity) assay was performed as previously described [229]. Images were acquired using a G-Box imaging system from SynGene and GeneSnap software.

Proteasome Purification – Overnight cultures in YPD were used to inoculate 4.5 liters of fresh YPD to a final OD_{600} of 0.5. Cells were allowed to grow for 6-8 hours before harvesting by centrifugation to produce a large pellet of logarithmically growing cells. Cells were washed with water before being resuspended in lysis buffer (1.5 pellet volumes: 50 mM Tris [pH 8.0], 5 mM $MgCl_2$, 1 mM EDTA, 1 mM ATP supplemented with ProBlock^{TM} protease inhibitor

cocktail from GoldBio. Cells were lysed using a French Press at a pressure of 1000 psi. To clear lysates, samples were centrifuged at 11,000 rpm in a Beckman Coulter Aventi J-E centrifuge (rotor: JA-17) for 20 minutes and the resulting supernatant was filtered through a cheesecloth. The cleared lysate was incubated with Antigen Affinity Gel Rabbit IgG resin (whole molecule from MP Biomedicals, LLC) for 1 hour at 4 ºC with constant rotation (750 µL of IgG slurry for 1.5 L of culture). Resin was collected using a Biorad econo-column (0.5 mL wide) and washed with 50 bed volumes of ice-cold Buffer 2 (50 mM Tris [pH 7.5], 5 mM $MgCl_2$, 1 mM EDTA, 1 mM ATP, and 20 mM NaCl). Next, resin was washed with 15 bed volumes ice-cold elution buffer (50 mM Tris [pH 7.5], 5 mM $MgCl_2$, 1 mM EDTA, 1 mM DTT, 1 mM ATP). Proteasome complexes were eluted by an incubation with 750 µL elution buffer containing 8 µL GST-Tev protease (stock concentration: 1.519 mg/mL) for 1 hour at 30 ºC. Collected eluate was incubated with constant rotation for 20 minutes at 4 ºC with glutathione resin to remove Tev protease. After removal of the resin using centrifugation and a spin column, proteasomes were concentrated using a concentrator with 100 kDa MW cutoff (PALL Life Sciences). Concentrated samples were analyzed by SDS-PAGE and native gel electrophoresis as described earlier.

Results

Overexpression of Blm10 leads to RP-CP dissociation

The proteasome core particle is a cylindrically shaped structure able to bind one of numerous regulators. However, binding of these regulators is mutually exclusive as they bind the same interface of CP. Thus, there are a variety of proteasome complexes that contain one or two copies of a particular regulator. Additionally, hybrid complexes (CP with two different regulators) can form. In all, there is the potential for a varied landscape of proteasome complexes. Several of these potential complexes have been observed in yeast as well as mammalian cells [231,232]; however, our understanding of the mechanisms and regulations that govern this landscape are limited.

In lysates of a strain where the endogenous copy of α1 was tagged with GFP, a number of these complexes can be distinguished on native gel (Fig. 2-1A, lane 1). Whole cell lysate prepared by cryo-grinding was separated on native gel and imaged for GFP to identify the native complexes that contained the CP subunit α1. A number of species can be readily identified; from top to bottom these are: CP with RP bound on both ends (RP_2-CP), CP-RP with Blm10 bound

(Blm10-CP-RP), CP with one RP (RP-CP), CP with Blm10 bound on both ends ($Blm10_2$-CP), CP with Blm10 bound on one end, and free CP. Assignment of these species is based on extensive work by us and other laboratories [233,234]. It should be noted that the Blm10-CP-RP band could contain Ecm29, as this proteasome associated 210 kDa protein can bind to both RP-CP, Blm10-CP-RP, and RP_2-CP complexes. Further, Ecm29 retards the migration of complexes on the gel when it is bound [178,180,186,235]. Consistent with the fluorescence based complex assignments, all these bands show hydrolytic activity towards the fluorogenic, model peptide substrate LLVY-AMC (Fig. 2-1A, right panel). We have previously shown that nitrogen starvation induces selective degradation of the proteasome through autophagy (proteaphagy) [176,177]. Here, we noticed the preferred disappearance of Blm10-CP and Blm10-CP-RP species over time (Fig. 2-1A). This disappearance was accompanied by an increase in the amount of a faster migrating GFP band. The migration behavior of this band is consistent with the migration of free GFP on our native gels [177]. Free GFP is formed when the GFP is proteolytically cleaved from a tagged protein in the yeast vacuole, but not yet degraded [177,236]. This suggests that either Blm10 containing proteasome species are preferably degraded via autophagy, or Blm10 dissociates from these complexes upon nitrogen starvation and the free GFP is derived from any form of CP containing complexes that undergo autophagy. Consistent with the latter, *blm10*Δ cells still displayed proteaphagy upon nitrogen starvation (Fig. 2-1B, 2-1C and [199]). Therefore, it is clear that Blm10-CP and Blm10-CP-RP proteasome complexes are not exclusively autophagy cargo.

Figure 2-1 - Blm10 containing complexes are reduced during nitrogen starvation

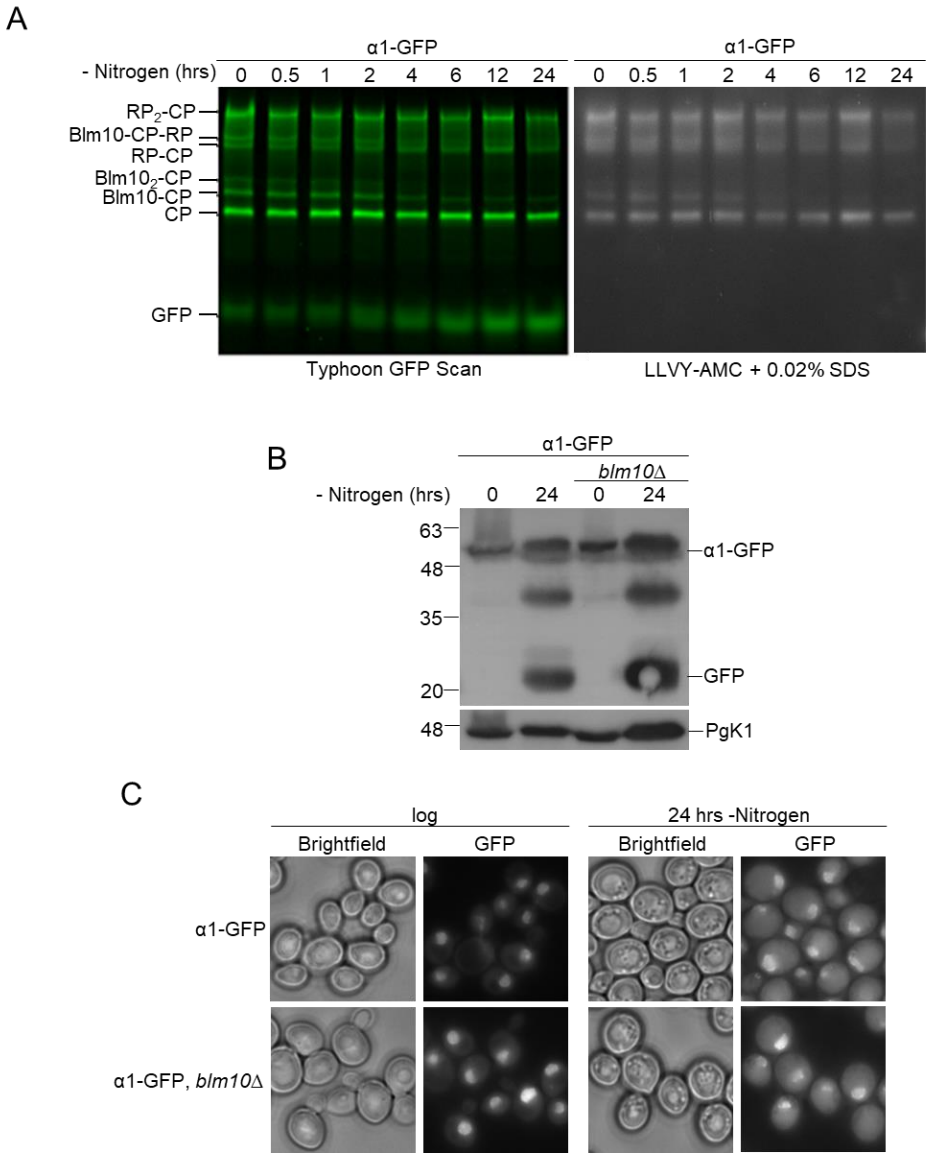

(A) Strains expressing α1 GFP-tagged proteasomes were analyzed by native gel electrophoresis to determine the effect of nitrogen starvation on proteasome complexes. Total protein lysates were obtained by cryogrinding and proteasomes were visualized using a Typhoon 9410 scanner. Following the GFP scan, a LLVY-AMC proteasome activity assay was conducted to determine the location of active proteasome complexes (CP bound with an activator). Use of 0.02 % SDS opens the CP gate and allows for visualization of proteasome complexes not bound by an activator. Over a 24-hour time course, the amount of proteasome complexes was reduced and free GFP was formed. Reduction of Blm10-CP complexes occurred approximately 2 hours earlier than what has been established for 26S proteaphagy. (B) To establish that Blm10 complexes were not exclusively degraded, proteaphagy was analyzed in strains lacking Blm10. Immunoblots for GFP showed the formation of free GFP which indicates vacuolar proteasome degradation through autophagy. PgK1 (phosphoglycerate kinase) was used as a loading control. (C) Strains as in B were analyzed by fluorescence microscopy. GFP localization was monitored in logarithmically growing cells as well as cells grown for 24 hours in minimal media lacking nitrogen.

As such, it is important to understand how the landscape of CP containing proteasome complexes is controlled by the protein levels of Blm10 in yeast and whether Blm10 containing complexes behave differently than RP containing complexes under stress conditions like nitrogen and glucose starvation. Although Blm10 overexpression has been studied previously [165,233], there have been some conflicting reports regarding its impact on growth. Furthermore, some studies were conducted with, or included strains, where Blm10 was tagged C-terminally [168,199,233]. However, C-terminal tagging renders Blm10 non-functional as the C-terminus of Blm10 is essential for its interaction with CP [107,165]. Here, we introduced an N-terminal fluorescent tag on Blm10 at its endogenous locus with different promotors. We either introduced the *CYC1, ADH,* or *GPD* promotors which provide increasing levels of Blm10 expression [237], or we retained the endogenous promotor using a Cre-Lox-based approach. The expression level we observed with the *CYC1* promoter was similar to the levels of Blm10 we observed with the endogenous promotor under conditions of logarithmic growth (Fig. 2-2A, lane 1 and 3). Replacement with either the *ADH* or *GPD* promoter resulted in strongly increased levels of Blm10 in total lysate immunoblots and an 8-fold (pADH) to 12-fold (pGPD) higher fluorescence intensity as compared to the endogenously expressed GFP-Blm10 (Fig. 2-2A, lanes 4 and 5). Regardless of the expression level, the signal for GFP-Blm10 remained predominantly nuclear (Fig. 2-2A).

Compared to CP, endogenous Blm10 levels are substoichiometric, and any increase in Blm10 could lead to either an accumulation of free Blm10, more Blm10 associated with CP, or both. That said, we are not aware of any reports showing the presence of wild type Blm10 that is not associated with proteasomes in cells. Therefore, to test how increased Blm10 expression influenced the proteasome landscape, we analyzed lysates expressing different levels of Blm10 on native gel. A β5-GFP expressing strain was used as a control to compare CP containing complexes. The β5-GFP tag resulted in a slight shift of CP species on the native gel as compared to non-tagged proteasomes (Figure 2-2B, lane 2). As expected, in cells that express GFP-Blm10 at levels similar to wildtype (*CYC1* promoter), the landscape consisted mostly of RP_2-CP, RP-CP, and CP complexes. Some RP-CP-Blm10 complexes were also visualized on native gel as indicated by LLVY-AMC active species (Figure 2-2B, right panel lane 3) which is very similar to wild type cells (lane 3 compared to 1 and 6). The fluorescent scan of the same gel shows the major band of RP-CP-Blm10 and a faint Blm10-CP species. With increased expression of

Blm10 (lanes 4 and 5), we observed a dramatic loss of the RP-CP and RP_2-CP species with only small amounts of RP-CP-Blm10 remaining. Most CP, however, could be found in a species hardly detectable in wildtype cells. Scanning the gel for GFP fluorescence (Fig. 2-2B, left panel), we observed GFP-Blm10 migrates at the same location as this species. Based on the shift, this band represents CP with both faces of the complex occupied with Blm10 ($Blm10_2$-CP) [233]. Interestingly, Blm10 levels appeared to be in excess of CP binding surfaces and accumulated free GFP-Blm10 could be observed on the native gel. Consistent with promoter activity, more free GFP-Blm10 was observed with *GPD* promoter then *ADH* promoter. In sum, Blm10 is a substoichiometric CP regulator that is normally found associated with a subset of CP. Increased expression resulted in reduced levels of free CP and 26S and led to an accumulation of free Blm10 which was in excess of the available CP binding surfaces .

As free Blm10 has never been reported on native gels, we wanted to confirm our assignment of free Blm10 by comparing Blm10 mutant strains that are defective in CP binding. Based on the crystal structure of Blm10-CP, the C-terminal tail is important for its interaction with CP and deletion of the last three amino acids of Blm10 has been shown to disrupt interactions between CP and Blm10 [107,165]. With the Blm10Δ3 mutant strain, we observed that even the strong overexpression of this mutant was not able to reduce the amount of RP-CP species normally found in yeast (Fig. 2-2C right panel, lane 5 compared to 6). Scanning the gels for bands that show GFP fluorescence, we observed that the $Blm10_2$-CP band was absent in the lysate from Blm10Δ3 cells while the other major band remained indicating this was indeed free Blm10 that migrated here on native gel (Fig. 2-2C, left panel). As there were no detectable levels of free Blm10 under endogenous expression (Fig. 2-2B, lane 3 and 6), increasing the levels of Blm10 appeared to directly affect the number of Blm10-CP complexes present in the cell as well as 26S proteasomes.

In the GFP-Blm10Δ3 expressing strain, we did observe a minor species migrating somewhat slower than CP with LLVY-AMC activity that is consistent with Blm10-CP. The strong overexpression of Blm10Δ3 appeared to compensate for the lower affinity and drive a minor fraction of Blm10Δ3 to associate with CP. More surprising was the appearance of a faster migrating band upon overexpression of Blm10 (Figure 2-2C, labeled #), which was unaffected by the deletion of the last three amino acids of Blm10. Considering that Blm10 is known to bind to immature forms of CP [102,168], it is likely these bands represent Blm10 bound to immature CP.

Similar observations have been made for overexpression of Pba1/2 which causes an accumulation of the immature 15S complex that migrates faster than CP on native gel [238]. Potentially, similar to Pba1-2, Blm10 binding to immature CP is structurally different as compared to mature CP and thus might depend less on the Blm10 Hb-Y-X motif [97].

RP is normally not found associated with immature CP because Pba1-Pba2 prevents this interaction. One possibility for the apparent increase in Blm10-CP complexes is that Blm10 binds to immature CP and has an extremely low off-rate, resulting in an inability of RP to compete with Blm10 for CP binding. To test if the overexpression of Blm10 caused excessive binding of Blm10 to immature CP, we sought to determine if Blm10 could displace the chaperone dimer Pba1-2 which binds to the same interface of immature CP as RP does to CP [208]. To assess changes in the levels of Pba1-2 bound to immature CP under conditions of Blm10 overexpression, we purified immature and mature CP from strains with endogenous or strongly overexpressed Blm10. Purified mature CP from cells that overexpressed Blm10 showed reduced levels of the RP subunit Rpn8 and increased levels of Blm10, indicating Blm10 competed with RP for CP binding (Supp. Figure 2-1A, lane 4). These results are consistent with our observations of whole cell extracts separated by native gel. Purified immature core particles, however, showed only slightly less Pba1-2 in the presence of increased levels of Blm10 (Supp. Fig. 2-1A, lane 2).

Figure 2-2 - Overexpression of Blm10 reduces RP-CP levels

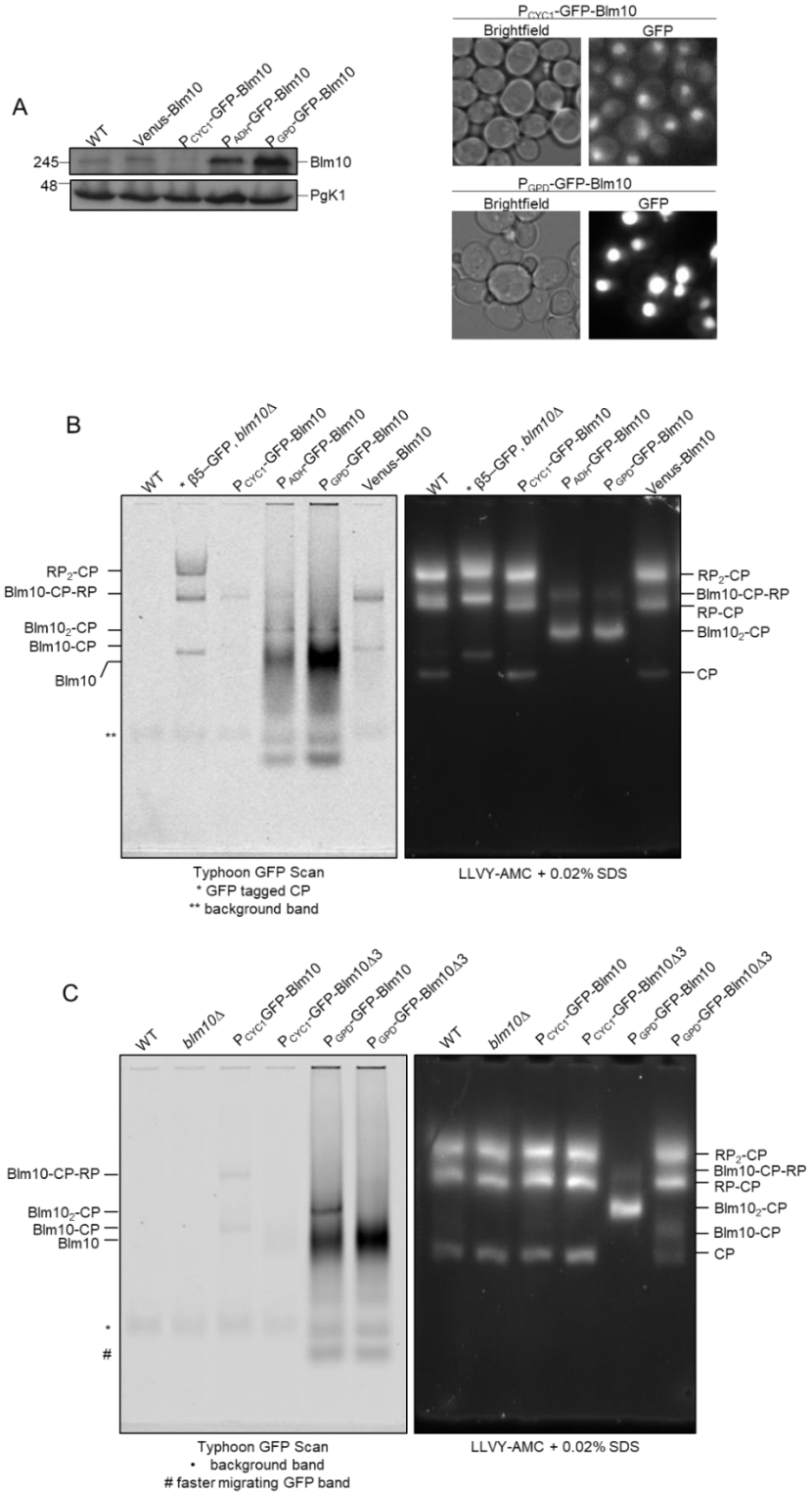

(A) Blm10 was N-terminally tagged with GFP and its expression levels were manipulated by changing its endogenous promoter to either the CYC1, ADH, or GPD promotors. The CYC1 promoter resulted in expression similar to WT Blm10 levels while the ADH and GPD promoter resulted in overexpression of the protein. Protein levels were determined and compared by immunoblotting for Blm10. Microscopic images showed similar increases in Blm10 levels when expression was driven by the GPD promoter. (B) Native gel electrophoresis was used to determine the effect of Blm10 overexpression on proteasome complexes. Gels were scanned using a Typhoon 9410 imager to identify GFP-Blm10 containing complexes (left panel). Proteasome activity was analyzed using LLVY-AMC (right panel). GFP-tagged CP (*) produces a shift on native gel. (C) Cell lysates from strains expressing Blm10 from the CYC1 and GPD promoters were compared with mutant versions of Blm10 lacking the C-terminal tail (YYA). The tail mutation prevented binding of Blm10 to CP even upon strong overexpression as shown by native gel electrophoresis.

To test if the Blm10 tail was expendable for Blm10-immature CP binding, as suggested by a lack of reduction for the faster migrating species in Fig. 2-2C, we next evaluated the impact of Blm10Δ3 expression on the purification of immature core particles. Purified immature CP showed reduced levels of Blm10 binding, both under the endogenous and GPD promotor, in strains expressing Blm10Δ3. This shows that the Hb-Y-X motif of Blm10 is critical for both CP and immature CP binding, suggesting that Blm10 interactions with the alpha ring of immature CP are similar to that of mature CP (Supp. Fig. 2-1B and 2-1C). This appears different than Pba1-2 which becomes embedded into immature CP but not mature CP [208,238]. Furthermore, the faster migrating species we observed at the bottom of the native gel in Fig. 2-2C is not Blm10 bound to immature CP, unless the purification conditions (as compared to lysis only) caused dissociation of only Blm10Δ3 from immature CP due to a weaker affinity as compared to full length Blm10.

Phenotypic Analysis of Blm10 Overexpression

With the exception of Rpn10, Rpn13, Sem1, and α3, all CP and RP subunits are essential, which is consistent with the important role for RP-CP complexes in the degradation of ubiquitinated proteins. Therefore, we anticipated that the very low level of RP-CP-Blm10 proteasomes we detected, together with the absence of 26S proteasomes in Blm10 overexpressed strains (Fig. 2-2B), would not suffice to maintain normal cellular proteostatic functions. To test the effect of Blm10 overexpression on proteasome substrates, we expressed an unstable N-end rule GFP proteasome substrate in a strain overexpressing Blm10. In cells containing 26S proteasomes, unstable GFP is present at a low steady state level (Figure 2-3A, lane 1). Overexpression of Blm10 increased these levels by almost 3-fold (2.8 ± 0.58 SEM) indicating a strongly reduced degradative capacity in these cells (Figure 2-3A, lane 2). To determine if the reduced degradation expanded beyond this model substrate, we examined overall levels of

ubiquitinated material by blotting for ubiquitin in cell lysate. Logarithmically growing cells containing high levels of Blm10 showed an increase in overall ubiquitinated material (Figure 2-3B, compare lanes 1 and 2). This accumulation was due to Blm10 binding to CP and displacing RP because the unbound form, Blm10Δ3, showed levels of ubiquitinated proteins similar to wildtype (Figure 2-3B, compare lanes 1 and 3). Thus, the overexpression of Blm10 reduces the ability of cells to degrade ubiquitinated substrates.

Despite the apparent loss in degradative capacity, strains overexpressing Blm10 were viable and did not show any apparent growth defects on YPD plates or in liquid culture for logarithmically growing cells despite the low levels of 26S proteasomes on native gels (RP-CP and RP_2CP) (Figure 2-3C and 2-3D). In fact, cells grew at normal rates and even better than a *rpn4*Δ strain (Figure 2-3D), which cannot upregulate proteasome levels, but retains higher basal proteasome levels [239–241]. These data suggest that, under these non-stress conditions, low proteasome levels are sufficient for survival. This also indicates that the slow growth of *rpn4*Δ in rich media under logarithmic growth conditions is not exclusively due to lower expression of proteasomes. Indeed, Rpn4 regulates the expression of numerous other proteins, such as Prb1 [239,242], some of which apparently contributes substantially to the slow growth phenotype. Alternatively, $Blm10_2$-CP could compensate for, or replace, the 26S degradative capacity. However, the latter is unlikely considering that Blm10, unlike many proteasome subunits, is not essential as it lacks ubiquitin receptors and does not have the ability to utilize ATP to unfold and translocate proteins into the degradative chamber of CP.

Compromised proteasome function or reduced proteasome levels, as has been observed with many mutants, is associated with increased sensitivity of strains to high temperature or the presence of the arginine analog canavanine. Under these conditions, protein misfolding and unfolding increases the demand for proteasomal degradation. Considering the low levels of 26S in the strain overexpressing Blm10, we expected to see a strongly reduced growth or survival for this strain compared to wildtype under these conditions. However, the GPD driven overexpression of Blm10 resulted in only a modestly reduced growth phenotype at 37 °C, and no detectable difference in the presence of canavanine (Fig. 2-3C and Supp. Fig. 2-2A). Moreover, the overexpression of Blm10Δ3, which is compromised in CP binding and has normal 26S proteasome levels, resulted in an almost similar reduction in growth as the Blm10

overexpression, indicating it is more likely the high levels of Blm10 itself (i.e. independent of its ability to reduce 26S proteasome levels) that are responsible for the phenotype (Figure 2-3C).

To understand why overexpression of Blm10 produced only a modest growth phenotype, we looked at the proteasome landscape for wildtype and Blm10 overexpressing strains under the conditions tested. For wildtype cells, the landscape of proteasome complexes remained similar when comparing growth in YPD over time (4 to 24 hours) or at 30 °C and 37 °C (Fig. 2-3E). As reported above, upon Blm10 overexpression, the landscape was comprised of mainly $Blm10_2$-CP complexes and a small amount of Blm10-CP-RP at 30 °C. A similar composition was also observed in logarithmically growing cells at 37 °C. However, growth of cells under these conditions for 24 or 48 hours induced dramatic changes in the proteasome composition as observed on native gel. At 24 hours, the levels of $Blm10_2$-CP were reduced, Blm10-CP-RP increased, and RP_2-CP was detectable at both temperatures (Figure 2-3E, lane 6 & 9 on right). Consistent with these gel analyses, microscopic analyses of cells at 37 °C showed reduced levels of GFP-Blm10 compared to 24 hours at 30 °C where we detect GFP-Blm10 in the nucleus. Intriguingly, the 37 °C stress response led to formation of proteasome granules that lacked GFP-Blm10 (α1-mCherry in Figure 2-3F). This was surprising as previous reports showed Blm10 and proteasomes colocalize in granules in stationary phase and upon carbon starvation [197,199]. The formation of these granule structures is thought to protect proteasomes from degradation, so failure of Blm10 to localize to these granules could lead to its reduced levels. However, apart from degradation, a reduction in Blm10 levels could also be caused by reduced transcription or translation and protein dilution resulting from cell division. To test how stable and an unstable proteins behave when driven by this promotor under these conditions, we introduced the same GPD promoter upstream of an open reading frame encoding a stable or an unstable form of GFP. The newly generated strains were subjected to the same conditions as the Blm10 overexpressing strains. Here, the cells expressing stable GFP maintained constant levels of GFP at both 30 °C and 37 °C for up to 24 hours of growth (Supp. Fig. 3A), while for the unstable GFP the equilibrium between expression and degradation resulted in a reduction of GFP levels, similar to what we saw for Blm10 . Thus, the reduction of Blm10 under these conditions cannot be explained simply by a lack of expression from this promoter and suggests the reduction in Blm10 levels results from degradation.

Figure 2-3 - Overexpression of Blm10 leads to proteasomal substrate accumulation

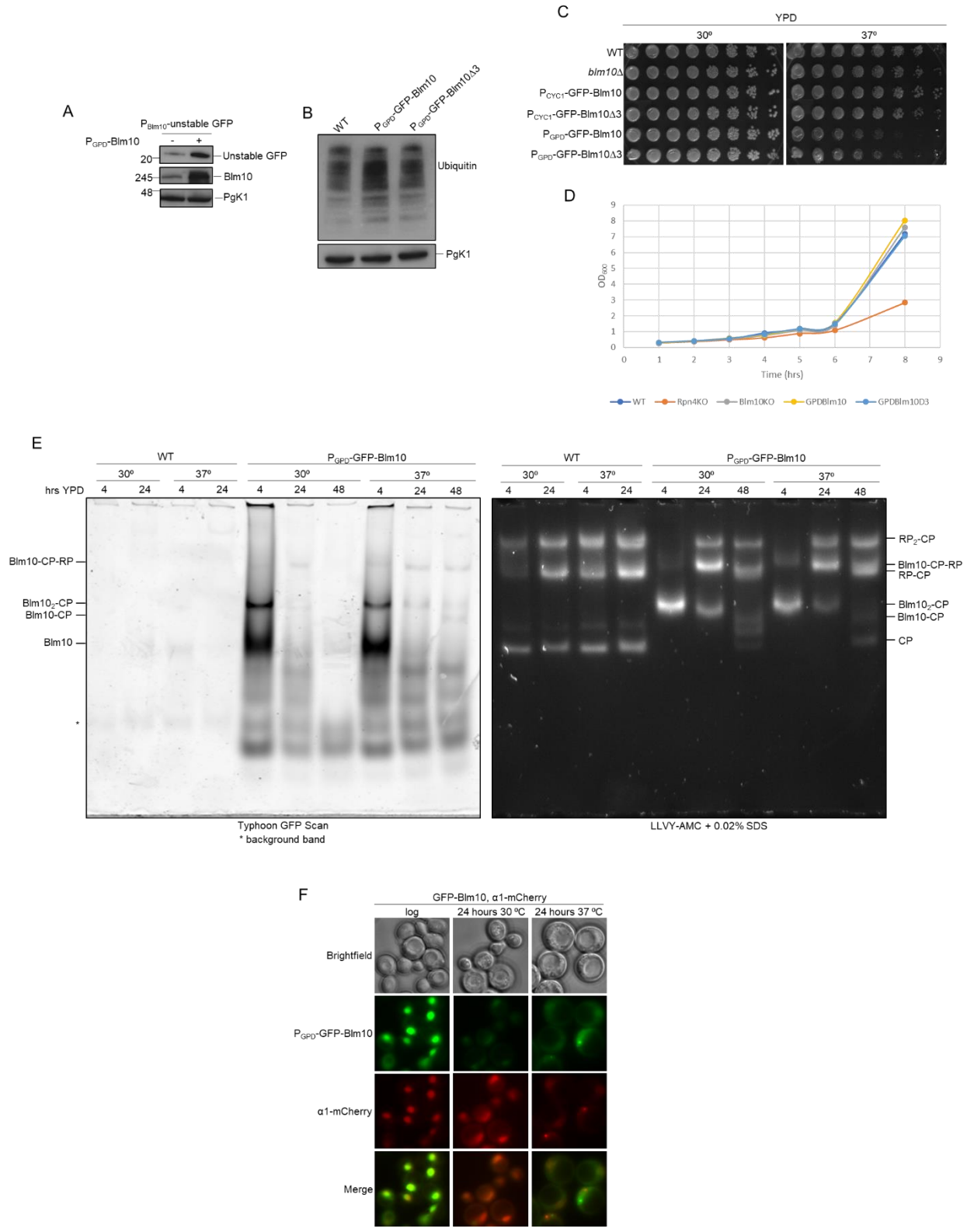

(A)Overexpression of Blm10 increased the amount of proteasomal substrates in the cell by reducing the amount of 26S proteasomes. Increased Blm10 levels in logarithmically growing cells lead to increased amounts of proteasomal substrate, unstable GFP, as analyzed by western blot. Elevated levels of unstable GFP upon Blm10 overexpression were observed in three independent experiments. Immunoblots of GFP and Blm10 were used to determine protein levels while PgK1 was used as a loading control. (B) An increase in overall ubiquitinated material resulted upon overexpression of WT Blm10 while no such increase was observed upon overexpression of the noncompetitive mutant of Blm10 which cannot bind CP. (C) Indicated strains were serially diluted following logarithmic growth and spotted on YPD plates to determine if Blm10 overexpression resulted in decreased cell survival. Plates were incubated at 30 degrees and 37 degrees Celsius for 48 hours . At 30 degrees, all strains grew similarly, but at elevated temperature, a modest growth phenotype was associated with overexpression of Blm10 which was partly rescued by the mutant version of Blm10. (D) A growth curve of the indicated strains was conducted to show that strains overexpressing Blm10 grew at similar rates to wildtype strains at 30 degrees. The rpn4Δ (rpn4KO) strain was used as a known slow-growth control as this deletion affects proteasome levels and results in poor growth. Cells were inoculated to an OD_{600} of 0.5. Cell density was monitored over a 24-hour period. Cell densities for all strains, except rpn4Δ, were similar at each timepoint. (E) Whole cell lysates from cells grown at 30 degrees and 37 degrees were resolved using native gel electrophoresis. GFP-Blm10 species were visualized using a Typhoon scanner while an in gel LLVY-AMC assay was conducted to determine the location of active proteasome complexes. Blm10 levels were reduced over time and 26S proteasomes had re-formed, which likely explains the modest growth phenotype observed in 3C. (F) Consistent with the native gel, GFP-Blm10 levels were reduced over time as determined by fluorescence microcopy. α1-mCherry localization at 30 degrees remained nuclear, while at 37 degrees, α1-mCherry formed granules that were devoid of GFP-Blm10.

CP-bound Blm10 is degraded by autophagy

As our data suggest reduction of Blm10 results from degradation, we next wanted to determine the degradative pathway responsible. Since the majority of protein degradation depends on either the autophagy-lysosome or the ubiquitin-proteasome pathway, we tested for the involvement of either system in the reduction of Blm10. We first used the proteasome inhibitor MG132 (100 μM) to test the extent to which the Blm10 reduction was dependent on proteasome activity. In cells overexpressing Blm10, the addition of proteasome inhibitor did not prevent the strong reduction of $Blm10_2$-CP complexes observed after growth for 24 or 48 hours in YPD (Fig. 2-4A). The band observed directly above Blm10-CP-RP in the proteasome inhibitor treated cells resulted from the association of Ecm29 with these complexes. Since *ECM29* has the PACE element in its promotor, it is recognized by Rpn4 [243] and upregulated in several strains with compromised proteasome function [180,186,244]. Therefore, upregulation of Ecm29 upon proteasome inhibition is expected. Ecm29 associates with RP-CP containing complexes as it has a binding site on RP as well as CP [178,179,187]. In all, proteasome inhibitor treatment did not block the reduction of Blm10-CP complexes.

Previous work in yeast has shown proteasomes (RP and CP) are degraded through autophagy under nitrogen starvation or upon proteasome inhibition [176,177,245]. To test for an autophagic contribution in reshaping the proteasome landscape, we deleted the *ATG7* gene. *ATG7* encodes for a protein that is required in both micro- and macroautophagy as it activates the

ubiquitin-like proteins Atg8 and Atg12, both of which are crucial for autophagosome formation [246]. In the *ATG7* knockout strain, we also observed a reduction in the levels of free Blm10; however, the levels of Blm10 that were complexed with the core particle were largely stabilized with hardly any reduction in Blm10-CP complexes even after 24 hours. This was in contrast to the autophagy capable cells, where barely any Blm10-CP was detected (Figure 2-4A). This indicates that Blm10-CP complexes are degraded through autophagy upon extended growth in YPD. The autophagic degradation is interesting under these conditions as it corroborates our original observations under nitrogen starvation (Fig. 2-1A) as well as previous work showing proteasomes (RP and CP) are degraded through autophagy under nitrogen starvation or upon proteasome inhibition [176,177,245].

Next, we tested if Blm10 levels would be affected similarly by nitrogen starvation as compared to prolonged growth. The reduction of Blm10 in wildtype cells began approximately two hours after starvation and steadily decreased with little to no detectable free Blm10 after 24 hours (Fig. 2-4B lane 1 to 5). In the *ATG7* knockout strain, free Blm10 levels remained steady up to four hours of nitrogen starvation and were not completely cleared after 24 hours. This indicates the free Blm10 was partially stabilized in the autophagy defective strain. Similar to prolonged growth, the CP bound Blm10 levels also remained almost constant, showing only a slight reduction at 24 hours (Figure 2-4B). Consistent with the autophagic degradation of Blm10, we observed the accumulation of free GFP on native gels after nitrogen starvation in an autophagy dependent fashion (Fig. 2-4B, see 4 hours wt versus *atg7*Δ). Furthermore, fluorescence could be observed in the vacuole of WT cells overexpressing Blm10, but not when *ATG7* was deleted (Figure 2-4C). Here, GFP-Blm10 was found in the nucleus and the vacuoles were void of fluorescent signal as reported previously [168,233]. Thus, Blm10 vacuolar targeting and degradation is mediated by autophagy and both prolonged growth and nitrogen starvation induce the autophagic degradation of Blm10-bound CP complexes.

Figure 2-4 - Blm10 is selectively degraded through autophagy

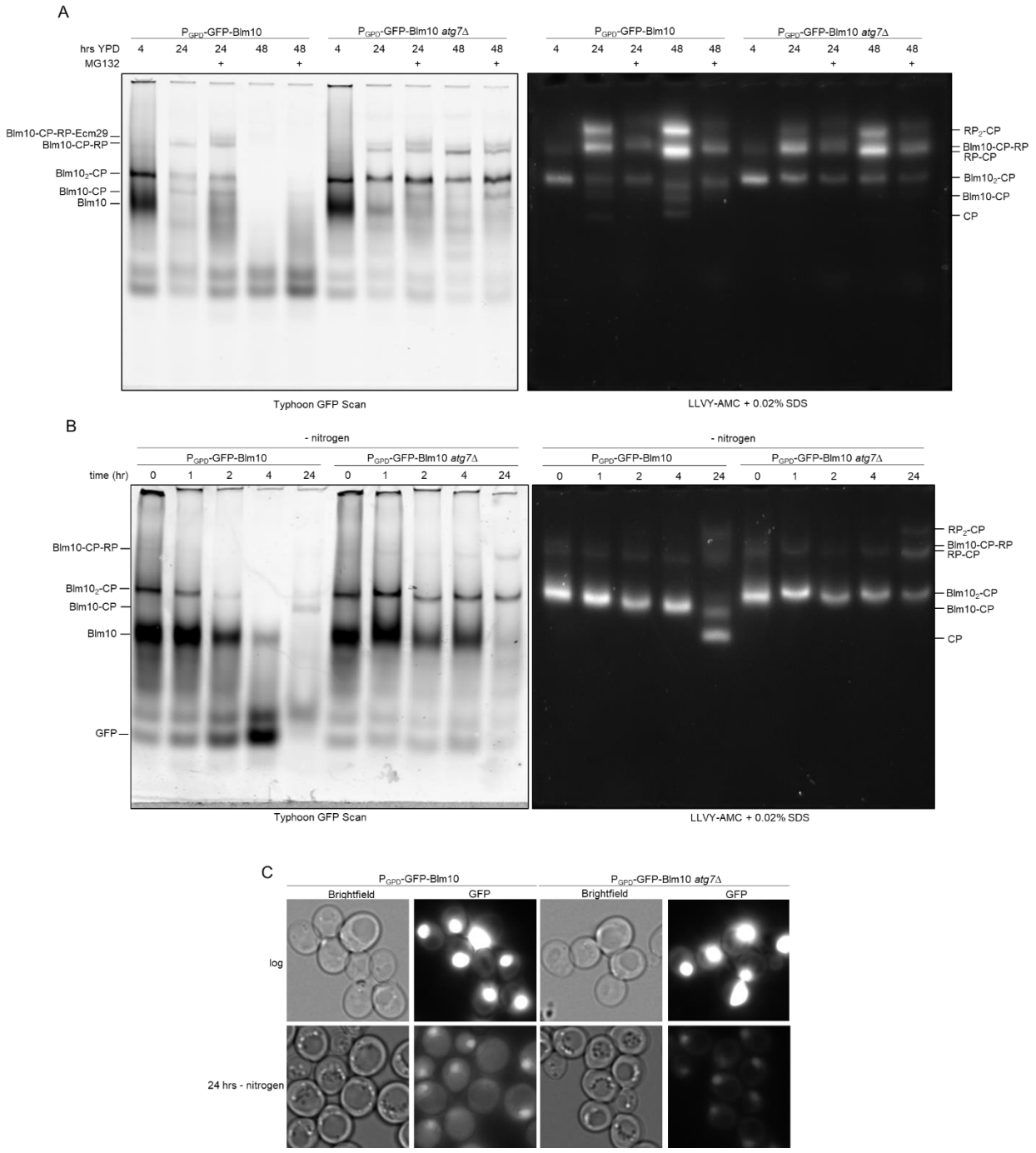

(A) GFP-Blm10 levels were monitored over a 48-hour time course in WT and atg7Δ strains in the presence of the proteasome inhibitor MG132 (100 µM). Proteasome complexes were separated using native gel electrophoresis. Blm10 bound CP complexes were stabilized in strains lacking Atg7 while proteasome inhibitor had no effect on Blm10 levels. (B) ATG7 deletion resulted in stabilized Blm10 bound complexes in nitrogen starved cells similar to cells grown in YPD for 24 and 48 hours. Samples were analyzed as in A. (C) Strains overexpressing Blm10 were analyzed using fluorescent microscopy. atg7Δ cells were consistently devoid of GFP signal in the vacuole while WT

strains showed GFP inside the vacuole indicating GFP-Blm10 complexes were targeted for autophagy upon nitrogen starvation.

Free Blm10 is degraded by both autophagy and the proteasome

While the data above show that Blm10 is targeted for vacuolar degradation by autophagy, this was under conditions of artificial overexpression of Blm10. To test Blm10 degradation when the protein was expressed from the endogenous promotor, we utilized the Venus-Blm10 tagged strain described earlier. To determine if changes in protein level were dependent on CP binding (all endogenously expressed Blm10 is CP bound) we also deleted the C-terminal three amino acids (YYA) resulting in free Blm10 (i.e. not associated with CP, Fig. 2-5A). First, we determined whether the levels of bound or free Blm10 changed upon nitrogen starvation or proteasome inhibitor treatment. Upon nitrogen starvation, both strains showed the appearance of free Venus together with a reduction in CP-bound Blm10 (left panel) and free Blm10 (right panel) (Fig. 2-5B). In strains defective in autophagy (by the deletion of *ATG7)*, the formation of free Venus was prevented indicating that Blm10 was at least in part degraded via autophagy. In the presence of Atg7, most free Blm10 was cleaved from Venus; however, in the *atg7*Δ we still saw a reduction in free Blm10, but no accumulation of Venus. This suggests clearance of unbound Blm10 is not mediated solely by autophagy but can presumably be degraded by the proteasome as well. Further, we observed higher migrating bands for Blm10Δ3 in the *atg7*Δ strain following nitrogen starvation. While we are not certain of the nature of these bands, one band is consistent with the migrating pattern for GFP-Blm10-CP-RP, suggesting that the Venus-Blm10Δ3 under these conditions is able to associate with CP. Since nitrogen starvation disrupts interactions between RP and CP, this might allow for more Blm10Δ3 to associate despite its reduced affinity for CP [177,245].

To test if proteasome activity was responsible for the decrease in Blm10 levels for cells grown for 24 hours in YPD, we next grew endogenously expressing Blm10 cells in the presence or absence of proteasome inhibitor. As expected, based on the data with GFP-Blm10 overexpression, Venus-Blm10 levels were reduced. This reduction of Blm10 was not prevented by proteasome inhibitor treatment but was limited in a strain defective for autophagy (Fig 2-5C, left panel). For unbound Blm10, we observed a similar reduction in levels for strains where autophagy was functional and these levels were also not stabilized with the addition of proteasome inhibitor, indicating degradation is primarily through the autophagy pathway (Fig. 2-5C, right panel, lane 3). However, in the *ATG7* knockout, although we still saw a reduction of

Blm10Δ3, the addition of proteasome inhibitor was able to stabilize the protein to a certain extent (Fig. 2-5C, right panel, lane 6). Thus, under both conditions unbound Blm10 was degraded by both autophagy and the proteasome, while proteasome bound Blm10 is largely cleared from cells via autophagy.

Figure 2-5 - Blm10 is degraded by the proteasome when autophagy is blocked

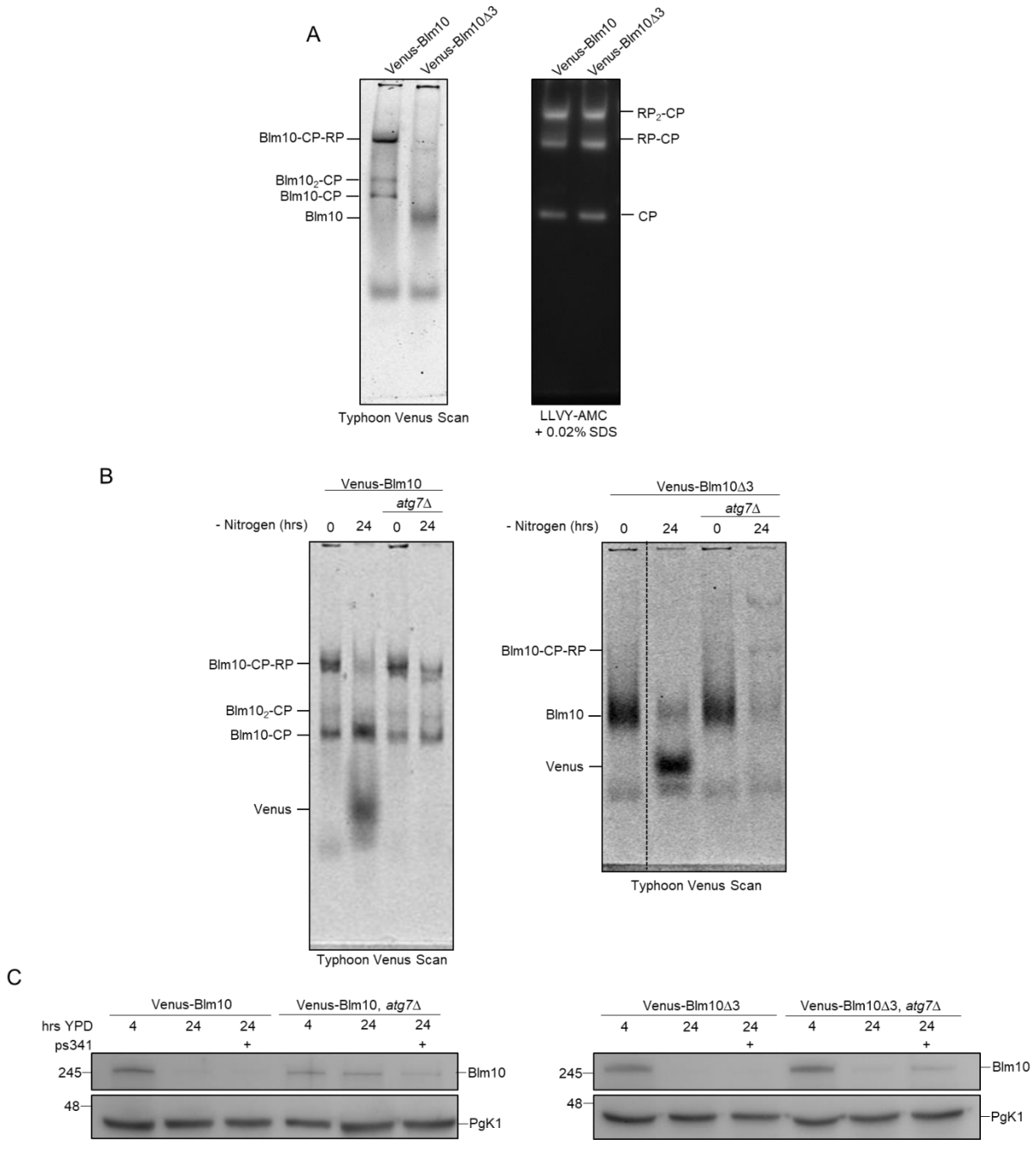

(A) Strains expressing Venus-Blm10 under the endogenous promoter were used to analyze the mechanism of degradation of free Blm10. Free Blm10 was generated by deleting the C-terminal tail of Blm10 (amino acids YYA) to prevent its ability to bind CP. Free Blm10 was confirmed using native gel electrophoresis and a Typhoon scanner as described above. (B) Native gel electrophoresis in strains where autophagy was induced through nitrogen starvation show degradation of bound Blm10 in the vacuole as indicated by the presence of free Venus. Dotted line in right panel, indicates a break in the same gel (one lane in between was cropped out). Blocking autophagy (atg7Δ) prevented the formation of free Venus and both Blm10 bound complexes and free Blm10 were stabilized. (C) SDS-PAGE separation and immunoblot analysis of Blm10 levels following 24 hours growth in YPD indicated bound Blm10 was stabilized when autophagy was blocked, but free Blm10 was not. Free Blm10 was degraded through autophagy, but when this pathway was blocked, it was instead degraded by the proteasome as levels were stabilized in the presence of proteasome inhibitor, PS341 (100 μM). A Blm10 specific antibody was used. PgK1 was used as a loading control.

Overexpression of Blm10 does not alter proteasome storage granule dynamics

In addition to autophagy, proteasomes and proteasome associated proteins are also regulated through re-localization. Under these conditions, UPS components are sequestered into cytoplasmic granules termed proteasome storage granules (PSGs). Previous reports indicated that Blm10 targets CP to proteasome storage granules (PSGs) [173,199] which have been proposed to provide a protective mechanism against autophagy [175,199,245]; however, we failed to observe Blm10 in CP containing granules at 37 °C (Fig. 2-3F) suggesting that granules formed under this stress might involve different targeting mechanisms. Therefore, we evaluated to what extent Blm10 is involved in other granule forming conditions such as glucose starvation as well as how Blm10 itself is affected by these stress conditions. As shown previously, Blm10 is found in the nucleus of logarithmically growing cells. Our data show that Blm10 is able to enter the nucleus independent of CP as conditions where most Blm10 is not bound to CP (strong overexpression or Blm10Δ3 truncation) showed Blm10 predominantly in the nucleus (Supp. Fig. 4A and [199]). Indeed, many Blm10 orthologs contain a canonical nuclear localization signal (NLS) within the C-terminal region of the protein. While bioinformatic analyses of Blm10 (*S. cerevisiae*) did not show a canonical NLS, deletion of the C-terminal region resulted in cytosolic localization of Blm10 [166,233]. This suggests that *S. cerevisiae* Blm10 has a noncanonical NLS.

Blm10 was reported to be required for the granular cytosolic localization of CP following 5 days of growth in YPD or a change in media from glycerol to no carbon source [173,199]. Furthermore, induced overexpression of Blm10 using a galactose inducible system led to CP sequestration into cytosolic granules [173]. We observed no change in CP localization upon overexpression of Blm10 using the GPD promoter in logarithmically growing cells maintained in the same carbon source (glucose). To test the impact of Blm10 overexpression on proteasome localization in cells completely deprived of carbon, we used a doubly tagged strain expressing

GFP-Blm10 from a GPD promoter, and endogenously expressed α1-mCherry. Consistent with strains that contain only one tagged protein, Blm10 and the proteasome can be found in the nucleus of logarithmically growing cells. In sum, overexpression of Blm10 in this doubly tagged strain did not affect localization of CP or induce proteasome granules during logarithmic growth (Fig. 2-6A).

Following 24 hours of glucose starvation, the proteasome can be found localized to granular structures in the cytoplasm. GFP-Blm10 did not colocalize with these granules, but instead remained nuclear (Figure 2-6A). This suggests that unbound Blm10 does not have the signal for granule targeting. It was surprising that we did not see any Blm10 granules as previous reports of quiescence or a switch from glycerol to no carbon have shown colocalization of Blm10 and CP in PSGs [197,199]; however, we cannot exclude that the strong signal in the nucleus obscured the presence of weaker GFP-Blm10 granules. It should be noted that native gel analysis did show a reduction of Blm10 binding to CP under these conditions as we could observe the appearance of RP2-CP and RP-CP complexes despite the presence of unbound Blm10 (Supp. Fig. 4B). Apparently, these conditions are less favorable for Blm10-CP interactions and it is possible that only CP complexes without Blm10 form granules under these conditions.

To further investigate the potential of Blm10 to form granules upon glucose starvation, we tagged Blm10 with GFP under its endogenous promoter using a Cre-Lox based approach. As expected, GFP-Blm10 localized to the nucleus along with α1-mCherry during logarithmic growth. Following glucose starvation, defined granules were observed for α1-mCherry while GFP-Blm10 appeared both diffuse in the cytoplasm as well as in granule-like structures. While both α1-mCherry and GFP-Blm10 showed a change in localization from the nucleus to the cytoplasm, we observed no colocalization of signals (Fig. 2-6B). Consistent with the lack of colocalization, the granules that formed under our assay conditions did not depend on Blm10 as a *blm10*Δ strain was able to successfully form proteasome granules (Fig. 2-6C). As Blm10 has been reported to both colocalize with and aide in PSG formation during quiescence, we tested both our strain and the previously reported strains (generous gift C. Enenkel) for granule formation following glucose starvation. It is possible that Blm10 may be important for granules that form under certain conditions of carbon limitation but not others.

Under the conditions used in our lab, strains expressing β5-GFP but lacking Blm10 readily formed granules similar to wildtype upon glucose starvation (Figure 2-6C). It should be noted that we recently observed that tagging β5, one of the catalytic subunits of CP, resulted in impaired growth (particularly in combination with a deletion of RPN4). A growth phenotype was also observed for the β5-GFP *blm10Δ* strain (Supp. Fig. 2A). While our lab has not observed aberrant proteasome localization with β5-GFP tagged strains under conditions of glucose starvation, we did observe β5-GFP tagged proteasomes in granules upon nitrogen starvation in strains defective for autophagy. This was unique for β5-GFP tagged proteasomes as it was not observed with several other CP-tagged strains, suggesting the GFP tag on β5 can alter the proteasome conformation, composition, or function. This may suggest that depending on the physiological state of the cells, β5 GFP-tagged proteasomes may behave differently. Nevertheless, in our hands, Blm10 was not essential for the formation of PSGs upon glucose starvation in either β5- or α1- GFP tagged strains.

Proteasome storage granules dissipate and proteasomes relocalize to the nucleus upon glucose reintroduction to starved cells. Blm10 has been shown to be required for efficient and timely relocalization of core particles under this condition. In wild-type cells, PSGs dissipate within 15 minutes of nutrient reintroduction, but cells lacking Blm10 showed a delay of CP reentry of about 2 hours [173]. To test whether Blm10 played a role in CP reentry into the nucleus, we first induced granule formation by glucose starvation followed by glucose reintroduction. α1-GFP granules disappeared within fifteen minutes upon glucose reintroduction with the majority of α1-GFP fluorescent signal relocalized to the nucleus (Figure 2-6D). The absence of Blm10 delayed nuclear re-localization by about 5 to 10 minutes, indicating the absence of Blm10 also impacts the efficiency of the process under our conditions. However, this was not nearly as dramatic as when glucose was added to quiescent cells. Thus, glucose starvation induced PSGs can form, and proteasomes can reenter the nucleus, in the absence of Blm10 (Figure 2-6D).

In light of these results, we next aimed to determine if Blm10 dynamics under glucose starvation were similar to proteasome CP dynamics. To test this, strains with endogenously expressed GFP-Blm10 and α1-mCherry were grown for 24 hours in media lacking glucose. This resulted in Blm10 localization to the cytosol and the formation of granule-like structures. 5-minutes after glucose reintroduction, the GFP-Blm10 fluorescence was less abundant in granules and fluorescence was observed in the nucleus and cytoplasm. After 15 minutes, GFP-Blm10 was

enriched in the nucleus to similar levels as seen during logarithmic growth (Figure 2-6E). Thus, Blm10 granules, like PSGs, are readily reversible and can disintegrate quickly following addition of glucose.

Figure 2-6 - Blm10 is not involved in the formation of PSGs following glucose starvation

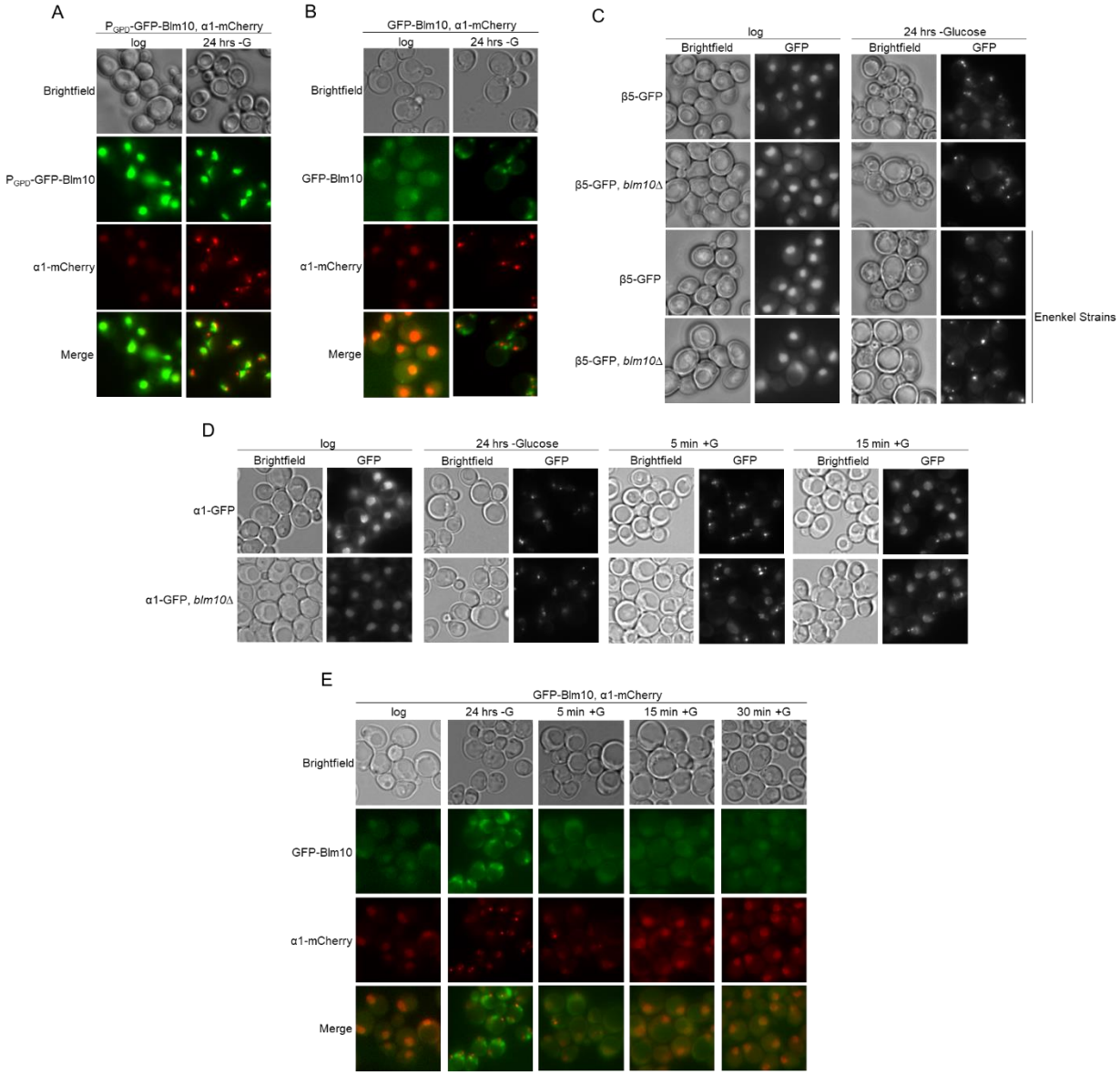

(A) Strains overexpressing GFP-Blm10 and α1-mCherry were visualized using fluorescence microscopy in logarithmically growing cells and following 24 hours of growth in media lacking glucose. GFP-Blm10 remained nuclear following glucose starvation where α1-mCherry formed proteasome storage granules (PSGs). The lack of GFP-Blm10 in these granules indicates that α1-mCherry forms glucose granules independently of GFP-Blm10. (B) Similar results were observed with GFP-Blm10 under its endogenous promoter. α1-mCherry again formed PSGs independent of Blm10 while Blm10 signal was seen both disperse in the cytoplasm and forming granule-like structures. (C) Two sets of strains (our lab and Enenkel lab) expressing β5-GFP but lacking Blm10 were monitored

for granule formation using fluorescence microscopy following 24 hours of glucose starvation. Both Blm10 mutant strains formed granules similar to wildtype indicating PSGs induced under glucose starvation form independently of Blm10. (D) Glucose reintroduction was used to determine if α1-GFP could relocate to the nucleus independently of Blm10. Cells expressing α1-GFP were initially glucose starved for 24 hours. Cells were collected and reinoculated in standard defined media containing glucose and monitored over a 15-minute time course. α1-GFP readily formed granules in the blm10Δ strain and reentered the nucleus similar to the control strain. (E) Glucose reintroduction as described in (D) for strains co-expressing GFP-Blm10 and α1-mCherry. Both GFP-Blm10 and α1-mCherry relocalized back to the nucleus within 15 minutes of glucose reintroduction.

Discussion

The CP houses the proteolytic active sites of the proteasome. However, the ability to degrade ubiquitinated and folded proteins is dependent upon the interaction of CP with RP. RP provides the receptors that recognize substrates, as well as contains the ATPase activity that unfolds and threads the substrates into the CP. Nevertheless, there are other regulators that can bind CP at the same surface as RP, such as human PI31, for which Fub1 seems to be the yeast ortholog, and Blm10 (PA200 in humans). How the cell controls or manages which regulator is bound to the CP is poorly understood [233,247,248]. In addition to competitive binding, which is modulated by affinity and protein levels, CP-regulator interactions could be actively controlled. To determine the extent to which the association between Blm10 and CP is actively regulated, we altered the expression of this regulator and determined the proteasome landscape under those conditions. Interestingly, while overexpression of Blm10 resulted in a dramatic reduction of RP bound to mature CP, we only saw a modest impact with respect to immature CP.

Blm10 and immature CP

Pba1-2 is a heterodimeric assembly chaperone that guides the formation of the CP α-ring as it aides in the incorporation of α5 and α6. Furthermore, its association with the α-ring physically blocks the surface where RP would bind CP, thereby preventing RP from binding to immature CP [97]. As Blm10 binding to CP involves a pocket between α5 and α6 and much of the α-ring surface, binding of Pba1-Pba2 and Blm10 is mutually exclusive. This suggests that either Blm10 binds to immature CP that is assembled independent of Pba1-Pba2, Blm10 binds to immature CP after Pba1-Pba2, or Blm10 binds immature CP prior to Pba1-Pba2. While our data cannot distinguish between these forms, it is intriguing that strong overexpression of Blm10 can readily displace RP from CP, but not Pba1-Pba2 from immature CP (Supp. Fig. 1A). Pba1-Pba2 has been shown to bind immature CP with very high affinity due to specific conformational changes within immature CP upon binding to both Pba1-2 and Ump1 [97,98,208]. Therefore, it seems that Blm10 works through an alternative pathway. Either Pba1-Pba2 is substoichiometric or a subset of immature CP must have a different conformation. Lack of Pba1-Pba2 in purifications

using Ump1-flag, where Blm10 was found and only β7 was missing [101], versus the observed presence of Pba1-Pba2 and Blm10 in Ump1-TAP purifications where both β6 and β7 were missing, might indicate that Pba1-Pba2 is lost late in ½ CP maturation. However, it is likely some conformational changes have to occur to facilitate an exchange between Pba1-2 and Blm10. That said, the human Pba1-Pba2 orthologues, PAC1-PAC2, are proposed to remain bound to immature CP until it matures, suggesting Blm10 would not replace it [211]. It remains to be determined if Blm10 binding to immature CP is structurally similar to its binding to mature CP [107,248]. Regardless, it appears that, unlike what we observed for CP binding, the binding of Blm10 to immature CP does not involve a simple distribution based on affinities and protein levels.

Blm10 binding to mature CP

Under normal physiological conditions, our data show that Blm10 is found solely bound to CP and not detectable as a free protein (see Fig. 2-2B). Consistent with this, increased levels of Blm10 seem to readily displace RP from CP to such an extent that free Blm10 only accumulates after the vast majority of CP has two Blm10 bound. That said, we do observe a small fraction of Blm10-CP-RP that remains present, but we are uncertain if this is a specific subpopulation (see Fig. 2-2B). Considering most CP and RP subunits are essential, we speculate that this amount of Blm10-CP-RP is the minimal amount of RP-CP required to perform the essential functions under normal growth conditions. Apparently, the low RP-CP levels in cells overexpressing Blm10 are sufficient to support cell growth under optimal conditions (see Fig. 2-3D).

Supporting our notion that there is direct competition between Blm10 and RP, RP-CP only reappeared in conditions that reduced the levels of free Blm10. Furthermore, the overexpression of Blm10Δ3 showed no ability to reduce RP-CP levels in the cell, indicating reduction of RP-CP is indeed due to direct competition between RP and Blm10. Interestingly though, we still see a small portion of bound Blm10 in the Blm10Δ3 mutant (see Fig. 2-5B). As a large surface of Blm10 rests upon the alpha ring of CP, it seems likely that weaker interactions might allow for some binding due to the increased abundance of Blm10; however, as the affinity is much lower, we failed to observe any competition with RP. An important implication of this observed competition is that changes in Blm10 levels have a direct impact on RP-CP levels in

the cell. Consistent with this, endogenous levels of Blm10 in the cell are normally substoichiometric allowing for an abundance of 26S (RP-CP complexes).

Blm10 stoichiometry and function

Blm10 is normally present at levels much lower than CP, which suggests that Blm10 either acts only on a subset of CP, or it functions in a temporal and reusable fashion on all CP. The former is consistent with a function in the degradation of certain substrates, like acetylated histones or tau-441 [164,165]. Here, depending on a cell's need, only a subset of Blm10-CP complexes would be required. For substrates to enter the CP they need to be recognized and unfolded. It remains unclear how Blm10-CP would recognize these substrates. Blm10 was reported to have a bromodomain-like region that can recognize acetylated substrates; however, recent structures raised some questions concerning this recognition [174,249]. As Blm10 lacks ATPase activity, its substrates must already be unfolded to allow for entry into CP, which would suggest specific substrates such as intrinsically disordered proteins or Blm10 requires the assistance of an unfolding ATPase. The ATPases p97/Cdc48 is known to assist the 26S proteasome in degradation of tail-lagging substrates [250]. Alternatively, there might be a role for hybrid proteasomes (Blm10-CP-RP) in degrading substrates. Hybrid complexes can be readily observed under normal conditions and the RP can bind and unfold ubiquitinated substrates. Since Blm10 would bind on the other end of CP, its role could then be either as an allosteric regulator or it could impact degradation by regulating peptide release [165,174,233,251].

Consistent with a role in a temporal, reusable fashion, Blm10 has been suggested to act as a chaperone in CP assembly due to its ability to bind immature CP [101,168]. However, to function effectively as a chaperone, one would expect the protein to be, to some extent, present in a free form that can readily associate with newly formed complexes and it remains unclear how it would function in this capacity compared to Pba1-Pba2. Alternatively, Blm10 could be reusable as a factor that facilitates CP cellular localization as has been observed during quiescence and carbon starvation [173,199]. A function for shuttling of CP into PSGs has been proposed; however, these studies indicate Blm10 colocalizes with the core particle in these granules. Considering the low endogenous levels of Blm10 relative to CP and the lack of apparent upregulation under stress conditions, like prolonged growth in YPD and glucose starvation, it would imply that only a small fraction of core particles could be targeted to proteasome storage granules by Blm10. If Blm10 were responsible for targeting all core particles to granules, it should be upregulated to

levels where one Blm10 can bind each CP or at least utilize a mechanism where Blm10 could bind and unbind core particles to shuttle them to these granules.

Autophagic degradation of Blm10

Nitrogen starvation and proteasome inhibitor treatment both induce autophagy of proteasomes (RP and CP complexes). However, it is less clear what happens to other proteasome regulators. Here, we show that nitrogen starvation also induces autophagy of Blm10-CP complexes as well as unbound Blm10. The latter is consistent with a previous report where Blm10-GFP was monitored following nitrogen starvation [199]. Since both Blm10 and RP-CP complexes are degraded, the reduction of Blm10 in the overexpressing strain does not cause any recovery of RP-CP complexes upon nitrogen starvation. When cells were grown in YPD for 24-48 hours or starved of glucose, there was no reported autophagy of proteasomes. Therefore, it was particularly surprising to observe that Blm10-CP complexes and unbound Blm10 were specifically targeted for autophagic degradation under these conditions. Indeed, cells overexpressing Blm10 showed a strong recovery of RP-CP complexes because Blm10 was degraded via autophagy. This suggests some syntheses of new CP complexes, or release of CP from Blm10 to allow for the formation of RP-CP complexes.

While these effects were more dramatically observed upon Blm10 overexpression, we also observed autophagic degradation of endogenously expressed Blm10 indicating these observations are physiologically relevant. While we report a strong stabilization of Blm10-CP complexes in strains defective for autophagy, we also observed some modest effect of treatment with proteasome inhibitor, in particular, for unbound Blm10Δ3. As this degradation was minor compared to the autophagy, we expect this to result from more general misfolded and protein quality control-based pathways than a specific cellular response or regulation of proteasome complexes. The ability of cells to degrade unbound Blm10 and CP-bound Blm10, but not other forms of CP, could indicate that Blm10 possesses a specific autophagy targeting signal although specific modifications have yet to be identified. Alternatively, the binding of Blm10 to the core particle might induce conformational changes within this complex that make it more readily recognized and targeted for degradation compared to CP alone or RP-CP complexes. The human orthologue of Blm10, PA200, has indeed been shown to induce conformational changes in CP as binding changes the specificity of the proteolytic active sites [174]. While the specific mechanism

of how Blm10 bound complexes are targeted for degradation remains to be determined, it is clear that they are degraded through the process of autophagy.

Blm10 and nuclear import

Under optimal growth conditions Blm10 is highly enriched in the nucleus, but it has been observed to be required for formation of cytosolic granules in quiescence as well as cells grown in and depleted of glycerol [173]. In our hands, endogenously expressed Blm10 was able to form granule-like structures under glucose starvation similar to what has been reported for cells starved of glycerol; however, most of these structures were void of CP [199]. Furthermore, Blm10 is important for efficient nuclear import of CP upon removal of nutrient stress (Fig. 2-6D and [173]) . While we observed a role for Blm10 in proteasome nuclear import after glucose starvation, this function was not as essential as has been reported for recovery from quiescence.

In all, our data show that Blm10 can directly compete with RP for binding to CP, suggesting Blm10 levels may be tightly regulated. As formation of 26S proteasomes is vital to cell survival, it's important to understand that any changes in levels of potential competitors like Blm10 can have effects on the proteasome as well as the cell as a whole. It appears that cells utilize a mechanism of clearing potential competitors as prolonged growth in YPD (24-48 hours) results in the selective autophagic degradation of Blm10 leading to reduced levels of Blm10-CP complexes and increased RP-CP levels. It will be important to understand the mechanisms of how these various complexes are differentially modified in response to specific stress conditions.

References

1. Groll, M. *et al.* Structure of 20S proteasome from yeast at 2.4 A resolution. *Nature* **386**, 463–71 (1997).

2. Marques, A. J., Palanimurugan, R., Matias, A. C., Ramos, P. C. & Dohmen, R. J. Catalytic mechanism and assembly of the proteasome. *Chem. Rev.* **109**, 1509–36 (2009).

3. Vigneron, N. & Van den Eynde, B. J. Proteasome subtypes and regulators in the processing of antigenic peptides presented by class I molecules of the major histocompatibility complex. *Biomolecules* **4**, 994–1025 (2014).

4. Reits, E. *et al.* Peptide Diffusion, Protection, and Degradation in Nuclear and Cytoplasmic Compartments before Antigen Presentation by MHC Class I. *Immunity* **18**, 97–108 (2003).

5. Groll, M. *et al.* A gated channel into the proteasome core particle. *Nat. Struct. Biol.* **7**, 1062–1067 (2000).

6. Groll, M. & Huber, R. Substrate access and processing by the 20S proteasome core particle. *Int. J. Biochem. Cell Biol.* **35**, 606–616 (2003).

7. Husnjak, K. *et al.* Proteasome subunit Rpn13 is a novel ubiquitin receptor. *Nature* **453**, 481–488 (2008).

8. Schreiner, P. *et al.* Ubiquitin docking at the proteasome via a novel PH domain interaction. *Nature* **453**, 548–552 (2008).

9. Shi, Y. *et al.* Rpn1 provides adjacent receptor sites for substrate binding and deubiquitination by the proteasome. *Science (80-.).* **351**, (2016).

10. Deveraux, Q., Ustrell, V., Pickart, C. & Rechsteiner, M. A 26 S protease subunit that binds ubiquitin conjugates. *J. Biol. Chem.* **269**, 7059–7061 (1994).

11. Smith, D. M. *et al.* Docking of the Proteasomal ATPases' Carboxyl Termini in the 20S Proteasome's α Ring Opens the Gate for Substrate Entry. *Mol. Cell* **27**, 731–744 (2007).

12. Sadre-Bazzaz, K., Whitby, F. G., Robinson, H., Formosa, T. & Hill, C. P. Structure of a Blm10 Complex Reveals Common Mechanisms for Proteasome Binding and Gate Opening. *Mol. Cell* **37**, 728–735 (2010).

13. Rabl, J. *et al.* Mechanism of gate opening in the 20S proteasome by the proteasomal ATPases. *Mol Cell* **30**, 360–368 (2008).

14. Strehl, B. *et al.* Interferon-γ, the functional plasticity of the ubiquitin-proteasome system, and MHC class I antigen processing. *Immunological Reviews* **207**, 19–30 (2005).

15. Stadtmueller, B. M. *et al.* Structure of a proteasome Pba1-Pba2 complex implications for proteasome assembly, activation, and biological function. *J. Biol. Chem.* **287**, 37371–37382 (2012).

16. McCutchen-Maloney, S. L. *et al.* cDNA cloning, expression, and functional characterization of PI31, a proline-rich inhibitor of the proteasome. *J. Biol. Chem.* **275**, 18557–18565 (2000).

17. Li, X., Thompson, D., Kumar, B. & DeMartino, G. N. Molecular and cellular roles of PI31 (PSMF1) protein in regulation of proteasome function. *J. Biol. Chem.* **289**, 17392–17405 (2014).

18. Wani, P. S., Rowland, M. A., Ondracek, A., Deeds, E. J. & Roelofs, J. Maturation of the proteasome core particle induces an affinity switch that controls regulatory particle association. *Nat. Commun.* **6**, 6384 (2015).

19. Hirano, Y. *et al.* A heterodimeric complex that promotes the assembly of mammalian 20S proteasomes. *Nature* **437**, 1381–1385 (2005).

20. Weberruss, M. H. *et al.* Blm10 facilitates nuclear import of proteasome core particles. *EMBO J.* **32**, 2697–2707 (2013).

21. Li, X. *et al.* The SRC-3/AIB1 coactivator is degraded in a ubiquitin- and ATP-independent manner by the REGγ proteasome. *Cell* **124**, 381–392 (2006).

22. Li, X. *et al.* Ubiquitin- and ATP-Independent Proteolytic Turnover of p21 by the REGγ-Proteasome Pathway. *Mol. Cell* **26**, 831–842 (2007).

23. Chen, X., Barton, L. F., Chi, Y., Clurman, B. E. & Roberts, J. M. Ubiquitin-Independent Degradation of Cell-Cycle Inhibitors by the REGγ Proteasome. *Mol. Cell* **26**, 843–852 (2007).

24. Nie, J. *et al.* REGγ proteasome mediates degradation of the ubiquitin ligase Smurf1. *FEBS Lett.* **584**, 3021–3027 (2010).

25. Suzuki, R. *et al.* Proteasomal turnover of hepatitis C virus core protein is regulated by two distinct mechanisms: a ubiquitin-dependent mechanism and a ubiquitin-independent but PA28gamma-dependent mechanism. *J. Virol.* **83**, 2389–92 (2009).

26. Hoffman, L., Pratt, G. & Rechsteiner, M. Multiple forms of the 20 S multicatalytic and the 26 S ubiquitin/ATP-dependent proteases from rabbit reticulocyte lysate. *J. Biol. Chem.* **267**, 22362–8 (1992).

27. Hendil, K. B., Khan, S. & Tanaka, K. Simultaneous binding of PA28 and PA700 activators to 20 S proteasomes. *Biochem. J.* **332**, 749–754 (1998).

28. Tanahashi, N. *et al.* Induction by interferon-gamma and contribution to ATP-dependent proteolysis. *J. Biol. Chem.* **275**, 14336–45 (2000).

29. Dick, T. P. *et al.* Coordinated dual cleavages induced by the proteasome regulator PA28 lead to dominant MHC ligands. *Cell* **86**, 253–62 (1996).

30. Murata, S., Takahama, Y., Kasahara, M. & Tanaka, K. The immunoproteasome and thymoproteasome: functions, evolution and human disease. *Nature Immunology* **19**, 923–931 (2018).

31. Zhang, Z. *et al.* Identification of an activation region in the proteasome activator REGalpha. *Proc. Natl. Acad. Sci. U. S. A.* **95**, 2807–11 (1998).

32. Förster, A., Masters, E. I., Whitby, F. G., Robinson, H. & Hill, C. P. The 1.9 A structure of a proteasome-11S activator complex and implications for proteasome-PAN/PA700 interactions. *Mol. Cell* **18**, 589–99 (2005).

33. Dange, T. *et al.* Blm10 Protein Promotes Proteasomal Substrate Turnover by an Active Gating Mechanism. *J. Biol. Chem.* **286**, 42830–42839 (2011).

34. Qian, M. X. *et al.* Acetylation-mediated proteasomal degradation of core histones during DNA repair and spermatogenesis. *Cell* **153**, 1012–1024 (2013).

35. Mandemaker, I. K. *et al.* DNA damage-induced replication stress results in PA 200-proteasome-mediated degradation of acetylated histones. *EMBO Rep.* **19**, (2018).

36. Krugel, U. *et al.* Proteasomal degradation of Sfp1 contributes to the repression of ribosome biogenesis during starvation and is mediated by the proteasome activator Blm10. *Mol. Biol. Cell* **22**, 528–540 (2011).

37. Kock, M. *et al.* Proteasome assembly from 15S precursors involves major conformational changes and recycling of the Pba1-Pba2 chaperone. *Nat. Commun.* **6**, 6123 (2015).

38. Fehlker, M., Wendler, P., Lehmann, A. & Enenkel, C. Blm3 is part of nascent proteasomes and is involved in a late stage of nuclear proteasome assembly. *EMBO Rep.* **4**, 959–963 (2003).

39. Marques, A. J., Glanemann, C., Ramos, P. C. & Dohmen, R. J. The C-terminal extension of the beta7 subunit and activator complexes stabilize nascent 20 S proteasomes and promote their maturation. *J. Biol. Chem.* **282**, 34869–76 (2007).

40. Ustrell, V., Hoffman, L., Pratt, G. & Rechsteiner, M. PA200, a nuclear proteasome activator involved in DNA repair. *EMBO J.* **21**, 3516–25 (2002).

41. Khor, B. *et al.* Proteasome Activator PA200 Is Required for Normal Spermatogenesis. *Mol. Cell. Biol.* **26**, 2999–3007 (2006).

42. Blickwedehl, J. *et al.* Proteasomes and Proteasome Activator 200 kDa (PA200) Accumulate on Chromatin in Response to Ionizing Radiation. *Radiat. Res.* **167**, 663–674 (2007).

43. Blickwedehl, J. *et al.* Role for proteasome activator PA200 and postglutamyl proteasome activity in genomic stability. *Proc. Natl. Acad. Sci. U. S. A.* **105**, 16165–70 (2008).

44. Tar, K. *et al.* Proteasomes associated with the blm10 activator protein antagonize mitochondrial fission through degradation of the fission protein dnm1. *J. Biol. Chem.* **289**, 12145–12156 (2014).

45. Toste Rêgo, A. & da Fonseca, P. C. A. Characterization of Fully Recombinant Human 20S and 20S-PA200 Proteasome Complexes. *Mol. Cell* **76**, 138-147.e5 (2019).

46. Goldstein, A. L. & McCusker, J. H. Three new dominant drug resistance cassettes for gene disruption in *Saccharomyces cerevisiae*. *Yeast* **15**, 1541–1553 (1999).

47. Longtine, M. S. *et al.* Additional modules for versatile and economical PCR-based gene deletion and modification in *Saccharomyces cerevisiae*. *Yeast* **14**, 953–961 (1998).

48. Prein, B., Natter, K. & Kohlwein, S. D. A novel strategy for constructing N-terminal chromosomal fusions to green fluorescent protein in the yeast *Saccharomyces cerevisiae*. *FEBS Lett.* **485**, 29–34 (2000).

49. Roelofs, J., Suppahia, A., Waite, K. A. & Park, S. Native gel approaches in studying proteasome assembly and chaperones. in *Methods in Molecular Biology* **1844**, 237–260 (Humana Press Inc., 2018).

50. Sundin, B. A., Chiu, C.-H., Riffle, M., Davis, T. N. & Muller, E. G. D. Localization of proteins that are coordinately expressed with Cln2 during the cell cycle. *Yeast* **21**, 793–800 (2004).

51. Cascio, P., Call, M., Petre, B. M., Walz, T. & Goldberg, A. L. Properties of the hybrid form of the 26S proteasome containing both 19S and PA28 complexes. *EMBO J.* **21**, 2636–2645 (2002).

52. Kopp, F., Dahlmann, B. & Kuehn, L. Reconstitution of hybrid proteasomes from purified PA700-20 S complexes and PA28αβ activator: Ultrastructure and peptidase activities. *J. Mol. Biol.* **313**, 465–471 (2001).

53. Schmidt, M. *et al.* The HEAT repeat protein Blm10 regulates the yeast proteasome by capping the core particle. *Nat. Struct. Mol. Biol.* **12**, 294–303 (2005).

54. Elsasser, S., Schmidt, M. & Finley, D. Characterization of the proteasome using native gel electrophoresis. *Methods in Enzymology* **398**, 353–363 (2005).

55. Leggett, D. S. *et al.* Multiple associated proteins regulate proteasome structure and function. *Mol. Cell* **10**, 495–507 (2002).

56. Kleijnen, M. F. *et al.* Stability of the proteasome can be regulated allosterically through engagement of its proteolytic active sites. *Nat. Struct. Mol. Biol.* **14**, 1180–1188 (2007).

57. Lee, S. Y.-C., De la Mota-Peynado, A. & Roelofs, J. Loss of Rpt5 protein interactions with the core particle and Nas2 protein causes the formation of faulty proteasomes that are inhibited by Ecm29 protein. *J. Biol. Chem.* **286**, 36641–51 (2011).

58. De La Mota-Peynado, A. *et al.* The proteasome-associated protein Ecm29 inhibits proteasomal ATPase activity and in vivo protein degradation by the proteasome. *J. Biol. Chem.* **288**, 29467–29481 (2013).

59. Marshall, R. S., Li, F., Gemperline, D. C., Book, A. J. & Vierstra, R. D. Autophagic Degradation of the 26S Proteasome Is Mediated by the Dual ATG8/Ubiquitin Receptor RPN10 in Arabidopsis. *Mol. Cell* **58**, 1053–66 (2015).

60. Waite, K. A., De-La Mota-Peynado, A., Vontz, G. & Roelofs, J. Starvation Induces Proteasome Autophagy with Different Pathways for Core and Regulatory Particles. *J. Biol. Chem.* **291**, 3239–53 (2016).

61. Klionsky, D. J. *et al.* Guidelines for the use and interpretation of assays for monitoring autophagy (3rd edition). *Autophagy* **12**, 1–222 (2016).

62. Marshall, R. S. & Vierstra, R. D. Proteasome storage granules protect proteasomes from autophagic degradation upon carbon starvation. *Elife* **7**, e34532 (2018).

63. Janke, C. *et al.* A versatile toolbox for PCR-based tagging of yeast genes: New fluorescent proteins, more markers and promoter substitution cassettes. *Yeast* **21**, 947–962 (2004).

64. Li, X., Kusmierczyk, A. R., Wong, P., Emili, A. & Hochstrasser, M. b-Subunit appendages promote 20S proteasome assembly by overcoming an Ump1-dependent checkpoint. *EMBO J.* **26**, 2339–2349 (2007).

65. Kock, M. *et al.* Proteasome assembly from 15S precursors involves major conformational changes and recycling of the Pba1-Pba2 chaperone. *Nat. Commun.* **6**, 6123 (2015).

66. Xie, Y. & Varshavsky, A. RPN4 is a ligand, substrate, and transcriptional regulator of the 26S proteasome: a negative feedback circuit. *Proc. Natl. Acad. Sci. U. S. A.* **98**, 3056–61 (2001).

67. Dohmen, R. J., Willers, I. & Marques, A. J. Biting the hand that feeds: Rpn4-dependent feedback regulation of proteasome function. *Biochimica et Biophysica Acta - Molecular Cell Research* **1773**, 1599–1604 (2007).

68. Kruegel, U. *et al.* Elevated proteasome capacity extends replicative lifespan in saccharomyces cerevisiae. *PLoS Genet.* **7**, (2011).

69. Shirozu, R., Yashiroda, H. & Murata, S. Identification of minimum Rpn4-responsive elements in genes related to proteasome functions. *FEBS Lett.* **589**, 933–940 (2015).

70. Enenkel, C. *et al.* Ubiquitin orchestrates proteasome dynamics between proliferation and quiescence in yeast. *Mol. Biol. Cell* **28**, 2479–2491 (2017).

71. Mannhaupt, G., Schnall, R., Karpov, V., Vetter, I. & Feldmann, H. Rpn4p acts as a transcription factor by binding to PACE, a nonamer box found upstream of 26S proteasomal and other genes in yeast. *FEBS Lett.* **450**, 27–34 (1999).

72. Park, S., Kim, W., Tian, G., Gygi, S. P. & Finley, D. Structural defects in the regulatory particle-core particle interface of the proteasome induce a novel proteasome stress response. *J. Biol. Chem.* **286**, 36652–36666 (2011).

73. Park, S., Kim, W., Tian, G., Gygi, S. P. & Finley, D. Structural defects in the regulatory particle-core particle interface of the proteasome induce a novel proteasome stress response. *J. Biol. Chem.* **286**, 36652–66 (2011).

74. Wani, P. S., Suppahia, A., Capalla, X., Ondracek, A. & Roelofs, J. Phosphorylation of the C-terminal tail of proteasome subunit α7 is required for binding of the proteasome quality control factor Ecm29. *Nat. Publ. Gr.* (2016). doi:10.1038/srep27873

75. Nemec, A. A., Howell, L. A., Peterson, A. K., Murray, M. A. & Tomko, R. J. Autophagic clearance of proteasomes in yeast requires the conserved sorting nexin Snx4. *J. Biol. Chem.* **292**, 21466–21480 (2017).

76. Reggiori, F. & Klionsky, D. J. Autophagic processes in yeast: Mechanism, machinery and regulation. *Genetics* **194**, 341–361 (2013).

77. Laporte, D., Salin, B., Daignan-Fornier, B. & Sagot, I. Reversible cytoplasmic localization of the proteasome in quiescent yeast cells. *J. Cell Biol.* **181**, 737–745 (2008).

78. Ortega, J. *et al.* The Axial Channel of the 20 S Proteasome Opens Upon Binding of the PA200 Activator. *J. Mol. Biol.* **346**, 1221–1227 (2005).

79. Iwanczyk, J. *et al.* Structure of the Blm10–20 S Proteasome Complex by Cryo-electron Microscopy. Insights into the Mechanism of Activation of Mature Yeast Proteasomes. *J. Mol. Biol.* **363**, 648–659 (2006).

80. Guan, H. *et al.* Cryo-EM structures of the human PA200 and PA200-20S complex reveal regulation of proteasome gate opening and two PA200 apertures. *PLoS Biol.* **18**, (2020).

81. Beskow, A. *et al.* A Conserved Unfoldase Activity for the p97 AAA-ATPase in Proteasomal Degradation. *J. Mol. Biol.* **394**, 732–746 (2009).

82. Formosa, T. *et al.* Structure of the Blm10–20 S Proteasome Complex by Cryo-electron Microscopy. Insights into the Mechanism of Activation of Mature Yeast Proteasomes. *J. Mol. Biol.* **363**, 648–659 (2006).

Chapter 3 - Rpn11 Integrity is Vital for Proteasome Assembly and Nuclear Export

Alicia Burris[1,2], Kenrick A. Waite[1], and Jeroen Roelofs[1,2#]

[1] Department of Biochemistry and Molecular Biology, University of Kansas Medical Center, Kansas City, 3901 Rainbow Blvd, HLSIC 1077,Kansas, USA

[2] Molecular, Cellular, and Developmental Biology Program, Division of Biology, Kansas State University, 338 Ackert Hall, Manhattan, Kansas 66506 USA

Abstract

Proteasomes are multisubunit complexes composed of two major subcomplexes, the core particle (CP) and the regulatory particle (RP), which can further be divided into the lid and base subcomplexes. Interactions between the RP and CP produce a functional protease that targets ubiquitinated substrates for degradation. While the CP contains proteolytic active sites to fragment the substrate protein, RP is responsible for binding the substrate, removing its ubiquitin tag and unfolding it into the core particle where its degraded. Removal of the ubiquitin tag is necessary as it impedes the ability of the proteasome to thread the unfolded substrate through the narrow channel of the core particle. The process of deubiquitination is facilitated by the RP subunit, Rpn11, which is one of nine subunits that make up the lid subcomplex of the regulatory particle. The N-terminal domain of Rpn11 is involved in its deubiquitinase activity while its C-terminus alpha helix is required for lid assembly and proteasome localization under stress. Here, we characterize a Rpn11 mutant, Rpn11-Δ31, which lacks the terminal alpha helix in an attempt to understand the mechanism behind how this truncation affects nuclear export of the proteasome. Rpn11-Δ31 prevents association of late stage lid subunits which include Rpn3, Rpn7 and Rpn12. Therefore, these unincorporated subunits could be central to proteasome nuclear export. To determine their involvement, we utilized tagged versions of Rpn7 and Rpn12 to establish whether these subunits could be exported independently of the rest of the proteasome. While our results show the formation of proteasome storage granules, which result from nuclear export, further analysis indicates that these subunits form foci when unincorporated into the proteasome rather than being exported specifically. Furthermore, while these subunits contain putative nuclear export signals for common export factor Crm1, our studies indicate that this export mechanism is not involved in nuclear export of the proteasome. In all, this work suggests that proper assembly of the proteasome is required for nuclear export and PSG formation during stress conditions.

Introduction

The optimal function of cells requires proteins to be properly folded and be present at a specific concentration. The regulation of this is known as proteostasis and involves processes that control synthesis, folding, localization, and degradation of proteins. Here, the ubiquitin-proteasome system (UPS) is responsible for the degradation of many misfolded proteins, like defective ribosomal products (DRiPs), or short-lived proteins, like cyclins, cyclin-dependent kinases, and transcription factors [252–254]. To target these substrates to the proteasome for degradation, they are labelled with a polyubiquitin chain. This labelling involves a number of enzymatic reactions where finally a ubiquitin E3 ligase recognizes the substrate and, with the assistance of a ubiquitin conjugating E2 enzyme, marks the substrates with a ubiquitin or a chain of ubiquitins. These marked substrates are recognized by ubiquitin receptors within the proteasome holoenzyme and sometimes with the help of adapter proteins known as shuttle factors. The proteasome consists of two major subcomplexes, the core particle (CP) and the regulatory particle (RP). The core particle consists of four heteroheptameric rings stacked together in the $\alpha_{1-7}\beta_{1-7}\beta_{1-7}\alpha_{1-7}$ conformation to form a cylinder with an inner chamber and one pore at either end. Three of the seven β subunits (β1, β2, β5) contain proteolytic active sites that lie within the chamber of the core particle. These sites have different specificities to facilitate the degradation of a wide range of substrates [103,201]. For CP by itself (free CP), the pores at either end are occluded by the N-termini of the alpha subunits. Collectively, they work as a gate since binding to an activator, like the regulatory particle, causes conformational changes that facilitate the movement of these N-termini resulting in an open pore which the substrate can enter the core particle through [104,112].

Furthermore, RP contains two enzymatic activities: deubiquitinase activity and ATPase activity [104,105]. A heterohexomeric ring of AAA-ATPases hydrolyzes ATP, which provides the energy to create a mechanical force that results in substrate unfolding and threading of the linear polypeptide through the gate and into the core particle [112]. The deubiquitinase activity removes ubiquitin from substrates to ensure it does not impede degradation. This activity also allows for the recycling of ubiquitin and can regulate substrate association with the proteasome [153,154]. The regulatory particle can be subdivided into the lid and base subcomplexes. The base of the regulatory particle is composed of Rpn1, Rpn2, Rpn13, and six Rpt AAA-ATPase subunits, Rpt1 to Rpt6. Rpn1, Rpn13, and Rpn10, a subunit that stabilizes lid-base interactions, function as

intrinsic ubiquitin receptors. The lid is composed of nine subunits, two MPN domain containing subunits, Rpn11 and Rpn8, six PCI domain-containing subunits, Rpn3, Rpn5-7, Rpn9 and Rpn12, and Rpn15. The MPN domain containing family can be subdivided into MPN+ and MPN- containing proteins. The MPN+ containing proteins, like Rpn11, are metalloenzymes that coordinate a zinc ion and facilitate isopeptidase activity while the MPN- proteins, like Rpn8, lack the proper residues for zinc binding and therefore have no catalytic activity [153]. For large complexes like the proteasome, the MPN+ and MPN- domain containing proteins often associate with one another although the reason for this dimerization remains unclear [155,255]. The PCI domains of the six lid subunits are thought to play a scaffolding role to help stabilize protein-protein interactions [256].

The MPN and PCI domain containing lid subunits all have either one or multiple C-terminal helices that combine to form a helical bundle which drives lid assembly [160]. First, Rpn11 and Rpn8 dimerize. Next, Rpn9 and Rpn5 interact with the Rpn11/Rpn8 dimer via their C-terminal helices which is followed by the addition of Rpn6. Next a complex of Rpn7, Rpn3 and Rpn15 associates [257–259]. The helical bundle is completed with the incorporation of Rpn12. Rpn12 acts as a quality control factor for bundle formation as it requires all other subunits to be present before binding. Furthermore, it is an essential subunit for lid and base interactions as it prevents incomplete lid subcomplexes from being incorporated into RP [260].

As mentioned, Rpn11 has isopeptidase activity which functions to remove the polyubiquitin tag from substrates to facilitate their entry into the core particle [153–155]. This activity is provided by the N-terminal domain of Rpn11. The C-terminal helix of Rpn11, however, also performs a number of crucial functions. At the core of the helical bundle, it is involved in lid stabilization [261]. Furthermore, it has some unique but poorly understood functions in mitochondrial morphology, cell cycle progression, and proteasome localization [262–264]. These latter functions were derived from studies that employed a mutant form of Rpn11 called *rpn11-m1* (*mpr1-1*) that contains a frameshift mutation at the C-terminus. This mutation replaces the last 31 amino acids with 9 arbitrary residues followed by a premature stop [263]. Under stressors like glucose starvation or quiescence, proteasomes, normally found in the nucleus, are exported to the cytoplasm where they form granular structures called proteasome storage granules (PSGs) [175]; however, strains harboring *rpn11-m1* displayed lidless proteasomes that failed to form these granules [153,261,262]. Therefore, we hypothesized that the Rpn11 tail was involved, either directly or

indirectly, in nuclear export and PSG localization. Here, we further characterize the C-terminal tail of Rpn11 to explore its effects on nuclear export.

Materials and Methods

Strains – Yeast strain information can be found in Table 3-1. Standard PCR-based approaches were used to truncate Rpn11, perform knockout genes and tag proteins at the endogenous loci. Primers utilized in these processes are provided in Table 3.2. The *crm1* strains were a generous gift from Dr. Rosbash at HHMI [265]. All strains in this paper, except for those indicated, come from a DF5 background genotype (*lys2-801 leu2-3, 2-112 ura3-52 his3Δ200 trp1-1*) except strains made from those provided by Dr. Rosbash (*). sJR1435 and sJR1560 came from sJR1360 (MNY7). sJR1436 and sJR1561 came from sJR1361 (MNY8) Background is: *MATA ade2, his3, leu2, trp1, ura3*. sJR1507 came from a knockout library with genotype *MATα his3Δ1 lysΔ0 ura2Δ0* [266].

Table 3-1 - Strains

Strain	*Genotype (lys2-801 leu2-3, 2-112 ura3-52 his3Δ200 trp1-1)*	Figure
sUB61	*MATα lys2-801 leu2-3, 2-112 ura3-52 his3Δ200 trp1-1*	S3B,3D-E
sJR622	*MATα pre1::PRE1-TevProA (HIS3) scl1::SCL1-CFP (HYGRO)*	S1A
sJR632	*MATα pre1::PRE1-TevProA (HIS3) pre8::PRE8-CFP (HYGRO)*	S1A
sJR797	*MATα pre1::PRE1-TevProA (HIS3) pup3::PUP3-YFP (KanMX)*	S1A
sJR861	*MATα rpn1::RPN1-GFP (HIS)*	1A,1C-E,2B,2D
sJR869	*MATα rpn11::RPN11-TevProA (HIS3)*	1A
sJR1084	*MATα scl1::SCL1-GFP (HIS)*	S3A
sJR1105	*MATα rpn1::RPN1-GFP (HIS) rpn11::Rpn11-TevProA (HIS3)*	1A
sJR1242	*MATα rpn1::RPN1-GFP (HIS) rpn11P276-307Δ (KanMX)*	1A,1C-E,2B-D,S3A-B
sJR1320	*MATα rpn1::RPN1-GFP (HIS) rpn11A298-307Δ (KanMX)*	2B
sJR1336	*MATα rpn1::RPN1-GFP (HIS) rpn11A284-307Δ (KanMX)*	2B
sJR1343	*MATA pre6::PRE6-GFP (HIS)*	1C
sJR1364	*MATA pre6::PRE6-GFP (HIS) rpn11P276-307Δ (KanMX)*	1C
sJR1365	*MATA rpn1::RPN1-GFP (TRP) rpn11P276-307Δ (KanMX) ura3-1::pRPN7rpn11P276-307(HIS)*	2C
sJR1366	*MATA rpn1::RPN1-GFP (TRP) rpn11P276-307Δ (KanMX) ura3-1::pGPDrpn11P276-307 (HIS)*	2C-D
sJR1409	*MATA pre6::PRE6-GFP (HIS) rpn11E286A,N290A*	S2A
sJR1421	*MATα rpn1::RPN1-GFP (HIS) rpn11P276-307Δ (KanMX) ecm29::TRP*	3A
sJR1432	*MATα rpn1::RPN1-GFP (HIS) rpn11L288A,I292A,V293A,V295A,L296A (KanMX)*	S2C

sJR1433	*MATα rpn1::RPN1-GFP (HIS) rpn11T287A,S294A,T297A (KanMX)*	S2C
sJR1435 *	*MATA crm1::KanMX + pDC-CRM1 (LEU2/CEN) scl1::SCL1-GFP (HIS)*	5B
sJR1436 *	*MATA crm1::KanMX + pDC-CRM1T539C (LEU2/CEN) scl1::SCL1-GFP (HIS)*	5B
sJR1460	*MATα rpn11::RPN11-TevProA (HIS3) ecm29::GPDpECM29 (KanMX) blm10::CloNAT*	S4A-B
sJR1506	*MATα pre1::PRE1-TevProA (HIS3) rpn11P276-307Δ (KanMX)*	3B
sJR1507	*MSN5:KanMX pre6::PRE6-GFP (HIS)*	5C
sJR1521	*MATA rpn5::ADHpGFP-RPN5 (CloNAT)*	3C
sJR1523	*MATA rpn7::ADHpGFP-RPN7 (CloNAT)*	3C,3E
sJR1524	*MATA rpn12::ADHpGFP-RPN12 (CloNAT)*	3C-E
sJR1525	*MATA rpn12::ADHpGFP-RPN12 (CloNAT) rpn11P276-307Δ (KanMX)*	3C-E
sJR1526	*MATA rpn7::ADHpGFP-RPN7 (CloNAT) rpn11P276-307Δ (KanMX)*	3C,3E,4B
sJR1527	*MATA rpn5::ADHpGFP-RPN5 (CloNAT) rpn11P276-307Δ (KanMX)*	3C
sJR1560 *	*MATA crm1::KanMX + pDC-CRM1 (LEU2/CEN) ura3-1::pRPN7NES-Unstable-GFP (HIS)*	5A
sJR1561 *	*MATA crm1::KanMX + pDC-CRM1T539C (LEU2/CEN) ura3-1::pRPN7NES-Unstable-GFP (HIS)*	5A
sJR1562	*MATA rpn7::ADHpGFP-RPN7 (CloNAT) rpn11P276-307Δ (KanMX) pre6::PRE6-mCherry (Hygro)*	4A,4C
sJR1563	*MATA rpn12::ADHpGFP-RPN12 (CloNAT) rpn11P276-307Δ (KanMX) pre6::PRE6-mCherry (Hygro)*	4A

Rpn11 mutant strains – The Rpn11 ORF was amplified by PCR using S. cerevisiae genomic DNA with primers designed to incorporate a PacI and AscI cut site at either end of Rpn11 (see Table 3.2). The resulting PCR product was cloned into pFA6-3HA-natMX6 using PacI (#R0547L: New England BioLabs) and AscI (#R0558L: New England BioLabs), which replaces the HA tag with the Rpn11 ORF. Mutations of the Rpn11 ORF were introduced into this plasmid by PCR (for primers see Table 3-2) and confirmed by sequencing. The newly created plasmids functioned as templates to amplify the (mutated) Rpn11 ORF, an aldehyde terminator and the ClonNAT selection cassette by PCR. These fragments were integrated at the endogenous locus and confirmed for proper integration with sequencing.

Table 3-2 - Primers

Manipulation	Frwd 5' – 3'	Rvrs 5' – 3'	Template
Rpn11 ORF amplification	pRL632 cccgggttaattaaatggaacgactacagagattgatg	pRL633 agaagtggcgcgccttatttaattgccactgaattaacacccg	sUB61 gDNA
blm10Δ	pf2Blm10 CTGTCATCAGGGCTTG-3	pr2Blm10 GTTGATCATTCTCAGTGG-3	sJR395 gDNA

rpn1-GFP	pRL560 TTG AGG GCG TAG TAA TTT TAA AGA AGA ACC CTG ACT ATC GTG AAG AGG AGC GTA CGC TGC AGG TCG AC	Rvrs/Rpn1 TTT GAA TTT TTC CTA TTC TGG TTG ATA TTG CCC AAA AGC TAT TCA GTT TAA TCG ATG AAT TCG AGC TCG	pNU293 (pYM28)
P_{GPD}Ecm29	pfEcm29Ntags1 CAATAATTATAGAAAAGTTTCTATTTCACCACGAACAAC ATTCGTACGCTGCAGGTCGAC	pRL273 TCTCCACGAGCTGTTTTTCTTTCGCTTCGTCAGAAGAA ATGGACATCGATGAATTCTCTGTCG	pNU326 (pYM-N14)
Rpn11P276-307Δ (Rpn11Δ31)	pRL656 GAAGAACTTAAGACAAGATACGTTGGTAGGCAAGATTA AGCGAATTTCTTATGA	Rvrs/Rpn11 AGT GGG CTT TCT AGT TAT TTA ATG CAT AAT GAC TTT ATA AAA TTT GTT TAA TCG ATG AAT TCG AGC TCG	pNU170 pFA6a-GFP (S65T)-kanMX6
Rpn11A298-307Δ (Rpn11Δ9)	pRL726 GAGACACTAGAGAACAATATTGTTTCTGTGCTGACGTAA GCGAATTTCTTATGA	Rvrs/Rpn11 AGT GGG CTT TCT AGT TAT TTA ATG CAT AAT GAC TTT ATA AAA TTT GTT TAA TCG ATG AAT TCG AGC TCG	pNU170 pFA6a-GFP (S65T)-kanMX6
Rpn11A284-307Δ (Rpn11Δ23)	pRL727 GGTAGGCAAGATCCAAAGAAGCACCTTTCCGAAACATA AGCGAATTTCTTATGA	Rvrs/Rpn11 AGT GGG CTT TCT AGT TAT TTA ATG CAT AAT GAC TTT ATA AAA TTT GTT TAA TCG ATG AAT TCG AGC TCG	pNU170 pFA6a-GFP (S65T)-kanMX6
P_{GPD}Rpn11P276-307	pRL558 GTTGACATTGCGAAGAGCGAC	pRL559 CGCCAGTACACCTTATCGGC	pJR865
P_{RPN7}Rpn11P276-307	pRL558 GTTGACATTGCGAAGAGCGAC	pRL559 CGCCAGTACACCTTATCGGC	pJR866
rpn11E286A,N290A	SP/Rpn11 Frwd CCG CGA AGG AAA CCA AGA TG	Rvrs/Rpn11 AGT GGG CTT TCT AGT TAT TTA ATG CAT AAT GAC TTT ATA AAA TTT GTT TAA TCG ATG AAT TCG AGC TCG	pJR870
rpn11L288A,I292A,V293A,V295A,L296A (rpn11ΔNES)	SP/Rpn11 Frwd CCG CGA AGG AAA CCA AGA TG	Rvrs/Rpn11 AGT GGG CTT TCT AGT TAT TTA ATG CAT AAT GAC TTT ATA AAA TTT GTT TAA TCG ATG AAT TCG AGC TCG	pJR875
rpn11T287A,S294A,T297A (rpn11ΔPhos)	SP/Rpn11 Frwd CCG CGA AGG AAA CCA AGA TG	Rvrs/Rpn11 AGT GGG CTT TCT AGT TAT TTA ATG CAT AAT GAC TTT ATA AAA TTT GTT TAA TCG ATG AAT TCG AGC TCG	pJR876
scl1-GFP	pRL589 TGC TGA GAA CAT CGA AGA AAG GCT AGT AGC AAT TGC TGA ACA AGA TCG TAC GCT GCA GGT CGA C	pRL36 GTG TTG ACG CGT GTG ATT TCA CAT TAT GTT GTG GCA GGA AGA TCG ATG AAT TCG AGC TCG	pNU293 (pYM28)

pre6-GFP	pRL602 AGAGCAGCAAGAGCAGGACAAAAAGAAAAAATCTAAC CAT CGTACGCTGCAGGTCGAC	pRL603 TATTTTATATAGGTTTTATGCCCAATATATATCGCCGTT TATCGATGAATTCGAGCTCG	pNU293 (pYM28)
scl1-mCherry	pRL600 TGCTGAGAACATCGAAGAAAGGCTAGTAGCAATTGCTG AACAAGATggtcgacggatccccggg	pRL36 GTG TTG ACG CGT GTG ATT TCA CAT TAT GTT GTG GCA GGA AGA TCG ATG AAT TCG AGC TCG	pJR655 (pBS34)
rpn5-GFP	pRL921 AATTACAAAAGAGGAAATCATGCACGGTTTGCAAGCTA AACGTACGCTGCAGGTCGAC	pRL922 CCGGATCTGAGATAATCCGACACTTACTCGAAAATCTC TATCGATGAATTCGAGCTCG	pNU293 (pYM28)
P_{ADH}*Rpn7*	pRL919 ATAGTTACTAATACACGCAAAAATTCTGGATAAACACG GC cgtacgctgcaggtcgac	pRL920 ATAGTTACTAATACACGCAAAAATTCTGGATAAACAC GGC cgtacgctgcaggtcgac	pNU321 (pYM-N9)
P_{ADH}*Rpn12*	pRL917 CCGGTGGAAAGTACTATTGAAGTGAGATAAGAAGCCAT CG cgtacgctgcaggtcgac	pRL918 AGGCTATGCTTAACGACTTGGTCAATTCGGCTAACGAG GG catcgatgaattctctgtcg	pNU321 (pYM-N9)
P_{RPN7}*NES-Unstable-GFP*	pRL964 CTAAACTCACAAATTAGAGCTTC	pRL559 CGCCAGTACACCTTATCGGC	pJR796

Upper- and lower-case lettering of primers has no special meaning.

Yeast Growth Conditions – Yeast cells were grown at 30 º C in YPD under constant shaking unless stated otherwise. For starvation experiments, cultures grown overnight were diluted to an OD600 of 0.5 in fresh YPD and grown for 4 hours (to an OD600 between 1 and 1.5). The cells were then harvested by centrifugation and washed with sterile MQ water. Cells were resuspended in starvation media (SD complete media without indicated nutrients) to an OD600 of 1.5. SD media contained yeast nitrogen base (0.17 %) and $(NH_4)_2SO_4$ (0.5 %) supplemented with appropriate nutrients (amino acids, uracil and adenine) and 2% dextrose. In glucose starvation media, dextrose was omitted while nitrogen starvation media lacked $(NH_4)_2SO_4$ and nutrients.

Western Blot Analysis – Cell lysates were made by cryogrinding (whenever native gels were a downstream application) or alkaline lysis. For cryogrinding, cells were harvested by centrifugation and frozen dropwise using liquid nitrogen and stored in -80 ºC or directly processed (detailed protocol Roelofs et al 2018)[229]. Frozen droplets were placed in mortars prechilled with liquid nitrogen and ground into a powder. The powder was transferred to a 1.5 mL tube and resuspended in lysis buffer (50 mM Tris-HCl [pH 7.5], 5 mM MgCl2, 1 mM ATP, 1 mM EDTA). The lysate was allowed to incubate on ice for 10 minutes and was cleared by centrifuging for 2 minutes in a microcentrifuge at 17,000 x g (4 ºC). The supernatant was

collected, and protein concentration determined using a NanoDrop (280 nm). For both native gel electrophoresis and SDS-PAGE, equal amounts of protein were used. For alkaline lysis, the cell equivalent to 1.5 mL of OD600 was collected by centrifugation, resuspended in 100 µL of MQ water, and mixed with 100 µL of 200 mM NaOH. Following, 5 minutes incubation at room temperature, samples were centrifuged in a microcentrifuge at 17,000 x g for 2 minutes. Next, the pellet was resuspended in 50 µL alkaline lysis buffer (60 mM Tris-HCl [pH 6.8], 5 % glycerol, 2 % SDS, 4 % β-mercaptoethanol, 0.0025 % bromophenol blue) and boiled for 3 minutes at 96 ºC. Followed by centrifugation at 13,200 rpm, 6 µL sample was used for SDS-PAGE. For immunoblotting, SDS-PAGE separated samples were transferred to PVDF membrane and immunoblotted for specific proteins. Primary antibodies used in this work include Pgk1 for a loading control (1:4000; Invitrogen, #459250), GFP (1:500; Roche, #11814460001), Rpn8 (1:10,000; #4797, generous gift of Dan Finley at Harvard Medical School in Boston, MA), and α7 (1:1000; Enzo Life Sciences, #02081203). Secondary antibodies used were conjugated to HRP (horseradish-peroxidase) (Rockland Immunochemicals). HRP activity was visualized using Immobilon Forte Western HRP substrate purchased from Millipore. Immunoblots were imaged using either a Syngene G-box imager (Syngene) along with GeneSnap software.

Native Gel Electrophoresis and Activity Assay– 300 µg of samples was lysed by cryogrinding, loaded on native gel (see Roelofs 2018)[229], and separated for 2.5 hours at 4 º C (96 volts). A Typhoon 9410 imager was utilized to visualize fluorescently tagged subunits of the proteasome within the native gel. An in-gel LLVY-AMC activity assay was utilized to visualize proteolytically active proteasome complexes (described previously by Roelofs 2018).

Phenotype Screen – Overnight cultures were diluted into 4 mL of fresh YPD to an OD600 of 0.5. Cultures were grown at 30 ºC with shaking until cells reached an OD600 of 1.0. The cell equivalent of 1 ml of OD600 1 was collected by centrifugation and washed with 500 µL sterile MQ water. Next, cells were resuspended in 133 µL sterile water and four-fold serial dilutions were prepared. Cell suspensions were spotted onto YPD plates using a pin array. Plates were incubated for 24 or 48 hours at indicated temperatures and imaged using a G-Box mini.

Fluorescence Microscopy – Live imaging of yeast cells expressing GFP or mCherry-tagged proteins was performed by collecting the equivalent of 2 OD600 of cells by centrifugation

and resuspending them in 20 µL of the growth media. 3 µL of this suspension was placed on an agar slide and covered with a coverslip for imaging. Agar slides were made by dissolving 1 % agarose in PBS. 30 µL of the melted agar solution was placed on a slide and covered with a second slide . Once dry, the top slide was removed leaving the agar pad behind on the original slide. Imaging was performed using a fluorescent microscope (Nikon Eclipse TE2000-S) at 600X magnification (Plan Apo 60x/1.40 objective) and camera from QImaging (Retiga R3tm). Images were taken using Metamorph software from Molecular Devices and analyzed using ImageJ.

Proteasome Purification – 4 mL of overnight culture was used to inoculate 1.5 liters YPD. Cells were grown for 24 hours and harvested by centrifugation at 3,000 rpm in a Beckman Coulter Aventi J-E centrifuge (rotor: JA-10) at room temperature for 3 minutes. After washing with water, cells were resuspended in 1.5 pellet volumes of lysis buffer (50 mM Tris [pH 8.0], 5 mM $MgCl_2$, 1 mM EDTA, 1 mM ATP). Cells were lysed by passing through a French press twice at 1000 psi. Lysates were cleared at 4 ºC and 11,000 rpm for 20 minutes (Beckman rotor: JA-17). Supernatant was filtered through a cheese cloth. 750 µL Antigen Affinity Gel Rabbit IgG resin (whole molecule from MP Biomedicals, LLC) was added to the cleared lysate and incubated under constant rotation at 4 ºC for 1 hour. Next, the IgG resin was collected in a Biorad econo-column and washed with 50 bed volumes of cold Buffer 2 (50 mM Tris [pH 7.5], 5 mM $MgCl_2$, 1 mM EDTA, 1 mM ATP, and 20 mM NaCl) and 15 bed volumes cold elution buffer (50 mM Tris [pH 7.5], 5 mM $MgCl_2$, 1 mM EDTA, 1 mM DTT, 1 mM ATP). To elute proteasomes, resin was incubated at 30 ºC for 1 hour under constant rotation with 750 µL elution buffer supplemented with 8 µL GST-Tev protease (1.5 mg/mL). Flow-through was collected and combined with a second elution of 1 bed volume elution buffer. The collected sample was incubated with glutathione resin at 4 ºC for 20 minutes with constant rotation. The glutathione resin was then removed by filtering the sample through a spin column. The elution was concentrated by centrifugation using a concentrator from PALL Life Sciences (100 kDa MW cutoff). Samples were stored in -80 ºC and analyzed by either native gel electrophoresis or SDS-PAGE.

Results

Rpn11 Truncation affects PSG formation following glucose starvation

Proteasomes localize to the nucleus of actively dividing cells, but as yeast cells experience nutrient loss, such as during quiescence or loss of glucose, proteasomes leave the nucleus and localize to granular structures in the cytoplasm termed proteasome storage granules (PSGs) [175,267]. How proteasomes are targeted to these storage granules and how proteasome nuclear export is controlled, however, remains elusive. In an effort to purify proteasome storage granules using the abundantly used Rpn11-ProtA tagged background, we surprisingly observed that our strain containing both the Rpn11-ProtA tag and Rpn1-GFP failed to form granules and remained nuclear (Fig. 3-1A). Strains with only one of these subunits tagged, either Rpn1-GFP or Rpn11-GFP, formed PSGs (Fig. 3-1A).

Interestingly, while no reports have indicated a lack of PSG formation using the C-terminally tagged Rpn11 subunit, strains expressing a mutant form of Rpn11 showed a similar lack in PSG formation during quiescence [262]. This mutant, *rpn11-m1* a.k.a. *mpr1-1*, has a frameshift mutation at amino acid 276, which translates into a truncated version of the protein where the C-terminal 31 amino acids are replaced with 9 non-native amino acids (Fig. 3-1B & [263]). To determine if the non-native amino acids or the loss of native amino acids at the C-terminus is responsible for the failure in PSG formation, we generated a strain that only expressed Rpn11 lacking the last 31 amino acids, Rpn11-Δ31, from the endogenous promotor (Fig. 3-1B).

We combined the Rpn11-Δ31 with a GFP tag on either the CP (α4) or the RP base (Rpn1) to follow 26S as well as proteasome subcomplex localization. The strains were starved of glucose for 24 hours. Strains containing either the RP base or CP tag alone successfully formed proteasome storage granules, however, those expressing the Rpn11 truncation failed to form granules. Instead, the proteasomes remained enriched in the nucleus suggesting a defect in nuclear export (Fig. 3-1C). This is similar to what has been reported for *rpn11-m1* in stationary phase [262]. While the Rpn11 tail affected nuclear export and PSG formation, we also observed a lethality phenotype associated with the truncation when combined with other tagged proteasome subunits. Following strain crossing and sporulation, spores containing Rpn11-Δ31, in combination with α1-GFP, α2-GFP, β5-GFP or *rpn4*Δ, failed to grow (Supp. Fig. 1). In all, these data indicate that the fluorescent tag on several CP subunits is unfavorable with other proteasome

mutations, something we had recently noticed in a different context when tagging the β5 subunit. The synthetic lethality with the *RPN4* knockout indicates that the Rpn11-Δ31 strain needs to upregulate proteasome levels to compensate for the reduced assembly and functionality of the proteasome. Nevertheless, the cross between α4 and Rpn11-Δ31 was viable enabling us to determine whether CP localization was altered in the presence of Rpn11-Δ31 following glucose starvation.

To determine if the Rpn11-Δ31 mutant affected nuclear export of the proteasome under other stress conditions, we tested growth at 37 °C as well as nitrogen starvation. Our lab has previously observed that yeast cells grown at elevated temperatures for prolonged amounts of time, such as 24 hours at 37 °C, form proteasome storage granules. However, Rpn1-tagged proteasomes failed to form PSGs in the presence of Rpn11-Δ31 following stress at 37 °C (Fig. 3-1D). Thus, the Rpn11 truncation appears to affect the formation of granules under a variety of granule-inducing conditions. While nitrogen starvation also induces nuclear export, it leads to vacuolar targeting and degradation through autophagy (proteaphagy) rather than the formation of PSGs [176,177]. While no specific receptor has been identified for targeting these proteasomes to autophagy, proteasomes do not appear to be degraded by bulk autophagy upon nitrogen starvation [176,177,245]. As expected, in the Rpn1-GFP tagged strain, nitrogen starvation led to a change in fluorescence from largely nuclear to mostly vacuolar, which is indicative of proteasomes being exported and targeted to the vacuole via autophagy (Fig. 3-1D). In the Rpn11 mutant strain, there was only a small amount of fluorescence that ended up in the vacuole following 24 hours nitrogen starvation and most proteasomes remained nuclear (Fig. 3-1D). The vacuolar targeting of proteasomes can also be monitored by observing the release of GFP from tagged proteasomes on SDS-PAGE [177,236]. Consistent with reduced lysosomal targeting in the presence of Rpn11-Δ31, cell lysates showed more Rpn1-GFP and 17.1% less free GFP (SEM = 8.05) (Fig. 1E, lane 4). This confirmed a reduced level of proteasome autophagy for strains containing the truncated version of Rpn11. In sum, the C-terminal tail of Rpn11 appears to be important for nuclear export of proteasomes, as Rpn11-Δ31 proteasomes remain nuclear under several conditions that induce the export.

Figure 3-1 - Truncation of Rpn11 affects nuclear export of proteasomes.

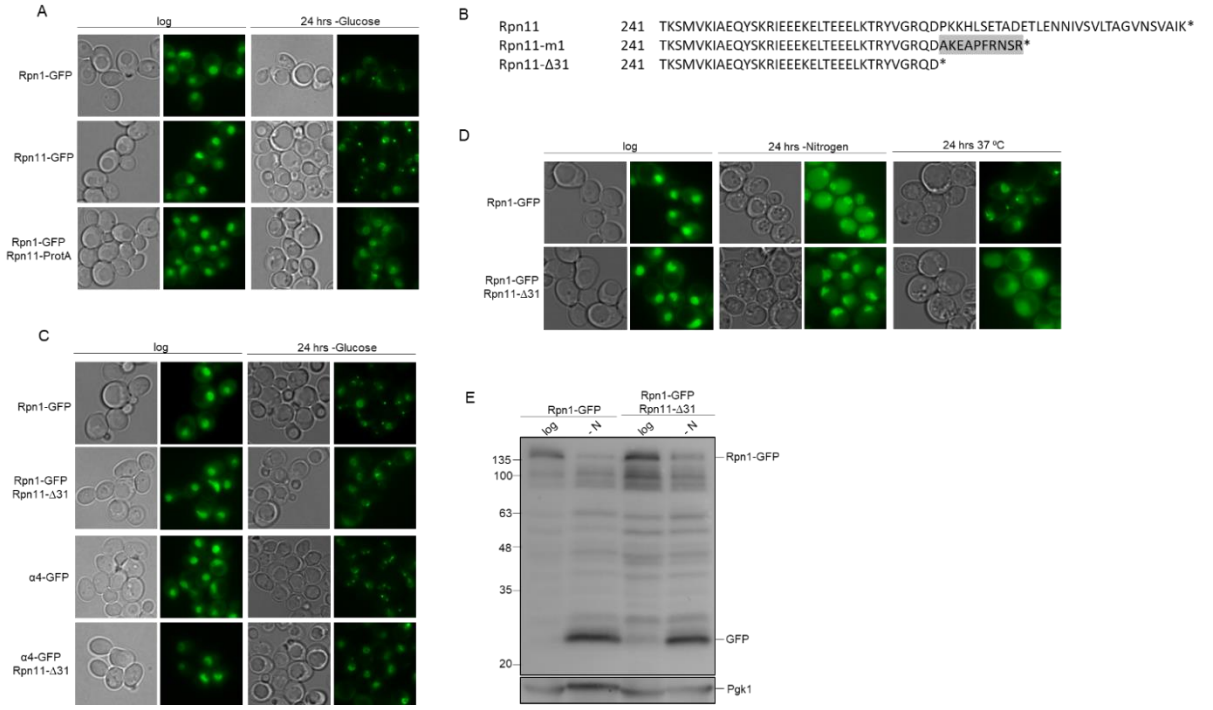

(A) Strains expressing both Rpn1-GFP and Rpn11-ProtA failed to form proteasome storage granules (PSGs) following glucose starvation. In comparison, strains containing a single GFP tag on either Rpn1 or Rpn11 successfully formed granules. (B) Sequence alignment of wild-type Rpn11 to the well characterized rpn11-m1, mpr1-1 sequence and Rpn11-Δ31. Shaded amino acids are the nonnative amino acids produced from the frameshift mutation. Asterisks indicate stop codons. (C) Rpn11-Δ31, in combination with Rpn1-GFP (RP) or α4-GFP (CP), produced the same phenotype present in (A) where the compromised tail of Rpn11 affected the formation of PSGs under glucose starvation. (D) Nuclear export of proteasomes occurs, not only by glucose starvation, but also by elevated temperatures and nitrogen starvation. Microscopy was performed to monitor export of proteasomes under these conditions in the presence of Rpn11-Δ31. Similar to what was observed for (B), there was a decrease in nuclear export of Rpn1-GFP when in combination with the Rpn11 truncation. Proteasome granules that typically form at elevated temperatures like 37 °C did not for Rpn11-Δ31. We also observed less fluorescent signal in the vacuole following nitrogen starvation indicating less export. This observation was verified using SDS-PAGE and immune-blotting for GFP (E). Protein lysates from Rpn11-Δ31 contained more Rpn1-GFP and less free GFP, which forms from proteolytic cleavage once inside the vacuole. Quantification of replicates and use of PgK1 confirmed less proteaphagy for Rpn11-Δ31 strains.

Analysis of the Rpn11 Tail Indicates its Effects are Structural

To determine the role of the C-terminal tail of Rpn11 in nuclear export, we looked for specific features within this sequence. The C-terminus of Rpn11 is folded into two antiparallel alpha helices which are both part of a helical bundle that binds most lid subunits together [160]. Both the *rpn11-m1* and the Rpn11-Δ31 mutant lacked the terminal alpha helix of Rpn11 (Helix H7) as well as an unstructured region following the helix (Fig. 3-2A & [262,264]). To determine the contribution of the unstructured C-terminal residues in Rpn11 functioning, we created a strain that lacked the last 9 amino acids of Rpn11 (Rpn11-Δ9) (Fig. 3-2A) [268]. The Rpn11-Δ9 strain

was glucose starved for 24 hours to induce granule formation and as shown, granules readily formed similar to wildtype. Thus, the 9 terminal amino acids of Rpn11 are not involved in nuclear export of proteasomes or the formation of PSGs following glucose starvation (Fig. 3-2B, 3rd row) and it is Helix 7 that is critical for this functionality. The structure of Rpn11 (PDB: 5wvi) indicates that two amino acids (E286 and N290) make interactions with the penultimate alpha helix of Rpn11. To determine if a loss of these intrahelical interactions affected the formation of PSGs, we introduced Rpn11-Δ23 which removed part of the terminal alpha helix that contained these two amino acids. This mutant failed to form proteasome storage granules similarly to Rpn11-Δ31 (Fig. 3-2B) and resulted in nuclear retention of proteasomes under these conditions. This defect was, however, not due to a simple disruption of the interaction between alpha helix 6 and 7 as a strain with Rpn11 $^{E286A,\ N290A}$ was able to export proteasomes and form PSGs (Supp. Fig. 3-2A and 3-2B). Overall, based on these results, nuclear export and PSG formation depends on 14 amino acids that make up the second half of the terminal alpha helix of Rpn11. As this sequence is involved in the helical bundle of the lid and is not easily accessible to export or cargo proteins, it is an unlikely candidate for being recognized by export machinery [269]. Consistent with this, mutating potential phosphorylation sites (Rpn11-ΔPhos) of Rpn11, as well as a putative NES (Rpn11-ΔNES), did not impact nuclear export or PSG formation (Supp. Fig 3-2C).

Therefore, it seems parsimonious that the truncation affects the structural integrity of the lid, as suggested previously [153,262,270], and thereby interferes with proteasome export. Previous reports showed that introducing the truncated portion of Rpn11 rescued phenotypes associated with *rpn11-m1*, including abnormal mitochondrial morphology, growth defects, proteasome instability, and lack of granule formation during stationary phase [262,264,270]. To test its effect on glucose granule formation, we introduced the terminal alpha helix *in trans* in strains containing Rpn11-Δ31. Interestingly, cells expressing the C-terminal alpha helix from the *RPN7* promoter, which should allow for expression at similar levels to Rpn11 itself, showed nuclear retention of the proteasome following 24 hours of glucose starvation similarly to the Rpn11-Δ31 cells. However, overexpression of the C-terminal tail using the *GPD* promoter did rescue the formation of PSGs (Fig. 3-2C & [262]). Since the terminal alpha helix of Rpn11 appears to make minimal interactions with neighboring residues, it's likely to have a low affinity for the helical bundle; therefore, we only observed a rescue when the tail was overexpressed which compensated for its

reduced ability to interact. In all, overexpression of the C-terminal tail of Rpn11 was able to rescue the granule phenotype associated with glucose starvation.

As reintroduction of the tail rescued granule formation, we further characterized our structural hypothesis using native gel electrophoresis and an in-gel activity assay for strains expressing the mutant form of Rpn11 in both the presence and absence of the C-terminal tail expressed *in trans.* Active proteasome complexes were visualized using LLVY-AMC, a fluorogenic substrate of the proteasome [229]. In wildtype cells, the majority of proteasomes are found as either doubly or singly capped complexes (RP_2CP and RP-CP); however, for Rpn11-Δ31, we observed base-CP complexes, as previously reported, as well as increased levels of free CP (Fig. 2D, compare lane 1 and 2 & [153,261,262,270]). The presence of base-CP complexes as well as high levels of free CP indicate a defect in 26S proteasome assembly, most likely in lid assembly due to the presence of lidless, base-CP complexes. While reports of base-CP complexes have been made, it has also been suggested that this defect in lid assembly leads to the formation of a lid intermediate containing Rpn11/8/5/9/6 (module 1) which can associate, under permissive temperatures, with base-CP and provide DUB activity [271]. However, this lid intermediate base-CP complex is highly unstable and readily dissociates. Therefore, it appears that while the Rpn11 truncation does affect lid assembly, it also causes instability within partially assembled complexes that may form. Defects in lid assembly as well as instability was partially rescued by introducing the C-terminal alpha helix of Rpn11 as seen by the loss of base-CP as well as free CP and reemergence of RP-CP levels similar to wildtype (Fig. 3-2D, lane 3 & [270,271]). Consistent with a defect in fully assembled 26S proteasomes, immunoblot analysis indicated an increased amount of ubiquitinated material in the presence of the Rpn11 truncation for both logarithmically growing cells and those grown for 24 hours in YPD (Supp. Fig. 3, compare lanes 1 & 4 and lanes 2 & 5) [153,261,263,270]. Levels of ubiquitinated material were not drastically different for glucose starved lysates (Supp. Fig. 3, compare lane 3 and 6). Taken together, these data indicate that the C-terminus of Rpn11 plays a structural role in assembling fully intact proteasomes which affects levels of ubiquitinated material, nuclear export and PSG formation during glucose starvation.

Figure 3-2 - Analysis of Rpn11 tail truncation narrows export phenotype down to 14 amino acids

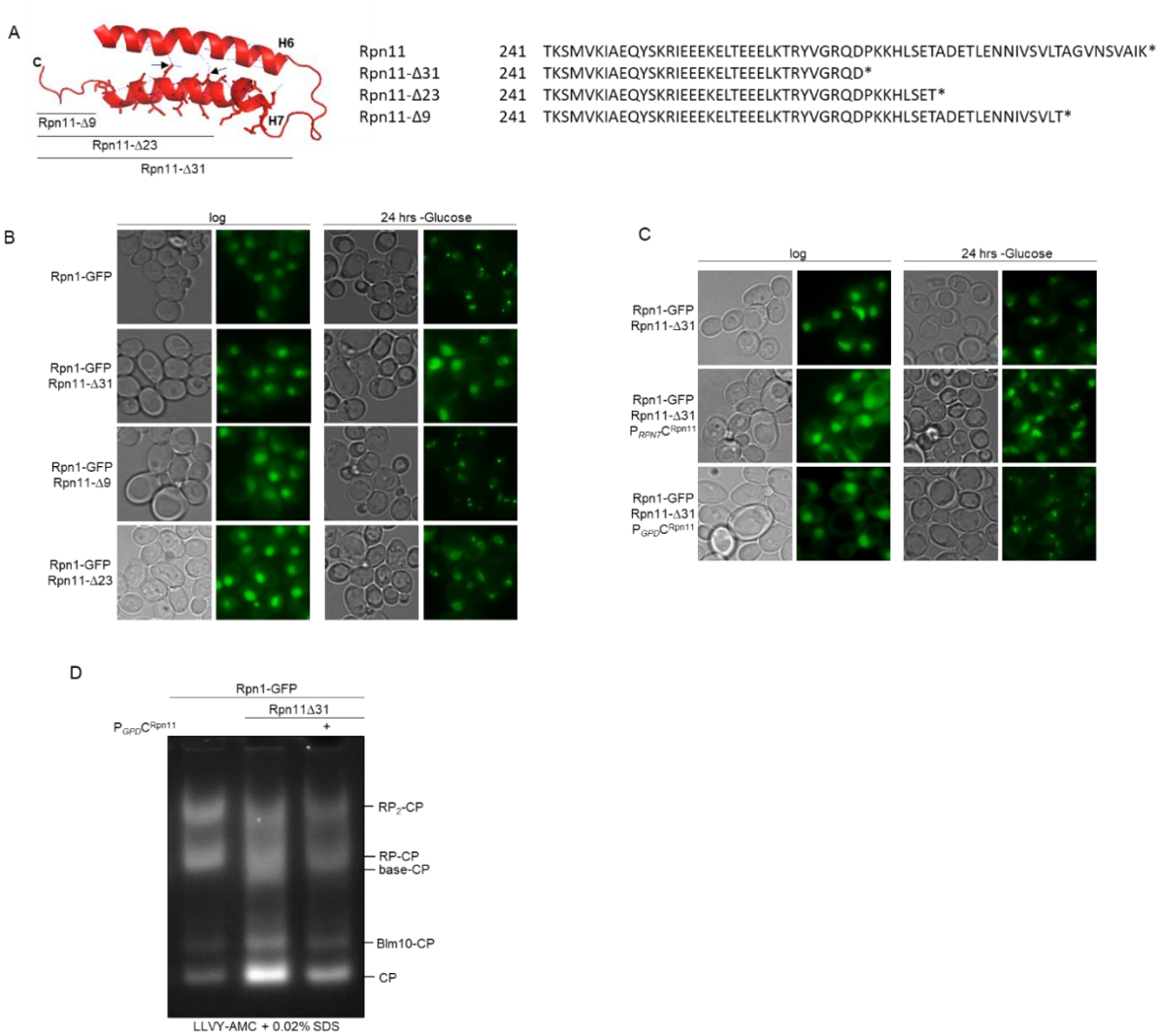

(A) Structure of Rpn11 C-terminal tail composed of two anti-parallel alpha helices. Three truncations were made as follows: Rpn11-Δ9 deleted the free C-terminal tail of Rpn11, Rpn11-Δ23 removed any intrahelical interactions, and Rpn11-Δ31 deleted the entire terminal alpha helix. For Rpn11-Δ23, the dotted lines potential interactions between amino acids. Arrows indicate amino acids capable of forming intrahelical interactions (PDB ID: 5wvi). Right panel shows sequence alignments for various Rpn11 tail truncations. (B) Rpn11 truncation variants were glucose starved for 24 hours to assess granule formation. (C) To assess the structural effects of the Rpn11 C-terminal alpha helix, the helix sequence was introduced in trans to strains containing Rpn11-Δ31. The C-terminal tail was expressed using either the RPN7 or GPD promoter. Microscopic analysis showed that overexpression of the tail using the GPD promoter rescued the formation of PSGs. (D) Proteasome samples were separated on native gel and visualized using an LLVY-AMC activity assay and 0.02 % SDS to determine structural phenotypes associated with the Rpn11 truncation. The truncation resulted in base-CP complexes and increased levels of CP consistent with assembly defects. These defects were rescued by overexpression of the C-terminal tail in trans.

Rpn11 Truncation affects lid assembly and incorporation into the proteasome

Ecm29 (KIAA0368 in mammalian cells) is a large proteasome associated protein thought to act as a quality control factor that binds faulty proteasomes that can arise from defects in assembly [178,186,188,244,272]. More specifically, it has been suggested as a regulator of RP assembly

as deletion of Ecm29 has been shown to rescue growth phenotypes associated with assembly defects caused by a loss of RP chaperones [178,244]. In strains lacking these RP chaperones, proteasomes are retained in the nucleus following certain stress conditions, like glucose starvation, which normally leads to the formation of PSGs (data unpublished). Furthermore, deletion of Ecm29 was able to not only rescue the growth phenotypes associated with the assembly mutants, but also partially rescue the formation of PSGs (data unpublished). As the Rpn11 truncation appears to cause proteasome assembly defects, we aimed to evaluate how Ecm29 might contribute to the lack of granule formation observed for the Rpn11-Δ31.

Localization of Rpn1-GFP containing proteasomes was monitored following glucose starvation in an *ecm29*Δ Rpn11-Δ31 strain. The presence or absence of Ecm29 had no detectable impact on localization as proteasomes were enriched in the nucleus both during logarithmic growth and following glucose starvation (Fig. 3-3A). Binding of Ecm29 to these mutant proteasomes is thought to inhibit them in order to prevent any adverse effects from the faulty assembly or mutant subunits. Ecm29 has been shown to inhibit proteasomes upon binding by closing the translocation channel of the core particle [186,244]. Interestingly, Ecm29 is the only proteasome associated protein shown to bind to both the core particle and the regulatory particle simultaneously [178,235,273]. In addition to affecting CP, it also inhibits RP by reducing the effectiveness of the ATPase ring which ultimately prevents substrate unfolding [178]. These data, along with the observation that Ecm29 is enriched on mutant proteasomes, led to the hypothesis that it functions as a quality control factor. As such, in order to inhibit the proteasome, Ecm29 must bind the proteasome. As no structure for Ecm29 has been solved, we sought to purify Ecm29 bound proteasomes to better understand its function as an inhibitor and why its deletion had no effect on the Rpn11-Δ31 aberrant proteasome phenotypes. Proteasomes, from strains overexpressing Ecm29, were purified and resolved on SDS-PAGE. Proteasome complexes were then separated using ultracentrifugation and fractions containing 26S proteasomes bound with Ecm29 (Supp. Fig. 4A, fractions 8 & 9) were combined and analyzed using native gel electrophoresis to confirm purity. Complexes containing Ecm29 show a shift on native gel, which verified purification of Ecm29-bound proteasomes (Supp. Fig. 4B, compare wild type and fractions 8 and 9). While 26S proteasomes bound with Ecm29 were successfully purified and, in collaboration with the Walters Lab at NIH we have seen negative EM stain showing apparent

Ecm29 containing proteasome particles, we have not yet been able to determine the structure of Ecm29-26S complexes using cryo-EM.

Although structural knowledge of Ecm29 is lacking, it is known to bind the Rpt5 subunit of RP and the α7 subunit of CP [178,179]. The inability of an Ecm29 knockout to (partially) rescue PSG formation of Rpn11-Δ31 might either indicate that Ecm29 interacts differently with this proteasome mutant compared to other assembly mutants we have analyzed or that Ecm29 does not recognize and bind Rpn11-Δ31 proteasomes. To test this, we purified proteasomes from a strain with a CP ProteinA tag and the Rpn11 truncation. While Ecm29 has been found enriched on many forms of aberrant proteasomes, we did not observe an enrichment of Ecm29 on Rpn11-Δ31 proteasomes (Fig. 3-3B). Further analysis of this purification showed that proteasomes purified using a β4-ProtA tag were almost completely devoid of essential proteasome subunits including lid subunits, Rpn8 and Rpn12, whereas base subunits and core particle subunits were present (Fig. 3-3B). This is consistent with native gels and previous reports which indicate the presence of base-CP complexes lacking lid subunits (Fig. 3-2E & [153,261,262,270,271]). Interestingly, although Rpt5 and α7 were present (subunits with which Ecm29 directly interacts), we still did not see any bound Ecm29, which suggests that Ecm29 requires specific lid subunits for binding in addition to the base and core particle. As mentioned previously, a lid intermediate containing Rpn11/8/5/9/6 has been shown to interact with base-CP; however, it readily dissociates in the presence of salt. This could suggest that while Ecm29 binds aberrant proteasomes, instability in the complex during purification could result in loss of some subunits as well as interacting proteins, like Ecm29. However, since microscopic analysis showed no difference in the presence of absence of Ecm29, it most likely indicates that Ecm29 does not recognize proteasomes in the presence of Rpn11-Δ31.

Lack of a fully assembled lid in these samples led us to focus on the assembly process and how the Rpn11 truncation could affect proteasome assembly and localization. Both antiparallel helices at the C-terminus of Rpn11 are part of the helical bundle, but deletion of the terminal helix alone caused the majority of lid subunits to separate into two lid particles, Rpn11/8/5/9/6 and Rpn7/3 when these subunits were heterologously expressed in *E. coli*. More so, all lid particles lacked Rpn12 [160]. Assuming that the cellular conditions in the Rpn11-Δ31 are still susceptive to proteasome nuclear export and PSG formation, one could hypothesize that the elements responsible for PSG targeting were absent from the GFP-tagged proteasome complexes

monitored previously. This raises the question whether the missing lid subunits contain their own NES and still localize to PSGs independently of the rest of the proteasome. To test this, we N-terminally tagged one subunit from each of these reported lid particles, Rpn5, Rpn7 and Rpn12. For Rpn5, a C-terminal GFP was introduced at the endogenous locus. For Rpn7 and Rpn12, the endogenous promotor was replaced by an *ADH* promoter while also introducing an N-terminal GFP-tag. This was due to the C-termini being buried within the structure of the helical bundle. As expected, in a wildtype Rpn11 background, these subunits localized to the nucleus of logarithmically growing cells and relocalized to proteasome storage granules upon glucose starvation. In the Rpn11-Δ31 background, Rpn5-GFP tagged proteasomes remained nuclear following glucose starvation. Thus, Rpn5 localization parallels Rpn1-GFP and core particle localization (Fig. 3-3C & Fig. 3-1C) consistent with previous reports showing Rpn5-GFP failed to form granules during stationary phase in the presence of *rpn11-m1* [262].

For GFP-Rpn12, we observed a decreased amount of signal in the nucleus upon glucose starvation along with 8 % of cells forming granules in the presence of the Rpn11 truncation compared to Rpn5-GFP Rpn11-Δ31 cells which failed to form granules (Fig. 3-3C, 4th row). We observed a similar phenotype for GFP-Rpn7 where 20 % of the cells formed granules. Interestingly, while we noticed a more intense fluorescent signal for granules formed following 24 hours of glucose starvation, we did observe faint granules in the cytoplasm of GFP-Rpn7 strains under logarithmic growth; however, the bulk of fluorescence was still nuclear (Fig. 3-3C, 2nd row). It has previously been observed that excess of certain proteasome subunits, like the Rpt subunits that form the base, form cytosolic puncta related to assembly defects [274]. Therefore, we next determined the expression level of the *ADH* promoter compared to endogenous levels. Using a Rpn12 specific antibody, we observed higher levels of Rpn12 under the *ADH* promoter, indicating this protein was expressed at higher levels (Fig. 3D).

To assess incorporation of GFP-Rpn12 and GFP-Rpn7, we analyzed lysates by native gel. On native gels, the majority of GFP containing bands correlated to proteolytic active complexes, as indicated by an in-gel LLVY-AMC activity assay. These bands represent typical proteasome complexes seen in wildtype samples, which include RP_2-CP, Blm10-CP-RP, RP-CP, and CP alone (Fig. 3-3E, compare lane 1 to 2 and 4). As seen previously for Rpn11-Δ31, we saw emergence of base-CP complexes (or base-CP bound with module 1 of the lid), in addition to increased levels of free CP (Fig. 3-3E, lane 3 and 5 & Fig. 3-2E & [153,261,262,270]). Furthermore,

we observed faster migrating bands when scanning for GFP which did not contain proteolytic activity. The migration pattern for one of these bands is consistent with a Rpn7 assembly intermediate which is a complex containing Rpn7, Rpn3, and Sem1 [162]. For Rpn12, however, we observed only one faster migrating band, which was present at increased levels in the Rpn11-Δ31 strain (Fig. 3-3E, left panel, compare lane 4 and 5). This band most likely represents Rpn12 as a single subunit. Overexpression leads to an abundance of this subunit that cannot all be incorporated into proteasome complexes. It seems reasonable to assume that the increase in free Rpn12 observed in the Rpn11-Δ31 background is due to defects in lid assembly as Rpn12 incorporates during the final step [160]. In sum, our data indicates that fluorescently tagged Rpn12 and Rpn7 can successfully incorporate into the proteasome. However, the increased expression from the *ADH* promoter, compared to endogenous levels, caused some accumulation of Rpn12 and Rpn7 outside of assembled proteasomes. Overexpressed base subunits were found in granules during logarithmic growth and that number increased during stress at elevated temperatures. Therefore, Rpn7 and Rpn12 granules may be an artifact of subunit overexpression [274].

Growth phenotypes, in strains with assembly defects, can sometimes be rescued by overexpression of specific subunits of the complex. For example, phenotypes caused by the loss of Hsm3, a base associated chaperone that binds to Rpt1, can be rescued upon overexpression of Rpt1 [139]. Previous reports have shown the *rpn11-m1* mutant produces temperature sensitive growth phenotypes [153,264,275]. The Rpn11-Δ31 strain similarly showed a modest growth phenotype at 30 °C, and a dramatically reduced growth at 37 °C (Fig. 3-3F, 2nd row, both panels). To test if the overexpression of Rpn12 and Rpn7 rescued the apparent assembly defect and associated growth phenotypes, we analyzed strains expressing either GFP-Rpn7 or GFP-Rpn12 in the wildtype and Rpn11-Δ31 background. Overexpression by itself did not cause any reduced growth, nor did the overexpression rescue the growth defects associated with the Rpn11 truncation (Fig. 3-3F, compare row 1 to 2, 4 and 6, both panels). In all, overexpression of lid subunits, GFP-Rpn7 and GFP-Rpn12, resulted in some recovery of Rpn11-Δ31 cells to from PSG with a more pronounced effect for Rpn7 overexpression. Since the overexpression did not rescue the growth phenotypes of Rpn11-Δ31, it does not appear this partial restoration of PSGs results from a rescue of assembled proteasomes in these cells. Since, we did observe that Rpn7 was capable of forming

Figure 3-3 - Rpn11 affects lid assembly and incorporation of late stage lid subunits.

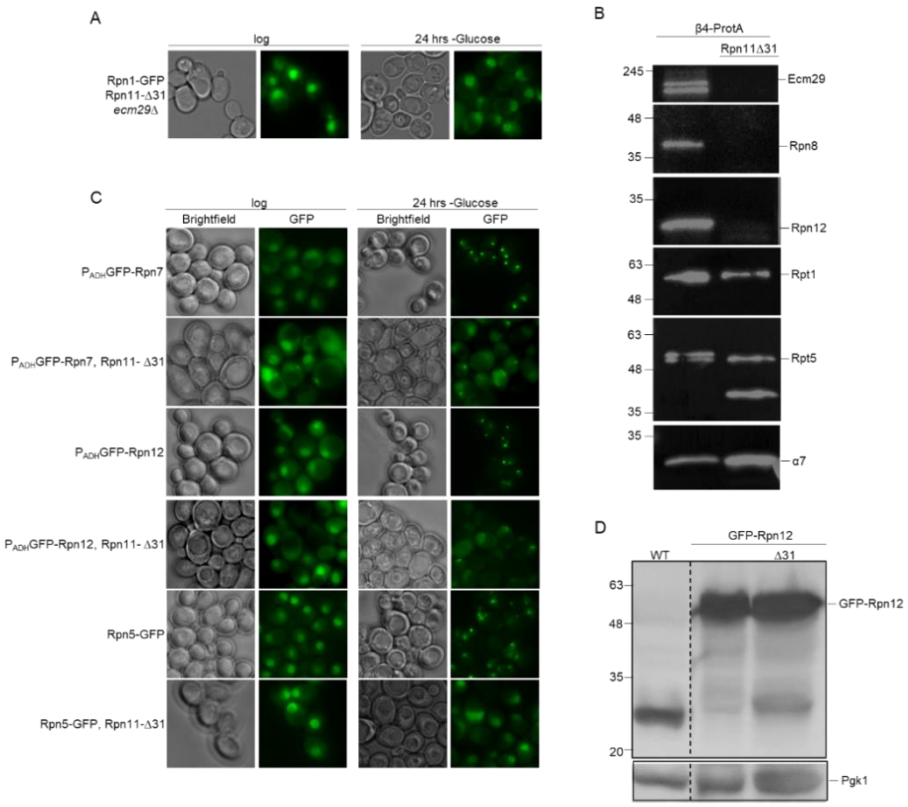
A
log
24 hrs -Glucose
Rpn1-GFP
Rpn11-Δ31
ecm29Δ
B
β4-ProtA
Rpn11Δ31
245
48
35
35
63
48
63
48
35
35
Ecm29
Rpn8
Rpn12
Rpt1
Rpt5
α7
C
log
24 hrs -Glucose
Brightfield
GFP
Brightfield
GFP
PADHGFP-Rpn7
PADHGFP-Rpn7, Rpn11- Δ31
PADHGFP-Rpn12
PADHGFP-Rpn12, Rpn11- Δ31
Rpn5-GFP
Rpn5-GFP, Rpn11-Δ31
D
GFP-Rpn12
WT
Δ31
63
48
35
20
GFP-Rpn12
Pgk1
E
PADHGFP-Rpn7
PADHGFP-Rpn12
PADHGFP-Rpn7
PADHGFP-Rpn12
WT
Δ31
Δ31
WT
Δ31
Δ31
RP2-CP
Blm10-CP-RP
RP-CP
CP
Rpn7/Rpn3/Sem1
Rpn12
RP2-CP
RP-CP
base-CP
Blm10-CP
CP
GFP Scan
LLVY-AMC + 0.02% SDS
F
24 hours
30 °
37 °
WT
Rpn11- Δ31
PADHGFP-Rpn7
PADHGFP-Rpn7, Rpn11- Δ31
PADHGFP-Rpn12
PADHGFP-Rpn12, Rpn11- Δ31
48 hours
30 °
37 °
WT
Rpn11- Δ31
PADHGFP-Rpn7
PADHGFP-Rpn7, Rpn11- Δ31
PADHGFP-Rpn12
PADHGFP-Rpn12, Rpn11- Δ31

(A) Fluorescent microscopy was used to assess a rescue in granule formation for strains with Rpn11-Δ31 and an Ecm29 knockout. Cells were glucose starved for 24 hours. (B) Rpn11-Δ31 proteasomes were affinity purified using a β4 protein A tag and IgG resin. Purified proteasomes were separated using SDS-PAGE and immunoblotting was used to determine incorporated subunits. Proteasomes were purified lacking the lid subcomplex. α7 was utilized as a loading control. (C) Expression using the ADH promoter, along with N-terminal tagging of late stage lid subunits Rpn12 and Rpn7, was utilized to determine if these subunits could form granules in the presence of Rpn11-Δ31. Following 24 hours of glucose starvation, GFP-Rpn7 formed granules in approximately 20 % of the cells, while GFP-Rpn12 granules were observed in about 8 % of the cells compared to control strain Rpn5-GFP which remained nuclear in the presence of the Rpn11 truncation. For strains harboring wild-type Rpn11, GFP-Rpn12, GFP-Rpn7, and Rpn5-GFP all relocated to PSGs following glucose starvation. (D) To assess expression of these lid subunits with the ADH promoter, logarithmically growing cells were lysed using the alkaline lysis method and proteins were resolved on SDS-PAGE followed by immunoblotting. Using PgK1 as a loading control we observed increased expression of lid subunit GFP-Rpn12 using the ADH promoter when compared to wild type. (E) Strains overexpressing GFP-Rpn7 and GFP-Rpn12 were analyzed using native gel electrophoresis. Gels were scanned for GFP containing complexes followed by an LLVY-AMC activity assay in the presence of 0.02 % SDS. Consistent with the Rpn11-Δ31, we observed increased levels of free CP as well as base-CP complexes. For Rpn11 truncation strains, there was a lack of Rpn12 and Rpn7 incorporation into the proteasome as observed by an accumulation of faster migrating GFP bands. (F) To determine if overexpression of these lid subunits rescued growth phenotypes associated with Rpn11-Δ31, we conducted a phenotype screen on indicated strains. 1 OD_{600} cell equivalents was collected and diluted 7-fold. Serial dilutions were plated on YPD plates and incubated at both 30 °C and 37 °C for 24 and 48 hours.

various assembly intermediates in the presence of Rpn11-Δ31, but Rpn12 was found as a single subunit, this might indicate that unincorporated lid subunits contain the features required for PSG localization; however, we cannot rule out the possibility that these granules are a direct cause of subunit overexpression as previously reported [274].

Unincorporated lid subunits can form granules independently

To address if the observed granules formed by these lid subunits are subcomplexes or assembled proteasomes, we generated Rpn11-Δ31 strains with either GFP-Rpn7 or GFP-Rpn12 in combination with α4-mCherry. As before, GFP-Rpn12 and GFP-Rpn7 were found mostly in the nucleus during logarithmic growth with a minor fraction of GFP-Rpn7 found in faint granules (Fig. 3-4A). Following glucose starvation, a small amount of the GFP-Rpn12 cells produced granules, all of which appeared to colocalize with α4 (Fig. 3-4A, right panel). This suggests that these cells have 26S proteasomes localized in granules indicating there is a subset of cells that show a rescue.

In contrast, Rpn7 readily formed cytoplasmic granules as previously observed. Unlike the GFP-Rpn12, α4 remained nuclear in these cells. Thus, Rpn7 can localize to granules without associating with CP in the Rpn11-Δ31 background under conditions that normally induce PSGs (Fig. 3-4A, left panel). To determine if these Rpn7 granules shared properties of PSGs, we tested their ability to disappear following glucose reintroduction and the concurrent enrichment of nuclear fluorescence. As reported before, PSGs dissolve within 15 minutes of glucose addition and proteasomes relocalize to the nucleus [173]. Even after 30 minutes of glucose add-

back, GFP-Rpn7 remained localized in cytosolic granules indicating that these granules behave differently from PSGs (Fig. 3-4B). The persistent GFP-Rpn7 granules remained devoid of CP (Fig. 3-4C).

In all, we observed that, in the presence of Rpn11-Δ31, GFP-Rpn7 is capable of forming granules independently of the rest of the proteasome and these granules appear to be distinct from the previously described proteasome storage granules. Thus, all together our data suggests the Rpn11 truncation does indeed affect lid assembly as excess unincorporated lid subunits form cytoplasmic foci similar to assembly defects for the base subcomplex. Furthermore, this implies that granule formation requires fully assembled proteasomes as inability to incorporate the Rpn7/Rpn3/Sem1 complex or Rpn12 affects granule formation of the lid subcomplex Rpn11/8/5/9/6 as well as the base and CP.

Figure 3-4 - Rpn7 granules behave differently than proteasome storage granules.

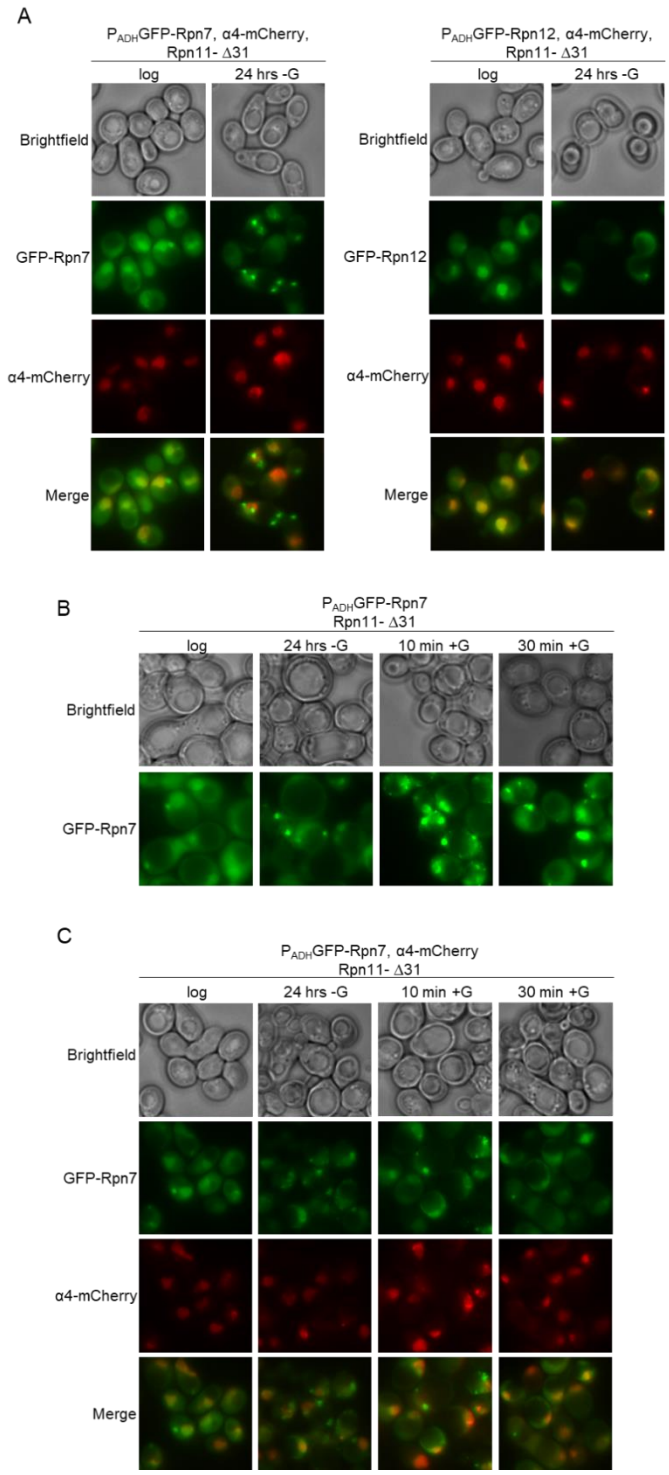

(A) To characterize the GFP-Rpn7 and GFP-Rpn12 granules, we introduced a CP mCherry tag and glucose starved these strains for 24 hours. GFP-Rpn7 granules formed independently of the proteasome, but Rpn12 granules co-localized with CP. (B) To characterize the GFP-Rpn7 granules, we performed a glucose reintroduction experiment. Cells were glucose starved for 24 hours, collected and reintroduced to fresh standard defined media containing 2 % glucose. Fluorescent microscopy was utilized to monitor granule dynamics over a 30-minute time course. Proteasomes exit PSGs and reenter the nucleus within 15 minutes of glucose reintroduction. GFP-Rpn7 granules

persisted even at the 30-minute timepoint indicating they behave dissimilarly to PSGs. (C) Doubly tagged strains underwent the same glucose reintroduction experiment as described in (B). GFP-Rpn7 granules persisted while CP remained nuclear over the course of the experiment in the presence of the Rpn11 truncation.

Common export factors are not involved in proteasome export

The export factor, Crm1 (exportin 1 or Xpo1), is responsible for nuclear export of both proteins and RNA molecules in eukaryotic cells and is known to recognize and bind leucine-rich nuclear export sequences [276]. Structural analysis of this short sequence of amino acids determined that the majority of NESs are involved in a helix-to-extended conformation or an alpha helix [269]. Since Rpn12 and Rpn7 are incorporated late in the lid assembly process, we determined whether these subunits contained Crm1 dependent export signals. If the Rpn11 truncation compromises their incorporation and they contain the signal responsible for proteasome export, this could explain why we see Rpn7 and Rpn12 granules while the rest of the proteasome remains nuclear. Analysis of the Rpn12 and Rpn7 sequences revealed putative Crm1 export signals. These signals are on regions exposed on the outer surface of the proteasome cryo-EM structure and are found as part of a helix-to-extended conformation (PDB: 5wvi) and therefore would be accessible to export machinery.

In mammalian cells and *Schizosaccharomyces pombe,* the drug leptomycin B (LMB), is a potent inhibitor of Crm1 mediated nuclear export as it binds and covalently modifies a cysteine residue within the active site of the protein rendering it non-functional [277–280]. LMB does not inhibit *Saccharomyces cerevisiae* as Crm1 contains a threonine at the homologous position. However, LMB-sensitive strains have been made by mutating the threonine to a cysteine, creating *crm1*^{T539C} [265]. We used this strain background to test whether LMB could inhibit Crm1 export of the proteasome or proteasome subcomplexes.

To ensure our granule-inducing starvation conditions allowed for nuclear export inhibition, we grew wild-type and mutant Crm1 strains for 24 hours in both YPD and glucose starvation media. To test for inhibition of nuclear export, we expressed stable GFP containing a Crm1-dependent NES (NINELALKFAGLDL). GFP has no specific localization and normally can be found in both the nucleus and cytoplasm of yeast cells. The presence of this NES caused GFP to be exported as soon as it entered the nucleus resulting in GFP localization around the nuclear periphery (Fig. 3-5A, 4-hour timepoint). LMB was added to logarithmically growing cultures containing either the sensitive or resistant version of Crm1. These cells were allowed to grow for 24 hours so export of stable GFP could be assessed. For wild-type Crm1, LMB had no

effect on nuclear export for glucose-starved or stationary phase cells as GFP was observed around the nuclear periphery irrespective of the presence of LMB (Fig. 3-5A, 1st & 3rd row, right panel). For LMB sensitive strain *crm1*^{T539C}, GFP signal was found diffuse throughout the cytoplasm and nucleus under both growth conditions indicating that Crm1 was successfully inhibited using these growth conditions (Fig. 3-5A, 2nd and 4th rows, right panel).

To determine whether Crm1 was involved in proteasome export from the nucleus, we tagged core particle subunit α1 with GFP. For logarithmically growing cells, the proteasome was localized to the nucleus and granule formation was monitored over a 24-hour time period. α1-GFP formed granules as early as 3 hours in glucose starvation media for both the sensitive and resistant LMB strains (Fig. 3-5B compare panel 2 top and bottom panel). For both strains, this phenotype was observed both in the presence and absence of LMB and granules persisted through the 24-hour timepoint (Fig. 3-5B, 3th and 4th panel). Altogether, this showed that, while Crm1 is involved in export of multiple cargoes, it is not essential in nuclear export of the proteasome under glucose starvation. This is consistent with previous work that showed that Crm1 was not involved in nuclear export of proteasomes during nitrogen starvation either [245].

Besides Crm1, another major nuclear export factor, Msn5, has been shown to preferentially bind phosphorylated proteins, which suggests it may play a role in regulated export mechanisms [281]. To test whether Msn5 is involved in proteasome export, we tagged core particle subunit α4 in a knockout library strain lacking *MSN5*. Consistently, the proteasome was localized to the nucleus in logarithmically growing cells, but similarly to Crm1 mutant strains, the proteasome was successfully exported from the nucleus and formed PSGs in the cytoplasm (Fig. 3-5C). In all, while Rpn7 and Rpn12 were hypothesized to contain Crm1-dependent nuclear export signals, neither Crm1 nor Msn5 were involved in nuclear export of the proteasome.

Figure 3-5 - Common export factors do not play a role in proteasome export.

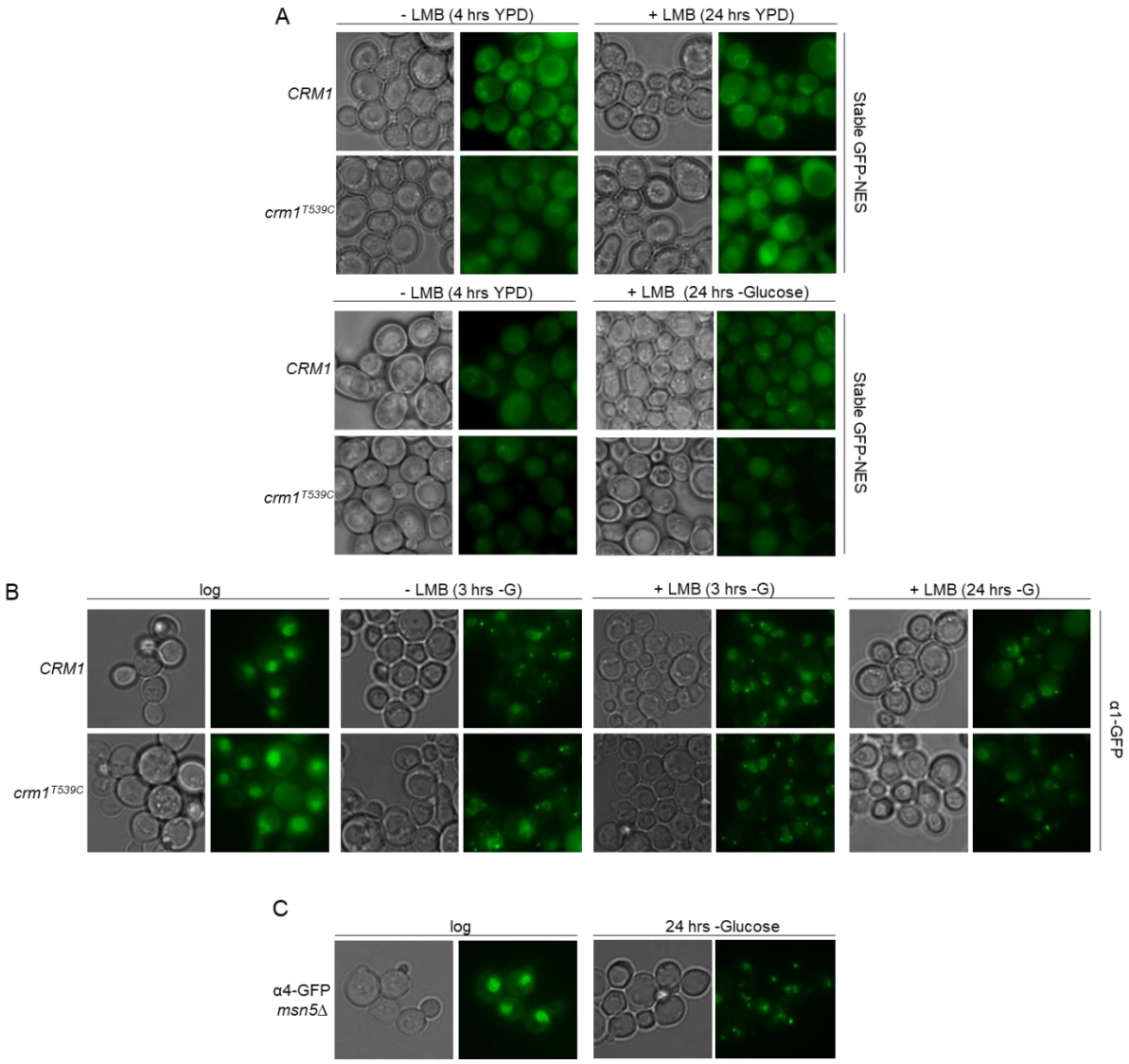

(A) Strains expressing either wild type or mutant ($crm1^{T539C}$) versions of nuclear export factor Crm1 were co-expressed with stable-GFP containing a nuclear export signal. $crm1^{T539}$ is sensitive to the drug leptomycin B (LMB) which blocks its export function. Strains were grown in YPD and glucose starvation media for 4 and 24 hours. Logarithmically growing cells containing either version of Crm1 successfully exported GFP-NES as indicated by the abundance of GFP signal around the nuclear periphery. Addition of LMB (200 nM) blocked nuclear export of GFP in the Crm1 mutant strain as indicated by diffuse signal in the nucleus. Block in export was similar for cells grown to stationary phase (24 hours YPD) and those glucose starved. (B) Export of the proteasome by Crm1 was monitored using fluorescent microscopy using the conditions for glucose starvation as described in (B). PSGs formed readily for both Crm1 strains despite the presence of LMB. Granules were present at both 3 hours and 24 hours of glucose starvation. (C) msn5Δ strains expressing α4-GFP were starved of glucose for 24 hours and nuclear export and granule formation was monitored using fluorescent microscopy.

Discussion

One of the commonly used tags to purify proteasomes is a ProteinA tag on the C-terminus of Rpn11 [282]. While strains with this tag have been instrumental in studies elucidating the biology and mechanisms of proteasomes, we noticed that a Rpn1-GFP Rpn11-ProtA strain starved of glucose did not form proteasome storage granules, while a Rpn1-GFP strain did. Thus, the Rpn11-ProtA tag might prevent proteasomes from forming PSGs similar to a well characterized Rpn11 mutant, *rpn11-m1,* that has a compromised C-terminal tail and fails to form granules during stationary phase [262]. However, Rpn11 strains with a C-terminal GFP-tag readily form PSGs following glucose starvation, indicating C-terminal tagging of Rpn11 is not detrimental per se. Instead, the manipulation of specific sets of proteasome subunits might lead to compromised proteasome dynamics or assembly.

CryoEM structural studies of the proteasome have revealed numerous conformations of the proteasome illustrating its complex nature and extensive changes during protein degradation [127,128]. For instance, during the course of binding ubiquitinated substrates, unfolding them and translocating them into the core particle, the regulatory particle undergoes numerous conformational changes in order to successfully manipulate substrates for deubiquitination and entry into the core particle. This involves delicate equilibria between conformations and requires subunits to move in unison to transition between states. The addition of a tag could change the thermodynamics of different states and thus impact conformational transitions and the function of the proteasome as a whole. Indeed, the Rpn11 subunit undergoes drastic conformational changes not only during substrate processing but also during assembly [158,159].

The inability of Rpn11-ProtA and *rpn11-m1* to form PSGs indicates a failure of proteasomes in these strains to be targeted to PSGs, an inability to export proteasomes out of the nucleus, or both. To assess a more general role in nuclear export and to more systematically study the role of the Rpn11 C-terminal region in this process, we created a clean mutation of Rpn11 called Rpn11-Δ31 based on the initial *rpn11-m1* frameshift mutant. We exposed this mutant to stress conditions that involved nuclear export and observed various phenotypes, such as reduced autophagy following nitrogen starvation and an inability to form PSGs upon carbon starvation or heat stress. The Rpn11 truncation prevented nuclear export under all these other conditions suggesting the inefficiency lies in the export mechanism itself. Together, this

suggests that the export of proteasomes under these conditions, at least in part, depends on a similar mechanism or prerequisite and that the C-terminal region of Rpn11 is important for this.

The C-terminal region of Rpn11 consists of two anti-parallel alpha helixes connected by a loop and followed by an unstructured tail. Initially, we hypothesized that loss of the C-terminal helix of Rpn11, as happened in the *rpn11-m1* as well as our Rpn11-Δ31 strain, could affect proteasome export in one of two ways. First, the Rpn11 sequence could be directly involved in the export mechanism, as in the export machinery specifically recognizes the C-terminal tail of Rpn11 to facilitate export. Loss of the C-terminal tail, or the motifs embedded within, would then prevent binding of the export machinery and the proteasome would fail to be exported. However, structural analysis of the C-terminal tail suggested that Rpn11 itself was not specifically recognized and targeted by export machinery as this segment is directly involved in formation of the helical bundle and is inaccessible for binding to export machinery. The second possibility is that truncating Rpn11 affects incorporation of other subunits within the complex which could be directly involved in export. This structural role was evaluated by making various truncations as well as through site-directed mutagenesis to determine residues that could affect the structural integrity of the C-terminal helix. While these mutations did not appear to have any affect, the alpha helix solely affected export and granular targeting. In addition, the observed assembly defects and base-CP complexes in *rpn11-m1* [153,261,262,271] as well as Rpn11-Δ31, and the ability of the Rpn11 C-terminal tail expressed *in trans* to restore proteasome assembly and PSG formation support more of a structural role in proteasome export (see Fig. 3-2E & [262,270]).

The proteasome associated protein Ecm29 functions as a quality control factor and binds aberrant proteasomes [178,186,188,244,272]. It binds the Rpt5 subunit of the base and α7 of the CP [178,179]. It inhibits proteasomal ATPase activity and a deletion can rescue growth phenotypes associated with various proteasome mutants. Our lab has also observed that PSG formation can, to some extent, be rescued when Ecm29 is knocked out in strains that fail to form PSGs due to deletion of specific proteasome assembly chaperones. Considering the Rpn11 truncation failed to form assembled proteasomes and accumulated base-CP complexes, we expected an increased amount of Ecm29 on these proteasomes. However, we did not observe increased levels of Ecm29 (see Fig. 3-3B) and a loss of Ecm29 did not rescue granule formation for Rpn11Δ31 proteasomes. This suggests this quality control factor cannot recognize proteasomes lacking the

lid. Either Ecm29 does not bind or recognize proteasomes lacking lid, or partially formed complexes are highly unstable and dissociate during purification.

Lid formation involves two major subcomplexes, Rpn11/Rpn8/Rpn5/Rpn9/Rpn6 and with Rpn7/Rpn3/Sem1 which combine and then associate with Rpn12 [162,257–259]. Rpn5, part of the Rpn11 complex, remained nuclear during stationary phase in the *rpn11-m1* mutant as well under glucose starvation in our Rpn11Δ31 strain (see Fig. 3-3C & [262]). This suggests that the Rpn11 subcomplex is not exported and, at least outside proteasome context, probably lacks the nuclear export signal responsible for the export of proteasomes under stress conditions. For Rpn7 and Rpn12, we observed a reduction in fluorescence intensity following glucose starvation, which likely resulted from reduced expression of the *ADH* promoter under glucose starvation, as we did not observe vacuolar accumulation of fluorescence and proteasomal activity is compromised in this mutant strain.

Nevertheless, we observed cytosolic granules. These granules could indicate that the PSG targeting sequences are located on these subunits and that they are targeted to PSGs independent of the remainder of the proteasome. However, one could argue this is unlikely considering the reported proteasome granules contain ubiquitin [197] and these lid subunits or subcomplexes have no reported ubiquitin binding capacity. Alternatively, overexpression of Rpn7 or Rpn12 might restore, in part, assembly of 26S proteasomes. Such a rescue has been observed with Rpt1 overexpression, which compensated for absence of the base assembly chaperone Hsm3. The ability to rescue 26S proteasome formation would allow for nuclear export and the formation of PSGs if these processes depended on fully formed 26S. However, self-assembly of the lid depends on the C-terminal alpha helices of all lid subunits and is independent of assembly chaperones making this mechanism unlikely. Indeed, strains overexpressing either lid subunit were not able to rescue growth defects associated with the Rpn11 truncation (see Fig. 3-3F).

In either of these cases, the granules would be predicted to behave similarly to PSGs. When we look at the dynamics of PSGs, we known they can dissociate, and proteasomes can reenter the nucleus within 15 minutes of nutrient replenishment [173]. However, when we characterized the Rpn7 granules, we observed that the GFP-Rpn7 signal remained granular in appearance even after 30 minutes of glucose addition (see Fig. 3-4B). This suggests that these granules are not in fact proteasome storage granules but are most likely derived from a different mechanism. Overexpressed base subunits have been shown to accumulate in granular structures

[274,283]. As lid assembly occurs without the help of any known chaperones, levels of individual lid subunits are more stoichiometric and normally expressed at fairly similar levels [283]. As such, overexpression of either Rpn7 or Rpn12 could cause the same effect where, under stress conditions, these excess individual subunits are sequestered into granules.

Interestingly, nutrient addition, following temperature stress, led to proteasomal degradation of the granule forming Rpt subunits. As the stress was alleviated, proteasome assembly and activity resumed which then targeted any excess base subunits for degradation [274]. In our strain, reduced proteasome activity resulting from Rpn11Δ31 would limit degradation of the excess lid subunits which could lead to their accumulation over time. While a few granules form in logarithmically growing cells, the granules increase in size and number following glucose starvation. These granules continue to grow after glucose addition, probably due to an increase in the levels of these subunits when transcription and translation is reinitiated. In all, it appears that overexpression of these lid subunits produced unforeseen phenotypes. As such, it would be interesting to test whether wildtype levels of these subunits have any effect on nuclear export of the proteasome.

Proteasomes are exported from the nucleus under various stress conditions (see Fig. 3-1D); however, several questions related to the transport process remain. For example, it remains unclear which export factors facilitate the transport. While common export factors Crm1 and Msn5 are involved in the export of numerous nuclear proteins [276,281], it appears that the proteasome does not (exclusively) depend on either (see. Fig. 3-5). It is also unclear in what state proteasomes traverse the nuclear pore and if this is the same under all conditions. While it has been established that 26S proteasomes can migrate through the nuclear pore as a complex [191,284], the efficiency of this remains unclear and several studies suggest proteasome subcomplexes migrate through the nuclear pore as well [194,195,285]. While this has been studied more from the perspective of nuclear import of proteasomes, a similar question for export can be posed. Do proteasomes dissociate into RP and CP before export or do they traverse the CP as an assembled complex? Under conditions of nitrogen starvation, data suggests that the proteasome dissociates prior to export [245]. However, our data indicate the Rpn11 truncation affects nuclear export of all proteasome subcomplexes. If dissociation occurs prior to export, one could reasonably expect the core particle to not be affected by the Rpn11 truncation and be transported to PSGs independently of the RP. So, either fully assembled proteasomes are required for export under

this condition or this indicates other factors control the export process. Assembled proteasome complexes could be distinguished based on CP and RP binding surfaces for an export complex, or certain conformations that are only stable in assembled proteasomes might be recognized. Such mechanisms could allow for exclusive recognition by export factors. Regardless, further studies will be necessary to determine the actual mechanism of nuclear export and which subcomplexes of the proteasome play a central role.

References

1. Kirschner, M. Intracellular proteolysis. *Trends Cell Biol.* **9**, M42–M45 (1999).

2. von Mikecz, A. The nuclear ubiquitin-proteasome system. *Journal of Cell Science* **119**, 1977–1984 (2006).

3. Qian, S. B., Princiotta, M. F., Bennink, J. R. & Yewdell, J. W. Characterization of rapidly degraded polypeptides in mammalian cells reveals a novel layer of nascent protein quality control. *J. Biol. Chem.* **281**, 392–400 (2006).

4. Groll, M. *et al.* Structure of 0 205 proteasome from yeast at 2.4A resolution. *Nature* **386**, 463–471 (1997).

5. Marques, A. J., Palanimurugan, R., Matias, A. C., Ramos, P. C. & Dohmen, R. J. Catalytic mechanism and assembly of the proteasome. *Chem. Rev.* **109**, 1509–36 (2009).

6. Nyquist, K. & Martin, A. Marching to the beat of the ring: polypeptide translocation by AAA+ proteases. *Trends Biochem. Sci.* **39**, 53–60 (2014).

7. Groll, M. *et al.* A gated channel into the proteasome core particle. *Nat. Struct. Biol.* **7**, 1062–1067 (2000).

8. Groll, M. & Huber, R. Substrate access and processing by the 20S proteasome core particle. *Int. J. Biochem. Cell Biol.* **35**, 606–616 (2003).

9. Verma, R. Role of Rpn11 metalloprotease in deubiquitination and degradation by the 26S proteasome. *Science (80).* **298**, 611–615 (2002).

10. Yao, T. & Cohen, R. A cryptic protease couples deubiquitination and degradation by the proteasome. *Nature* **419**, 403–407 (2002).

11. Maytal-Kivity, V., Reis, N., Hofmann, K. & Glickman, M. H. MPN+, a putative catalytic motif found in a subset of MPN domain proteins from eukaryotes and prokaryotes, is critical for Rpn11 function. *BMC Biochem.* **3**, 1–12 (2002).

12. Ambroggio, X. I., Rees, D. C. & Deshaies, R. J. JAMM: A metalloprotease-like zinc site in the proteasome and signalosome. *PLoS Biol.* **2**, (2004).

13. Hofmann, K. & Bucher, P. The PCI domain: A common theme in three multiprotein complexes. *Trends Biochem. Sci.* **23**, 204–205 (1998).

14. Estrin, E., Lopez-Blanco, J. R., Chacón, P. & Martin, A. Formation of an Intricate Helical Bundle Dictates the Assembly of the 26S Proteasome Lid. *Structure* **21**, 1624–1635 (2013).

15. Fukunaga, K., Kudo, T., Toh-e, A., Tanaka, K. & Saeki, Y. Dissection of the assembly pathway of the proteasome lid in Saccharomyces cerevisiae. *Biochem. Biophys. Res. Commun.* **396**, 1048–1053 (2010).

16. Sharon, M., Taverner, T., Ambroggio, X. I., Deshaies, R. J. & Robinson, C. V. Structural organization of the 19S proteasome lid: Insights from MS of intact complexes. *PLoS Biol.* **4**, 1314–1323 (2006).

17. Bai, M. *et al.* In-depth analysis of the lid subunits assembly mechanism in mammals. *Biomolecules* **9**, (2019).

18. Tomko, R. J. & Hochstrasser, M. Incorporation of the Rpn12 Subunit Couples Completion of Proteasome Regulatory Particle Lid Assembly to Lid-Base Joining. (2011). doi:10.1016/j.molcel.2011.11.020

19. Rinaldi, T. *et al.* Participation of the proteasomal lid subunit Rpn11 in mitochondrial morphology and function is mapped to a distinct C-terminal domain. *Biochem. J.* **381**, 275–85 (2004).

20. Saunier, R., Esposito, M., Dassa, E. P. & Delahodde, A. Integrity of the Saccharomyces cerevisiae Rpn11 Protein Is Critical for Formation of Proteasome Storage Granules (PSG) and Survival in Stationary Phase. *PLoS One* **8**, (2013).

21. Rinaldi, T., Ricci, C., Porro, D., Bolotin-Fukuhara, M. & Frontali, L. A mutation in a novel yeast proteasomal gene, RPN11/MPR1, produces a cell cycle arrest, overreplication of nuclear and mitochondrial DNA, and an altered mitochondrial morphology. *Mol. Biol. Cell* **9**, 2917–2931 (1998).

22. Rinaldi, T. *et al.* Dissection of the Carboxyl-Terminal Domain of the Proteasomal Subunit Rpn11 in Maintenance of Mitochondrial Structure and Function. *Mol. Biol. Cell* **19**, 1022–1031 (2008).

23. Laporte, D., Salin, B., Daignan-Fornier, B. & Sagot, I. Reversible cytoplasmic localization of the proteasome in quiescent yeast cells. *J. Cell Biol.* **181**, 737–745 (2008).

24. Neville, M. & Rosbash, M. The NES-Crm1p export pathway is not a major mRNA export route in Saccharomyces cerevisiae. *EMBO J.* **18**, 3746–3756 (1999).

25. Winzeler, E. A. *et al.* Functional characterization of the S. cerevisiae genome by gene deletion and parallel analysis. *Science (80).* **285**, 901–906 (1999).

26. Roelofs, J., Suppahia, A., Waite, K. A. & Park, S. Native gel approaches in studying proteasome assembly and chaperones. in *Methods in Molecular Biology* **1844**, 237–260 (2018).

27. Peters Lee Zeev, Z., Hazan, R., Breker, M., Schuldiner, M. & Ben-Aroya, S. Formation and dissociation of proteasome storage granules are regulated by cytosolic pH. *J. Cell Biol.* **201**, 663–671 (2013).

28. Waite, K. A., De-La Mota-Peynado, A., Vontz, G. & Roelofs, J. Starvation Induces Proteasome Autophagy with Different Pathways for Core and Regulatory Particles. *J. Biol. Chem.* **291**, 3239–53 (2016).

29. Marshall, R. S., Li, F., Gemperline, D. C., Book, A. J. & Vierstra, R. D. Autophagic Degradation of the 26S Proteasome Is Mediated by the Dual ATG8/Ubiquitin Receptor RPN10 in Arabidopsis. *Mol. Cell* **58**, 1053–66 (2015).

30. Nemec, A. A., Howell, L. A., Peterson, A. K., Murray, M. A. & Tomko, R. J. Autophagic clearance of proteasomes in yeast requires the conserved sorting nexin Snx4. *J. Biol. Chem.* **292**, 21466–21480 (2017).

31. Klionsky, D. J. *et al.* Guidelines for the use and interpretation of assays for monitoring autophagy (3rd edition). *Autophagy* **12**, 1–222 (2016).

32. Ding, Z. *et al.* High-resolution cryo-EM structure of the proteasome in complex with ADP-AlFx. *Cell Res.* **27**, 373–385 (2017).

33. Lee, Y., Pei, J., Baumhardt, J. M., Chook, Y. M. & Grishin, N. V. Structural prerequisites for CRM1-dependent nuclear export signaling peptides: accessibility, adapting conformation, and the stability at the binding site. *Sci. Rep.* **9**, (2019).

34. Chandra, A., Chen, L., Liang, H. & Madura, K. Proteasome assembly influences interaction with ubiquitinated proteins and shuttle factors. *J. Biol. Chem.* **285**, 8330–8339 (2010).

35. Yu, Z. *et al.* Base-CP proteasome can serve as a platform for stepwise lid formation. *Biosci. Rep.* **35**, (2015).

36. Lehmann, A., Niewienda, A., Jechow, K., Janek, K. & Enenkel, C. Ecm29 Fulfils Quality Control Functions in Proteasome Assembly. *Mol. Cell* **38**, 879–888 (2010).

37. Park, S., Kim, W., Tian, G., Gygi, S. P. & Finley, D. Structural defects in the regulatory particle-core particle interface of the proteasome induce a novel proteasome stress response. *J. Biol. Chem.* **286**, 36652–36666 (2011).

38. Panasenko, O. O. & Collart, M. A. Not4 E3 Ligase Contributes to Proteasome Assembly and Functional Integrity in Part through Ecm29. *Mol. Cell. Biol.* **31**, 1610–1623 (2011).

39. Lee, S. Y.-C., De la Mota-Peynado, A. & Roelofs, J. Loss of Rpt5 protein interactions with the core particle and Nas2 protein causes the formation of faulty proteasomes that are inhibited by Ecm29 protein. *J. Biol. Chem.* **286**, 36641–51 (2011).

40. De La Mota-Peynado, A. *et al.* The proteasome-associated protein Ecm29 inhibits proteasomal ATPase activity and in vivo protein degradation by the proteasome. *J. Biol. Chem.* **288**, 29467–29481 (2013).

41. Leggett, D. S. *et al.* Multiple associated proteins regulate proteasome structure and function. *Mol. Cell* **10**, 495–507 (2002).

42. Kleijnen, M. F. *et al.* Stability of the proteasome can be regulated allosterically through engagement of its proteolytic active sites. *Nat. Struct. Mol. Biol.* **14**, 1180–1188 (2007).

43. Wani, P. S., Suppahia, A., Capalla, X., Ondracek, A. & Roelofs, J. Phosphorylation of the C-terminal tail of proteasome subunit α7 is required for binding of the proteasome quality control factor Ecm29. *Nat. Publ. Gr.* (2016). doi:10.1038/srep27873

44. Nahar, A., Fu, X., Polovin, G., Orth, J. D. & Park, S. Two alternative mechanisms regulate the onset of chaperone-mediated assembly of the proteasomal ATPases. *J. Biol. Chem.* **294**, 6562–6577 (2019).

45. Tomko, R. J. & Hochstrasser, M. Incorporation of the Rpn12 Subunit Couples Completion of Proteasome Regulatory Particle Lid Assembly to Lid-Base Joining. *Mol. Cell* **44**, 907–917 (2011).

46. Roelofs, J. *et al.* Chaperone-mediated pathway of proteasome regulatory particle assembly. *Nature* **459**, 861–865 (2009).

47. Hofmann, L. *et al.* A nonproteolytic proteasome activity controls organelle fission in yeast. *J. Cell Sci.* **122**, 3673–3683 (2009).

48. Weberruss, M. H. *et al.* Blm10 facilitates nuclear import of proteasome core particles. *EMBO J.* **32**, 2697–2707 (2013).

49. Wen, W., Meinkotht, J. L., Tsien, R. Y. & Taylor, S. S. Identification of a signal for rapid export of proteins from the nucleus. *Cell* **82**, 463–473 (1995).

50. Kudo, N. *et al.* Leptomycin B inactivates CRM1/exportin 1 by covalent modification at a cysteine residue in the central conserved region. *Proc. Natl. Acad. Sci. U. S. A.* **96**, 9112–9117 (1999).

51. Wolff, B., Sanglier, J. J. & Wang, Y. Leptomycin B is an inhibitor of nuclear export: Inhibition of nucleo-cytoplasmic translocation of the human immunodeficiency virus type 1 (HIV-1) Rev protein and Rev-dependent mRNA. *Chem. Biol.* **4**, 139–147 (1997).

52. Fornerod, M., Ohno, M., Yoshida, M. & Mattaj, I. W. CRM1 is an export receptor for leucine-rich nuclear export signals. *Cell* **90**, 1051–1060 (1997).

53. Askjaer, P., Jensen, T. H., Nilsson, J., Englmeier, L. & Kjems, J. The specificity of the CRM1-Rev nuclear export signal interaction is mediated by RanGTP. *J. Biol. Chem.* **273**, 33414–33422 (1998).

54. Aitchison, J. D. & Rout, M. P. The yeast nuclear pore complex and transport through it. *Genetics* **190**, 855–83 (2012).

55. Leggett, D. S., Glickman, M. H. & Finley, D. Purification of proteasomes, proteasome subcomplexes, and proteasome-associated proteins from budding yeast. *Methods Mol. Biol.* **301**, 57–70 (2005).

56. Unverdorben, P. *et al.* Deep classification of a large cryo-EM dataset defines the conformational landscape of the 26S proteasome. *Proc. Natl. Acad. Sci. U. S. A.* **111**, 5544–9 (2014).

57. Wehmer, M. *et al.* Structural insights into the functional cycle of the ATPase module of the 26S proteasome. *Proc. Natl. Acad. Sci. U. S. A.* **114**, 1305–1310 (2017).

58. Dambacher, C. M., Worden, E. J., Herzik, M. A., Martin, A. & Lander, G. C. Atomic structure of the 26S proteasome lid reveals the mechanism of deubiquitinase inhibition. *Elife* **5**, e13027 (2016).

59. Worden, E. J., Padovani, C. & Martin, A. Structure of the Rpn11-Rpn8 dimer reveals mechanisms of substrate deubiquitination during proteasomal degradation. *Nat. Struct. Mol. Biol.* **21**, 220–227 (2014).

60. Enenkel, C. *et al.* Ubiquitin orchestrates proteasome dynamics between proliferation and quiescence in yeast. *Mol. Biol. Cell* **28**, 2479–2491 (2017).

61. Ghaemmaghami, S. *et al.* Global analysis of protein expression in yeast. *Nature* **425**, 737–741 (2003).

62. Pack, C. G. *et al.* Quantitative live-cell imaging reveals spatio-temporal dynamics and cytoplasmic assembly of the 26S proteasome. *Nat. Commun.* **5**, (2014).

63. Panté, N. & Kann, M. Nuclear pore complex is able to transport macromolecules with diameters of ~39 nm. *Mol. Biol. Cell* **13**, 425–434 (2002).

64. Andrea Lehmann, Katharina Janek, B. B. & Peter-Michael Kloetzel and Cordula Enenk. 20 S proteasomes are imported as precursor complexes into the nucleus of yeas. *J. Mol. Biol. (* **317**, 401–413 (2002).

65. Wendler, P., Lehmann, A., Janek, K., Baumgart, S. & Enenkel, C. The Bipartite Nuclear Localization Sequence of Rpn2 Is Required for Nuclear Import of Proteasomal Base Complexes via Karyopherin αβ and Proteasome Functions. *J. Biol. Chem.* **279**, 37751–37762 (2004).

66. Isono, E. *et al.* The assembly pathway of the 19S regulatory particle of the yeast 26S proteasome. *Mol. Biol. Cell* **18**, 569–580 (2007).

Chapter 4 - Discussion

The proteasome in proteostasis

Cellular protein levels must be controlled in order to maintain protein homeostasis (proteostasis). A network of regulatory mechanisms, such as those involved with protein folding, localization, and degradation, work collectively to ensure proper protein function and cell viability [1]. A vital branch of this network is the ubiquitin-proteasome system (UPS) that works to maintain proper protein levels through selective degradation of ubiquitinated substrates. Through the addition of ubiquitin, marked substrates, such as cyclins, cyclin-dependent kinases, and defective ribosome products, can be recognized and degraded by the proteasome [252–254]. This selective degradation can prevent accumulation of misfolded proteins as well as control cellular processes like the cell cycle. Therefore, proper functioning of the UPS is vital for cell survival and proliferation. While the proteasome is a key player in proteostasis, it is affected by other branches of proteostasis including assembly and degradation. As a fully functional proteasome involves assembly of 66 individual subunits, mechanisms are in place that aid in the formation of mature proteasome complexes. Furthermore, activity is regulated (e.g. phosphorylation of 26S) as well as its cellular localization. Finally, proteasomes can be subjected to degradation if they become non-functional or when physiological conditions change. Due to its large size, complexity, and numerous conformational states, it can be hard to dissect which subunits, posttranslational modifications, or external factors trigger specific regulatory events. While we have gained a better understanding of proteasome assembly with the discovery of proteasome-dedicated chaperones for each of the proteasome's two subcomplexes, the regulatory particle (RP) and the core particle (CP), factors that regulate proteasome localization and composition during specific stress conditions remain poorly understood [88,89,92–94,139,208]. Both of these mechanisms are central to the work discussed in this thesis.

Regulation of proteasome composition

The standard 26S proteasome is composed of RP and CP. However, multiple other proteasome-associated proteins and complexes exist. While many of these indirectly regulate the degradative process of the proteasome, e.g. by bringing substrates to the proteasome (Rad23, Dsk2), or by regulating the ubiquitin chains of substrates (Hul5, Ubp6), there is a subset of proteasome-associated proteins that directly bind CP. This binding is mutually exclusive with RP

and creates a number of alternative proteasome complexes, each one, presumably, with a specific function. The function of RP is to facilitate the degradation of folded, ubiquitinated substrates. RP has deubiquitinating and ATPase activity that enables it to, respectively, remove the ubiquitin tag and unfold the substrate. These unfolded substrates are translocated through a narrow channel of CP [111,153,154]. How other proteins/complexes that bind to the core particle, at the same interface as RP, function with CP remains poorly understood. One of these activators, Blm10 (PA200 in mammalian cells) was reportedly involved in numerous cellular processes including core particle assembly, proteasome nuclear import, and trafficking of proteasomes into proteasome storage granules (PSG) [101,168,173]. While these numerous functions have been suggested, few have tried to understand the dynamics behind proteasome complex formation or how different complexes are affected by stress conditions, such as those that affect proteasome localization and degradation. Here, we wanted to understand how the formation of Blm10-CP complexes were regulated by studying the variety of complexes that were found in the cell upon varying Blm10 expression levels. In fact, we show that by creating an overabundance of Blm10, we shift the equilibrium from mostly RP-CP complexes, that are responsible for degradation of ubiquitinated material, to primarily Blm10-CP complexes. Considering RP-CP complexes are essential, and we observed that increased levels of Blm10 directly displace RP from CP, it is evolutionarily speaking, logical that Blm10 would exist at substoichiometric levels to RP to ensure sufficient RP-CP levels are maintained.

This shift in complex composition led to an accumulation of proteasome-specific substrates. Reduced levels of Blm10 during particular stress conditions would allow for more RP-CP complexes, as we have shown Blm10 and RP compete for CP binding. An increase in 26S complexes would allow the cell to degrade more ubiquitinated substrates. Thus, degradation of Blm10 might be a regulatory mechanism to increase the cell's degradative capacity. Our observation that Blm10 is degraded during particular stress conditions, might indicate cells require an increased degradative capacity. Upon nitrogen starvation, proteasomes are selectively targeted for degradation in the vacuole through the process of autophagy [176,177]. RP-CP complexes are targeted for degradation approximately 6 hours post nitrogen starvation while Blm10 containing complexes begin disappearing around 2 hours. Earlier degradation could indicate that the cell is attempting to increase the levels of RP-CP complexes to aid in the degradation of accumulating substrates. The degradation of Blm10 and disappearance of Blm10-

CP complexes can result from two distinct processes. First, induction of stress conditions could lead to dissociation of Blm10 and CP followed by subsequent degradation of Blm10. This would increase the levels of free CP which could, in turn, bind more RP and increase the levels of 26S proteasomes. Therefore, as stress conditions or nutrient starvation persists, Blm10 levels decline and the levels of RP-CP complexes increases. Secondly, CP could be degraded along with its bound Blm10; however, in this case, new CP would need to be made in order to explain the newly emerging RP-CP complexes. This scenario seems unlikely as general protein synthesis is reduced during nutrient starvation [286]. The first model is also consistent with our observations that Blm10 can still be degraded through autophagy independently of CP. Therefore, we propose that Blm10 is selectively degraded through autophagy in order to increase 26S proteasome levels and circumvent the ramifications caused by nutrient stress. While the dynamics behind how these activators interchange with one another remains unknown, it could be based on conformational changes. Evidence suggests that CP adopts different conformations when Blm10 binds to it than when RP binds [287]. These different conformations could allow for specific targeting of Blm10-CP complexes through post-translational modifications. These modifications could further alter either the conformational state of Blm10 or the core particle that could lead to its release of CP and subsequent degradation (Fig. 1). However, with the multitude of potential modification sites on numerous subunits of the CP, as well as Blm10, this hypothesis poses difficult to test.

Figure 4-1 – Effects of Blm10 on proteasome dynamics

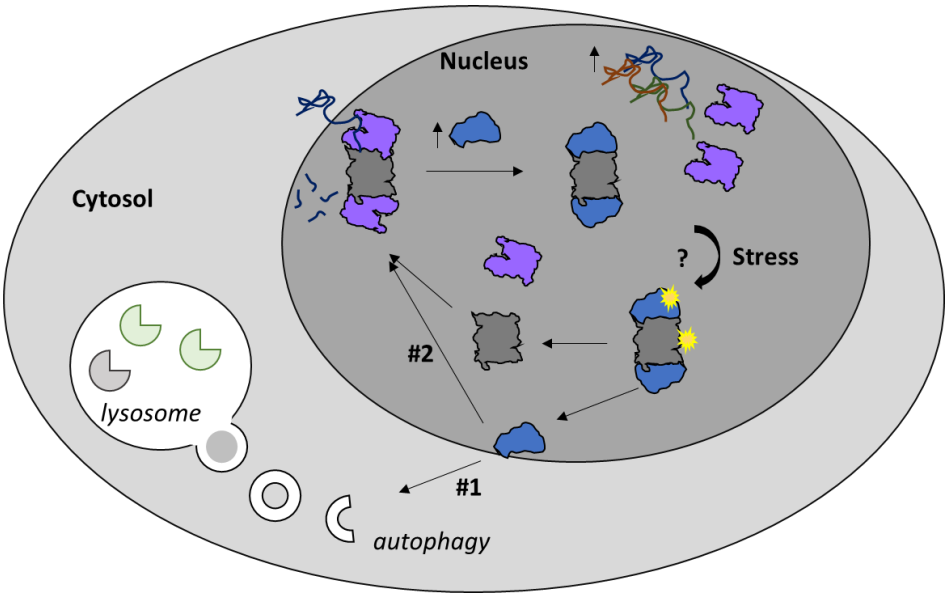

Model: 26S proteasomes composed of RP and CP degrade ubiquitinated substrates. Increased levels of Blm10 compete with RP to form $Blm10_2$-CP complexes which increases ubiquitinated substrate levels. Prolonged cell stress and increasing levels of substrates could lead to modification of either Blm10 or CP which leads to dissociation of Blm10. This would allow for CP to bind to the regulatory particle and for the cell to regain its degradative capacity. #1 Blm10 appears to be selectively degraded through autophagy; however, when autophagy is blocked, it appears that Blm10 can be degraded through the proteasome (#2).

Factors affecting proteasome localization

For proper functioning, proteins not only need to be present at the optimal concentration, but also be present at the correct location in the cell. As the cell encounters various stress conditions, such as nutrient starvation, it adapts to ensure cell survival. The proteasome, depending on the stress conditions encountered, changes localization; however, the specific mechanisms or signaling pathways involved in these processes remains obscure. My thesis focuses on two specific stress conditions, nitrogen starvation and glucose starvation, which affect proteasome localization differently [177,199]. As shown for the proteasome and Blm10, nitrogen starvation induces autophagy which causes the proteasome, normally enriched in the nucleus, to be exported to the cytoplasm and targeted to the lysosome/vacuole for degradation. While the proteasome appears to be essential during nutrient stress, its degradation appears to be much later than that of other proteins. Perhaps, as starvation persists, the cell's need for nutrients surpasses its need for proteasome activity thus leading to its degradation in the vacuole to produce more nutrients for cell survival [176,177]. While degradation appears imminent, the process, including what signals lead to proteasome export from the nucleus as well as what modifications might cause the proteasome to be recognized as cargo for the autophagosome, is relatively unknown. Other studies have attempted to understand the phenotype associated with glucose starvation as

well. While glucose starvation also causes nuclear export of the proteasome, the end result is the formation of granules in the cytoplasm, called proteasome storage granules, rather than degradation [175]. In fact, these granules are proposed to protect proteasomes from damage or degradation during this type of starvation. Therefore, when cells are relieved of starvation or quiescence, the intact proteasomes can quickly regain normal distribution by utilizing the complexes stored in granules. This allows for quicker resumption of proteolytic activity function as compared to the production of new proteasome complexes which improves efficiency and cell fitness [175,199]. Addition of nutrients, to alleviate the stress, causes the granules to rapidly resolve and the proteasomes to reenter the nucleus within minutes. While we know these granules form, it remains a challenge to understand how the proteasomes localize to these structures. We still don't understand what factors signal and facilitate nuclear export of the proteasome or what factor nucleates and maintains the proteasome in these granules. Similarly, the mechanism involved in granule disintegration and proteasome nuclear import following nutrient addition remains poorly understood. Previous work using a Blm10 knockout suggested that this protein was required for PSG formation of the CP alone as well as its nuclear import following the addition of nutrients to cells grown to stationary phase [173,175].

However, our work in Chapter 2 indicates that, while Blm10 may be responsible for proteasome movement during and following quiescence, its effects are dispensable for granule formation and nuclear import following glucose starvation. So, how is proteasome localization differently regulated under these different conditions? Changes in cell state can activate signaling pathways, like the PKA or TORC pathways, which can lead to different posttranslational modifications. Post-translational modifications, such as phosphorylation or acetylation, are known to affect protein localization [288,289]. Therefore, I propose that deprivation of a specific nutrient activates unique signaling pathways that each target the proteasome differently, resulting in a difference in recognition by associated factors which alter localization. However, for the proteasome there is a multitude of potential modification sites and PTMs could also lead to conformational changes and thereby affect which activators bind and how different complexes are affected during different conditions. As such, elucidating the mechanism(s) involved in potential proteasome modifications, as well as the subunits and sequences involved in proteasome localization, remains a challenging question to answer. Regardless, our work

provides a more intricate understanding of the dynamics that govern proteasome complex formation as well as their fate, which appears to differentiate based on the stress condition.

Factors affecting proteasome nuclear export

Consistent with our hypothesis that proteasome localization could be affected by various conformations and post-translational modifications, we observed differences in proteasome localization upon modification of specific subunits. Tagging proteins with fluorescent tags can create abnormal phenotypes induced by the tag. We suspect that these phenotypes can be more drastic in larger complexes where many subunits interaction and transition simultaneously through multiple conformational states as the complex performs its function. This appears to be true for the proteasome. The proteasome interacts with many proteasome associated factors, so tagging certain subunits could interfere with specific binding factors or functions. More so, as the proteasome cycles through the steps of substrate recognition, deubiquitination, unfolding, and cleavage, various subunits, as well as subcomplexes, move accordingly to facilitate the function at hand [127,128]. Therefore, by adding an additional folded domain to one or more of these proteasomal subunits, we can affect its ability to change conformations which, in turn, can affect proteasome efficiency or cellular location. We observed such an effect in proteasome localization when tagging both Rpn1 and Rpn11 of the regulatory particle. Proteasomes containing both tags failed to be exported from the nucleus or form proteasome storage granules (Chapter 3). As mentioned, these tags could affect the proteasome's ability to form interactions, change conformations or expose residues that could be modified and affect its recognition by export machinery. Alternatively, while the proteasome was shown to be able to pass through the nuclear pore complex, addition of bulky tags could prevent its ability to fit through the pore [191,284]. However, this seems less likely as proteasomes, in other strains, containing these same tags were able to be exported.

Regardless, we focused on Rpn11, a subunit of the regulatory particle lid, to study how modification of this subunit affects nuclear export. Rpn11 is one of nine subunits that form the lid. The lid has been shown to self-assemble in a process that requires interactions between each of the lid subunits. Lid subunits associate stepwise: Rpn11 binds with Rpn8 followed by Rpn5, Rpn9, and Rpn6, which forms what is called module 1 of the lid subcomplex. Module 1 combines with a lid complex composed of Rpn7, Rpn3 and Sem1. The final subunit to bind is Rpn12, which serves to assure correct incorporation of all other lid subunits [162,257–259]. Apart

from the dimerization of Rpn11 and Rpn8, each of these interactions occurs between C-terminal alpha helices of each of the subunits [115,160]. Interestingly, previous reports identified a frameshift mutation in Rpn11 that prevented granule formation during quiescence [262]. Based on this, we designed a Rpn11 mutant that was informed by more recent structural insights and lacked the terminal alpha helix. This mutant led to mislocalization of the proteasome which remained nuclear under glucose starvation rather than forming PSGs. Additionally, we observed an abnormal proteasome landscape, which included an abundance of free CP as well as complexes that appeared to contain CP along with the base and module 1 of the regulatory particle. This suggests that our proteasomes lack lid subcomplex Rpn7/3/Sem1 as well as Rpn12. Either these subunits fail to incorporate as a direct result of the Rpn11 truncation, or they can associate transiently, but under lysis conditions, they dissociate. Regardless, our observation concerning a lack of lid subunits led to one of two hypotheses. First, by affecting the structure of the proteasome, we affect its ability to undergo conformational changes that could lead to its recognition and modification by export machinery. Secondly, if a defect in lid assembly is true, then these subunits could be the direct targets of export machinery and proteasomes lacking these subunits fail to be recognized.

The latter led to our analysis of Rpn7 and Rpn12. Each of these subunits was predicted to contain an export signal recognized by well-known export factor Crm1. By tagging these subunits, we tested whether they could form PSGs independently of the rest of the proteasome in the presence of the Rpn11 truncation. Following glucose starvation, we did observe a slight increase in granule formation for both subunits; however, as these subunits were under the control of the overexpressing *ADH* promoter, we suspected that these granules might not, in fact, be PSGs. Overexpression of the base subunit Rpt1, for example, led to its localization to cytoplasmic granules similar to what was observed for Rpn7 and Rpn12 [274]. Further analysis of these granules indicated that they did not behave similarly to PSGs because they did not dissolve upon addition of nutrients. Therefore, this work establishes that overexpressed, or unincorporated, lid subunits can be sequestered into granular structures. Similar to the idea that PSGs protect proteasomes, these granules could store these unincorporated subunits until they can be used to assemble more proteasome complexes.

Figure 4-2 - Effects of the Rpn11 truncation proteasome complexes

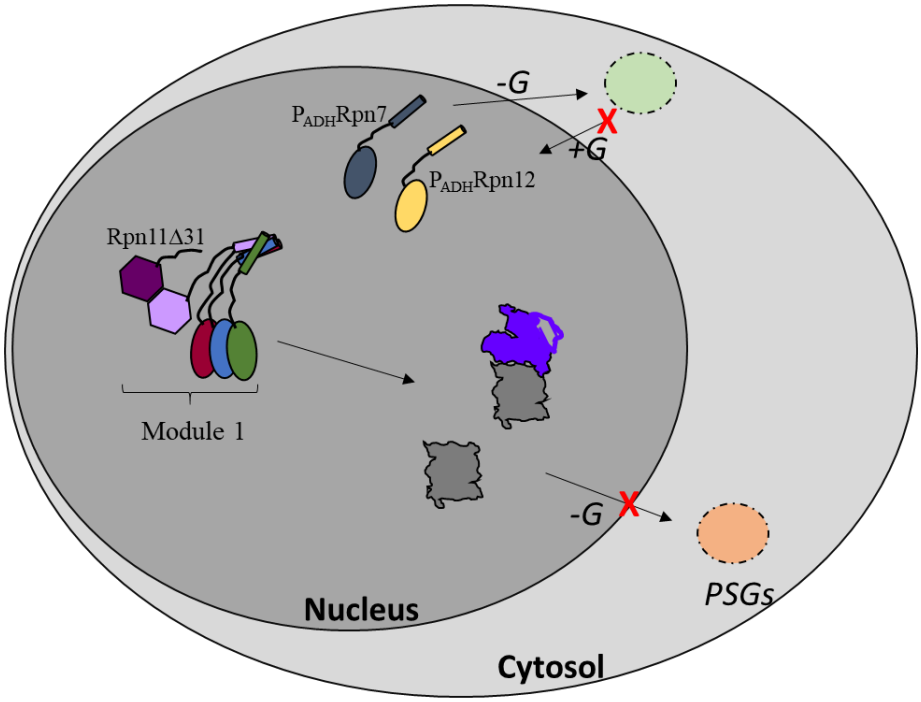

The Rpn11 truncation affects proteasome complex formation that results in increased levels of CP as well as complexes thought to contain CP, base and module 1 of the lid which all fail to form PSGs upon glucose starvation. However, lid subunits Rpn7 and Rpn12, expressed using the overexpressing ADH promoter, did form granule-like structures upon glucose starvation. These granules behaved dissimilarly to PSGs as addition of glucose had no effect on them. This indicates that unincorporated lid subunits can be stored in granules.

While Rpn7 and Rpn12 formed granular structures, we could not confirm whether they formed from subunits in the cytoplasm or whether these unincorporated subunits were exported from the nucleus based on their putative Crm1 NES. Therefore, we took advantage of a strain that expressed a form of CRM1 that could be inactivated with the drug leptomycin B. Upon drug treatment, we observed wildtype proteasomes were still exported upon glucose starvation indicating Crm1 is not required for proteasome export. It remains unclear whether components of the Rpn7 complex or Rpn12 are central to proteasome export or if affecting their interactions with the rest of the proteasome causes other defects. As stated, addition of a tag(s) on the proteasome can affect localization, so affecting subunit interactions could very well induce the same phenotype.

Work on proteasome storage granules suggest that RP and CP, while found in the same granule, are not associated with each other, and exist as individual subcomplexes. If this is accurate, does the proteasome dissociate before or after nuclear export? Our data suggests that the 26S proteasome is exported rather than individual subcomplexes. The Rpn11 truncation, which is part of RP, not only affects RP localization but CP as well. If the proteasome

dissociates prior to nuclear export, then it is reasonable to predict that CP would be exported and sent to PSGs independently of RP. As this does not occur, it appears that RP and CP are exported together.

Together, this work highlights the complexity of proteasome dynamics. By altering expression of proteasome associated factors or manipulating proteasome subunits, we drastically change proteasome function as well as how the proteasome responds to particular stress conditions.

References

1. Powers, E. T., Morimoto, R. I., Dillin, A., Kelly, J. W. & Balch, W. E. Biological and Chemical Approaches to Diseases of Proteostasis Deficiency. *Annu. Rev. Biochem.* **78**, 959–991 (2009).

2. Kirschner, M. Intracellular proteolysis. *Trends Cell Biol.* **9**, M42–M45 (1999).

3. von Mikecz, A. The nuclear ubiquitin-proteasome system. *Journal of Cell Science* **119**, 1977–1984 (2006).

4. Qian, S. B., Princiotta, M. F., Bennink, J. R. & Yewdell, J. W. Characterization of rapidly degraded polypeptides in mammalian cells reveals a novel layer of nascent protein quality control. *J. Biol. Chem.* **281**, 392–400 (2006).

5. Roelofs, J. *et al.* Chaperone-mediated pathway of proteasome regulatory particle assembly. *Nature* **459**, 861–865 (2009).

6. Takagi, K. *et al.* Pba3–Pba4 heterodimer acts as a molecular matchmaker in proteasome α-ring formation. *Biochem. Biophys. Res. Commun.* **450**, 1110–1114 (2014).

7. Kusmierczyk, A. R., Kunjappu, M. J., Funakoshi, M. & Hochstrasser, M. A multimeric assembly factor controls the formation of alternative 20S proteasomes. *Nat. Struct. Mol. Biol.* **15**, 237–244 (2008).

8. Hirano, Y. *et al.* Dissecting β-ring assembly pathway of the mammalian 20S proteasome. *EMBO J.* **27**, 2204–2213 (2008).

9. Ramos, P. C., Höckendorff, J., Johnson, E. S., Varshavsky, A. & Dohmen, R. J. Ump1p is required for proper maturation of the 20S proteasome and becomes its substrate upon completion of the assembly. *Cell* **92**, 489–99 (1998).

10. Kusmierczyk, A. R., Kunjappu, M. J., Kim, R. Y. & Hochstrasser, M. A conserved 20S proteasome assembly factor requires a C-terminal HbYX motif for proteasomal precursor binding. *Nat. Struct. Mol. Biol.* **18**, 622–629 (2011).

11. Stadtmueller, B. M. *et al.* Structure of a proteasome Pba1-Pba2 complex implications for proteasome assembly, activation, and biological function. *J. Biol. Chem.* **287**, 37371–37382 (2012).

12. Tomko, R. J., Funakoshi, M., Schneider, K., Wang, J. & Hochstrasser, M. Heterohexameric Ring Arrangement of the Eukaryotic Proteasomal ATPases: Implications for Proteasome Structure and Assembly. *Mol. Cell* **38**, 393–403 (2010).

13. Verma, R. Role of Rpn11 metalloprotease in deubiquitination and degradation by the 26S proteasome. *Science (80).* **298**, 611–615 (2002).

14. Yao, T. & Cohen, R. A cryptic protease couples deubiquitination and degradation by the proteasome. *Nature* **419**, 403–407 (2002).

15. Weberruss, M. H. *et al.* Blm10 facilitates nuclear import of proteasome core particles. *EMBO J.* **32**, 2697–2707 (2013).

16. Fehlker, M., Wendler, P., Lehmann, A. & Enenkel, C. Blm3 is part of nascent proteasomes and is involved in a late stage of nuclear proteasome assembly. *EMBO Rep.* **4**, 959–963 (2003).

17. Marques, A. J., Glanemann, C., Ramos, P. C. & Dohmen, R. J. The C-terminal extension of the beta7 subunit and activator complexes stabilize nascent 20 S proteasomes and promote their maturation. *J. Biol. Chem.* **282**, 34869–76 (2007).

18. Marshall, R. S., Li, F., Gemperline, D. C., Book, A. J. & Vierstra, R. D. Autophagic Degradation of the 26S Proteasome Is Mediated by the Dual ATG8/Ubiquitin Receptor RPN10 in Arabidopsis. *Mol. Cell* **58**, 1053–66 (2015).

19. Waite, K. A., De-La Mota-Peynado, A., Vontz, G. & Roelofs, J. Starvation Induces Proteasome Autophagy with Different Pathways for Core and Regulatory Particles. *J. Biol. Chem.* **291**, 3239–53 (2016).

20. Onodera, J. & Ohsumi, Y. Autophagy is required for maintenance of amino acid levels and protein synthesis under nitrogen starvation. *J. Biol. Chem.* **280**, 31582–31586 (2005).

21. Toste Rêgo, A. & da Fonseca, P. C. A. Characterization of Fully Recombinant Human 20S and 20S-PA200 Proteasome Complexes. *Mol. Cell* (2019). doi:10.1016/j.molcel.2019.07.014

22. Marshall, R. S. & Vierstra, R. D. Proteasome storage granules protect proteasomes from autophagic degradation upon carbon starvation. *Elife* **7**, e34532 (2018).

23. Laporte, D., Salin, B., Daignan-Fornier, B. & Sagot, I. Reversible cytoplasmic localization of the proteasome in quiescent yeast cells. *J. Cell Biol.* **181**, 737–745 (2008).

24. Hirano, H., Kimura, Y. & Kimura, A. Biological significance of co- and post-translational modifications of the yeast 26S proteasome. *Journal of Proteomics* **134**, 37–46 (2016).

25. Kors, S., Geijtenbeek, K., Reits, E. & Schipper-Krom, S. Regulation of Proteasome Activity by (Post-)transcriptional Mechanisms. *Front. Mol. Biosci.* **6**, (2019).

26. Unverdorben, P. *et al.* Deep classification of a large cryo-EM dataset defines the conformational landscape of the 26S proteasome. *Proc. Natl. Acad. Sci. U. S. A.* **111**, 5544–9 (2014).

27. Wehmer, M. *et al.* Structural insights into the functional cycle of the ATPase module of the 26S proteasome. *Proc. Natl. Acad. Sci. U. S. A.* **114**, 1305–1310 (2017).

28. Pack, C. G. *et al.* Quantitative live-cell imaging reveals spatio-temporal dynamics and cytoplasmic assembly of the 26S proteasome. *Nat. Commun.* **5**, (2014).

29. Panté, N. & Kann, M. Nuclear pore complex is able to transport macromolecules with diameters of ~39 nm. *Mol. Biol. Cell* **13**, 425–434 (2002).

30. Fukunaga, K., Kudo, T., Toh-e, A., Tanaka, K. & Saeki, Y. Dissection of the assembly pathway of the proteasome lid in Saccharomyces cerevisiae. *Biochem. Biophys. Res. Commun.* **396**, 1048–1053 (2010).

31. Sharon, M., Taverner, T., Ambroggio, X. I., Deshaies, R. J. & Robinson, C. V. Structural organization of the 19S proteasome lid: Insights from MS of intact complexes. *PLoS Biol.* **4**, 1314–1323 (2006).

32. Bai, M. *et al.* In-depth analysis of the lid subunits assembly mechanism in mammals. *Biomolecules* **9**, (2019).

33. Tomko, R. J. & Hochstrasser, M. Incorporation of the Rpn12 Subunit Couples Completion of Proteasome Regulatory Particle Lid Assembly to Lid-Base Joining. *Mol. Cell* **44**, 907–917 (2011).

34. Beck, F. *et al.* Near-atomic resolution structural model of the yeast 26S proteasome. *Proc. Natl. Acad. Sci. U. S. A.* **109**, 14870–14875 (2012).

35. Estrin, E., Lopez-Blanco, J. R., Chacón, P. & Martin, A. Formation of an Intricate Helical Bundle Dictates the Assembly of the 26S Proteasome Lid. *Structure* **21**, 1624–1635 (2013).

36. Saunier, R., Esposito, M., Dassa, E. P. & Delahodde, A. Integrity of the Saccharomyces cerevisiae Rpn11 Protein Is Critical for Formation of Proteasome Storage Granules (PSG) and Survival in Stationary Phase. *PLoS One* **8**, (2013).

37. Nahar, A., Fu, X., Polovin, G., Orth, J. D. & Park, S. Two alternative mechanisms regulate the onset of chaperone-mediated assembly of the proteasomal ATPases. *J. Biol. Chem.* **294**, 6562–6577 (2019).

Appendix A - Supplementary Information for Chapter 2

Supplementary Figure 1 - Blm10 fails to outcompete Pba1-2 as it does RP

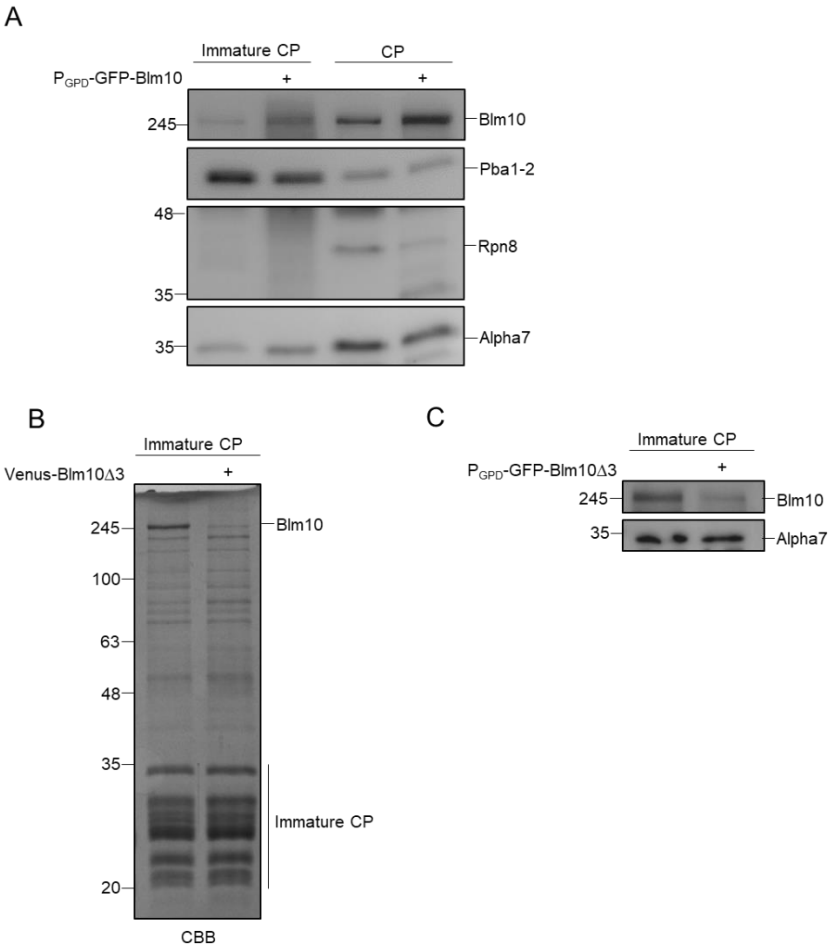

(a) β4 ProtA-tagged strains were used to purify mature proteasomes while Ump1 ProtA-tagged strains allowed for purification of immature CP. Purified complexes were resolved using SDS-PAGE to determine the extent to which Blm10 could compete with RP and Pba1-2 for binding to mature and immature CP, respectively. Competition was determined through overexpression of Blm10. Immunoblotting for Blm10 allowed determination of the amount of Blm10 bound and co-purified with mature and immature CP. α7 was used as a loading control while antibodies against Pba1-2 and Rpn8, a subunit of RP, were used to determine the extent of Blm10 competition (b) Immature CP was purified from strains expressing endogenous levels of Blm10Δ3. Samples were separated using SDS-PAGE followed by staining with CBB. The mutant form of Blm10 showed reduced binding to immature CP similarly to mature CP. (c) To determine whether overexpression of Blm10 could force binding to immature CP, Ump1-ProtA tagged strains overexpressing Blm10 were used to again purify immature CP complexes. Immunoblots against Blm10 were utilized to determine the extent of Blm10 binding and subsequent purification. α7 was used as a loading control.

Supplementary Figure 2 - Blm10 overexpression is not associated with growth phenotype on canavanine

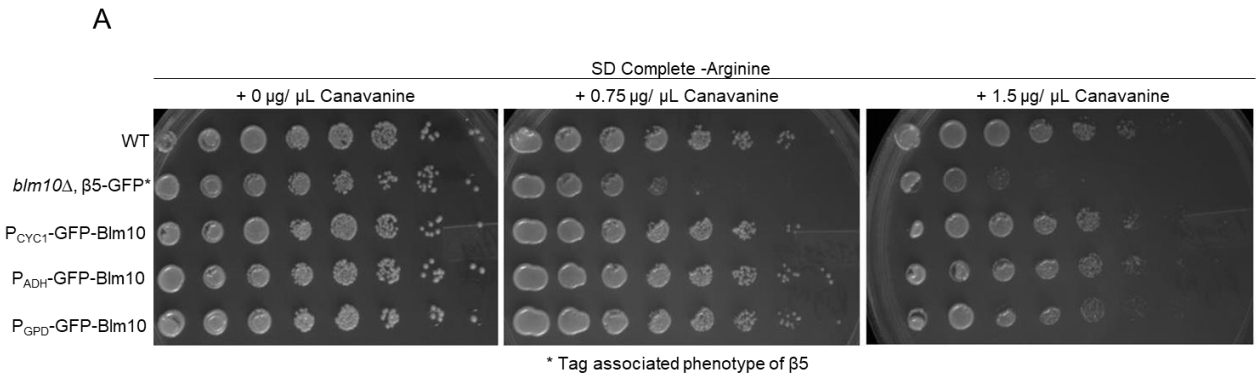

(a) A phenotype screen was conducted as in 3C. 1.0 (OD_{600}) cell equivalents were diluted seven-fold and plated on SD complete plates lacking arginine and containing increasing amounts of canavanine (0-1.5 µg/µL). Plates were incubated at 30 degrees for 48 hours. Overexpression of Blm10 was not associated with a growth phenotype.

Supplementary Figure 3 – GPD promoter remains active under prolonged cell growth and heat stress

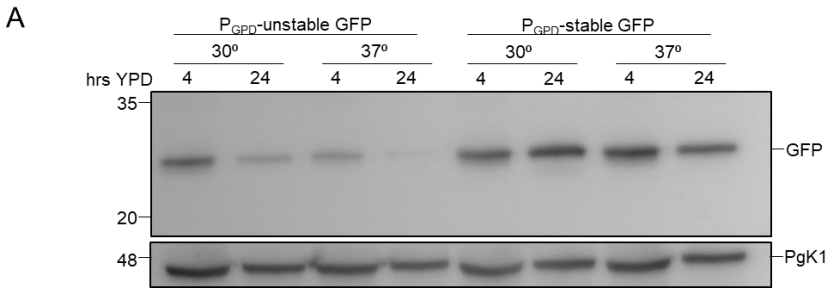

(a) As Blm10 expression decreased during prolonged cell growth, the expression level from the GPD promoter was analyzed using stable and unstable GFP. Constructs were integrated into the URA3-TIM9 region of the genome. Levels of stable GFP remained steady following 24 hours at 30 degrees and 37 degrees. Levels of unstable GFP were reduced at both 30 degrees and 37 degrees, but still detectable indicating the GPD promoter is moderately active.

Supplementary Figure 4 - Blm10 levels are not affected by glucose starvation

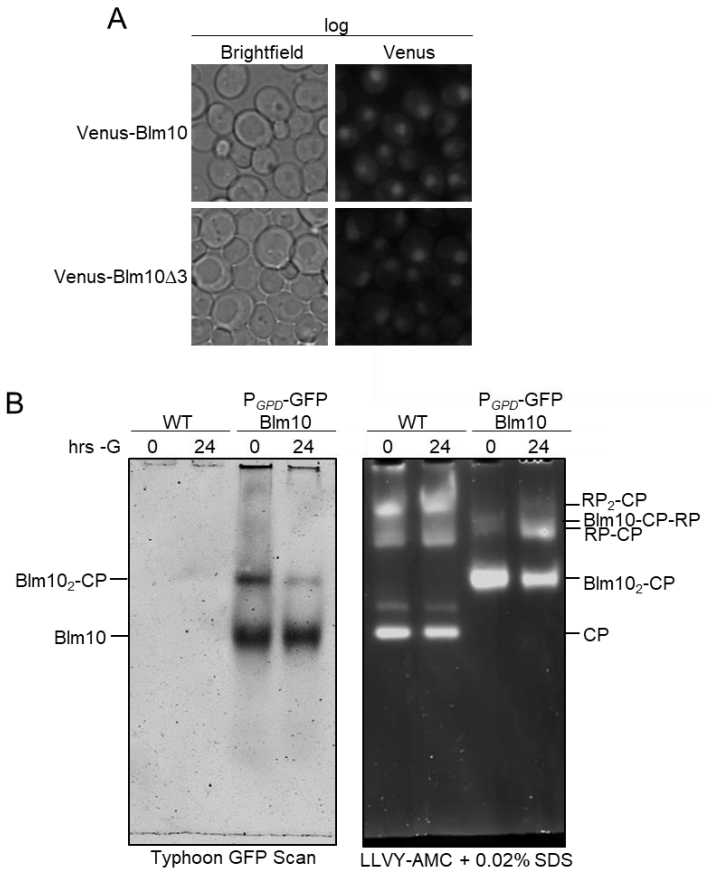

(a) Strains expressing either bound or unbound Venus-Blm10 were monitored for cellular localization using fluorescent microscopy. Both strains showed nuclear signal indicating both forms of Blm10 can be imported into the nucleus. (b) Whole cell lysates for endogenous and GPD controlled expression of Blm10 were monitored by native gel electrophoresis following 24 hours of glucose starvation. Following starvation, unbound Blm10 remains present (left panel, lane 4). Despite this observation, RP-CP complexes begin to reform in the absence of glucose indicating that this condition is unfavorable for Blm10-CP complexes. (right panel lane 3 versus lane 4).

Appendix B - Supplementary Information for Chapter 3

Supplementary Figure 1. Certain combinations of tagged proteasome subunits affect proteasome localization.

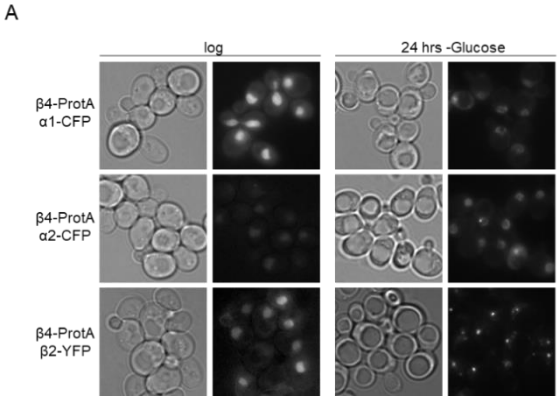

(A) Strains containing various combinations of tagged proteasome subunits were glucose starved for 24 hours. α1- and α2-CFP in combination with a β4-ProtA tag failed to form PSGs while β4-ProtA with β4-YFP formed granules similarly to singly tagged strains.

Supplementary Figure 2. Rpn11 mutations readily formed PSGs similar to wild type.

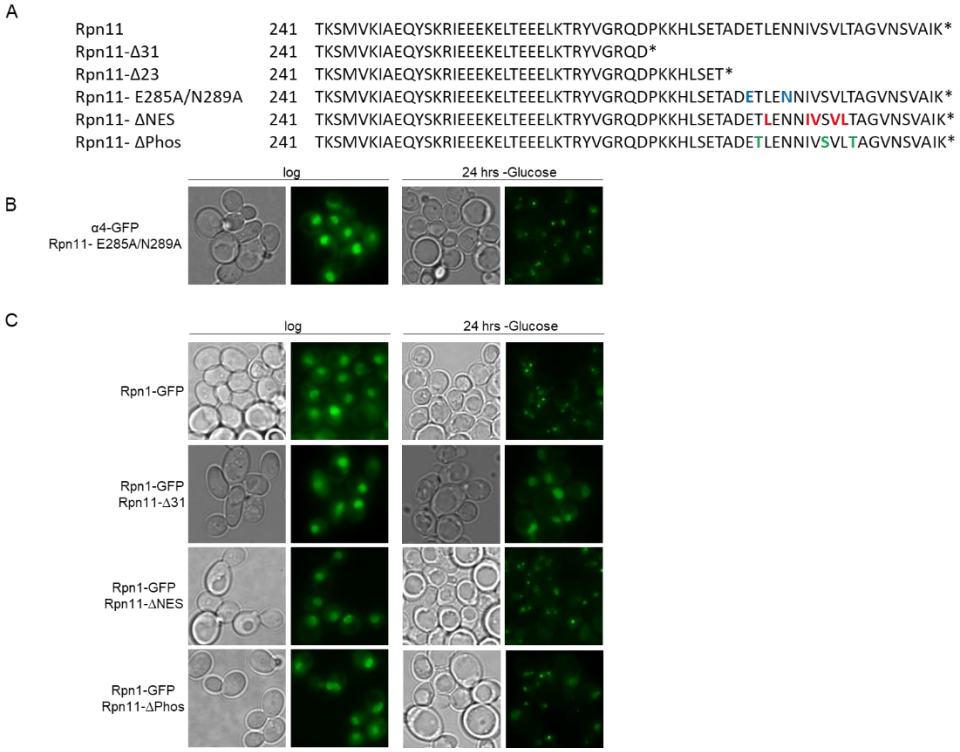

(A) Sequence alignment for Rpn11 mutations. Rpn11-E285A/N289A sequence shows the wild-type sequence of Rpn11; however, amino acids indicated in blue are those involved in intrahelical interactions. Rpn11ΔNES highlights a putative Crm1-dependent NES. Amino acids of this sequence are indicated in red. Potential phosphorylation sites (Rpn11ΔPhos) for common kinases are indicated in green. Colored amino acids were mutated to alanine. (B) The Rpn11-E285A/N289A mutant strain (in combination with α4-GFP) was starved of glucose and granule formation was assessed using fluorescent microscopy. (C) Rpn11ΔNES and Rpn11ΔPhos in combination with Rpn1-GFP were starved of glucose for 24 hours. Both mutant strains formed granules similarly to wild type.

Supplementary Figure 3. The Rpn11 truncation becomes lethal in combination with certain proteasome tags.

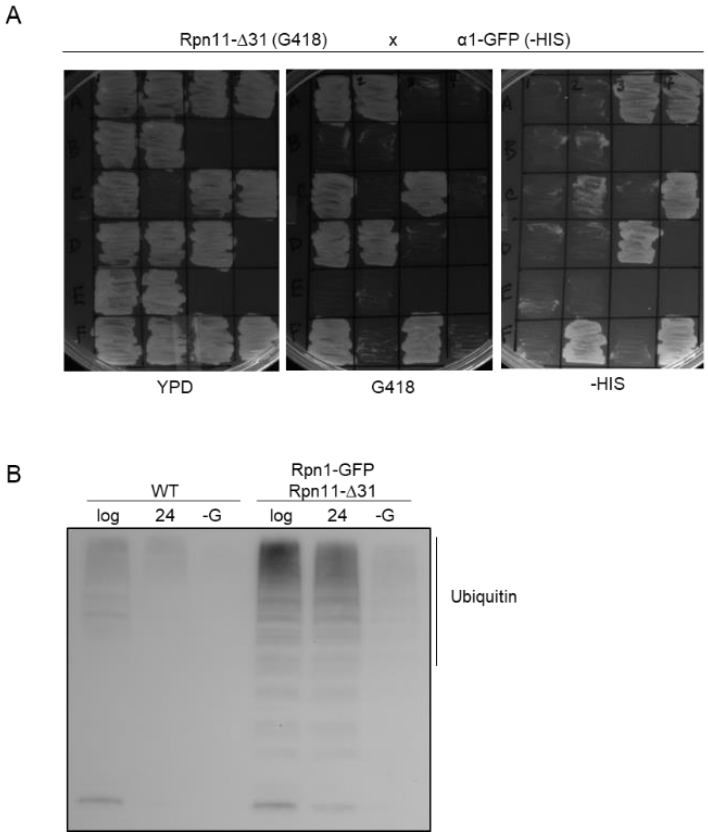

(A) Stains containing the Rpn11 truncation were crossed with multiple strains containing fluorescently tagged proteasome subunits to create diploid strains for sporulation. Spores derived from tetrad dissections were re-streaked on YPD plates and selection plates specific for the Rpn11 truncation (G418) and tagged proteasome subunits (-HIS). Spores that were viable did not contain both G418 and -HIS selections indicating that the Rpn11 truncation is lethal in combination with some tagged proteasome subunits. (B) SDS-PAGE analysis of Rpn11-Δ31 showed increased levels of ubiquitinated proteins during both log phase and 24 hours of growth on YPD compared to wild type.

Supplementary Figure 4. Purification of Ecm29 bound proteasomes.

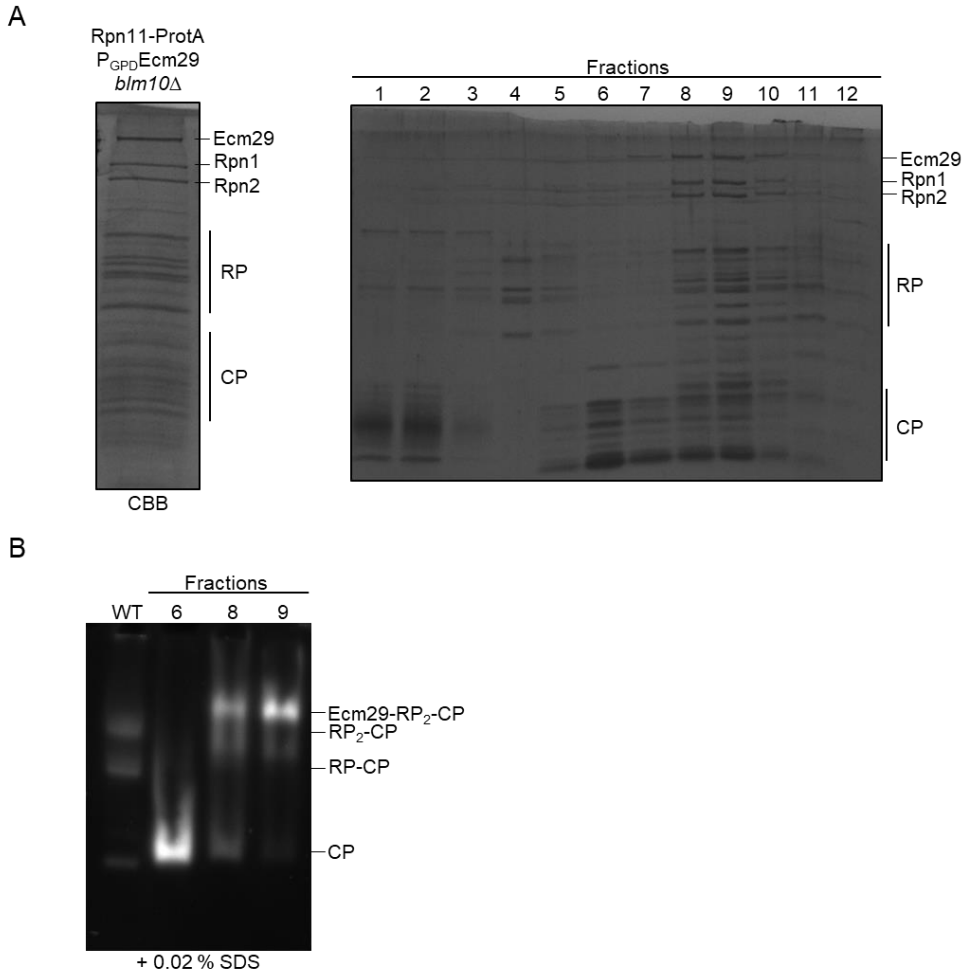

(A) Proteasomes containing a ProtA affinity tag on Rpn11 were purified using IgG affinity resin. Purified samples were analyzed on SDS-PAGE to ensure Ecm29 bound proteasomes (left panel). Samples were ultracentrifuged on a glycerol gradient at 100,000 x g for 18 hours at 4 °C to separate proteasome complexes. 1 mL fractions were collected from the top of the gradient. 10 µL of each fraction was analyzed on SDS-PAGE to determine which fractions contained Ecm29 bound proteasomes. (B) 10 µL of fractions containing Ecm29 bound proteasomes were analyzed for purity on native gel electrophoresis and proteasome complexes were visualized using an in-gel LLVY-AMC activity assay with 0.02 % SDS.